NASA CONTRACTOR REPORT 177360

USAAVSCOM TR 85-A-2

AD-B094967

UH-60 BLACK HAWK ENGINEERING SIMULATION MODEL VALIDATION AND PROPOSED MODIFICATIONS

Thaddeus T. Kaplita

IN-08
58119
P-125

CONTRACT NAS2- 11570
July 1985

Date for general release January 1987

NASA

United States Army
Aviation Systems
Command

NASA CONTRACTOR REPORT 177360

USAAVSCOM TR 85-A-2

UH-60 BLACK HAWK ENGINEERING SIMULATION MODEL VALIDATION AND PROPOSED MODIFICATIONS

Thaddeus T. Kaplita
Sikorsky Aircraft
Division of United Technologies Corporation
Stratford, CT 06601

Prepared for
Aeroflightdynamics Directorate
U. S. Army Research and Technology
Activity (AVSCOM)
under Contract NAS2-11570

July 1985

Date for general release January 1987

National Aeronautics and
Space Administration

Ames Research Center
Moffett Field, California 94035

United States Army
Aviation Systems
Command

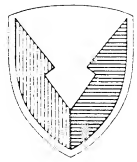

FOREWORD

This report was prepared by the Sikorsky Division of United Technologies Corporation for the National Aeronautics and Space Administration, Ames Research Center, Moffett Field, California under Contract NAS2-11570.

This contract, to validate and update the engineering simulation model of the UH-60A BLACK HAWK helicopter at the Ames Research Center, was funded by the U. S. Army Research and Technology Laboratories (USARTL), Ames Research Center and administered by the National Aeronautics and Space Administration. Mr. William McKenna was the Contract Administrator and E. W. Aiken, Army Aeromechanics Laboratory, was the Technical Monitor. The Sikorsky Division Program Manager for this contract was Mr. J. Howlett. Simulation software support was provided by Messrs. K. Arifian, R. Brand, and D. Simpson.

SA 1114

SUMMARY

The BLACK HAWK Engineering Simulation Model is validated and updated. Model calculated data for transient responses to control inputs and for steady trimmed flight are compared with corresponding flight test data. The test data were acquired by the U. S. Army Aviation Engineering Flight Activity (USAAEFA) flying the UH-60A BLACK HAWK Helicopter S/N 77-22716, Reference (1). Ninety time histories of transient responses to step and pulse control inputs and 16 sets of steady flight data, supplied by the Army on magnetic tapes, were processed and simulated on the BLACK HAWK simulation mathematical model at Sikorsky.

Comparison plots of calculated and test data are analyzed to assess simulation model fidelity and to identify unsatisfactory areas of comparison. The existing simulation model is deemed to simulate the UH-60A BLACK HAWK with good accuracy. It is an acceptable engineering design and evaluation analytical tool. Acceptable but unsatisfactory areas are defined and potential approaches to create a more descriptive and representative simulation of the BLACK HAWK are listed and evaluated.

Modifications to update the existing simulation model are formulated. These include, in their order of priority, the following:

- Substitute main rotor torque for engine torque in main rotor moment matrix.
- Program first order lag in Load Demand Spindle (LDS) of the engine simulation.
- Update moment equations of motion for lateral CG offsets.
- Program first order lag on tail rotor downwash.
- Modify equations for main rotor wake interaction with empennage.
- Introduce equations for tail rotor downwash interaction with vertical tail in forward flight.

The collective lag in the LDS will significantly improve the rotor and engine response to collective inputs. The modified equations for rotor-wake/empennage interaction provide improved roll response to pedal inputs. The first two items are simple to implement and most important.

SA 1114

TABLE OF CONTENTS

SA 1114

LIST OF TABLES

LIST OF FIGURES

LIST OF FIGURES (Cont'd)

LIST OF FIGURES (Cont'd)

SA 1114

LIST OF SYMBOLS

CG	Center of Gravity
DWSHTR	Uniform downwash velocity at tail rotor disk non-dimensionalized by tail rotor tip speed.
EKTRVT	Ratio of tail rotor downwash at the vertical tail to the downwash at the tail rotor disk.
FSCG	Fuselage station of center of gravity, in.
GGRPM	Engine gas generator speed, %
h_d	Density altitude, ft
Ihl	Stabilator angle, positive leading edge up, deg
KN, KTS	Knots
LDS	Engine Load Demand Spindle
LDSCAM	Engine load demand system spindle cam, deg
LPLADD	Roll moment damping of horizontal tail, ft-lb
LT	Left
MUZTR	Velocity component parallel to tail rotor shaft and normalized by tail rotor tip speed, positive to port
NGGLDS	Engine load demand spindle cam output, %
N_r	Main rotor rotational speed, %
OMEGTR	Tail rotor rotational speed, rad/sec
OMGRAT	Main rotor rotational speed ratio, 1.0 = 100% = 27.0 rad/sec
p	Helicopter body axis roll rate, rad/sec
PS2	Location of nose accelerometer
PS3	Location of cg accelerometer
PS4	Location of velocity sensor
QFRE	Free stream dynamic pressure, lb/ft^2
RT	Right

LIST OF SYMBOLS - (Cont'd)

RTR	Tail rotor radius, ft
S	Laplace operator, 1/sec
SAV	Simulation calculated variables data file
TDW	Tail rotor downwash lag time constant, sec
THETTR	Tail rotor blade pitch angle at center of rotation, deg
TST	Flight test variables data file
TXC	LDS/Collective lag time constant, sec
VKT	True airspeed, knots
VXB	Component of airspeed along body longitudinal axis, positive forward, ft/sec
VYTRV1	Interference velocity at vertical tail due to tail rotor downwash, ft/sec
WLCG	Waterline position of center of gravity, in.
XA	Lateral cyclic stick position, positive right, in.
XB	Longitudinal cyclic stick position, positive aft, in.
XC	Collective stick position, positive up, in.
XP	Pedal position, positive right, in.
$\theta_{.75}$	Main rotor or tail rotor blade pitch angle at 0.75 blade span station, deg

SA 1114

LIST OF REFERENCES

1. Abbott, W.Y., Benson, J.D., Oliver, R.G., and Williams, R.A., "Validation Flight Test of UH-60A For Rotorcraft Systems Integration Simulator (RSIS)," USAAEFA Project No. 79-24, September 1982.

2. Howlett, J.J., "UH-60A BLACK HAWK Engineering Simulation Program: Volume I - Mathematical Model," NASA Contractor Report 166309, December 1981.

3. Hoak, D.E., "USAF Stability and Control Datcom," Revised April 1978.

4. McFarland, R.E., "The N/Rev Phenomenon in Simulating a Blade-Element Rotor System," NASA TM-84344, March 1983.

INTRODUCTION

The United States Army Aviation Engineering Flight Activity (USAAEFA) flight tested the UH-60A BLACK HAWK Helicopter (S/N 77-22716) at Edwards Air Force Base for the Aeromechanics Laboratory (AL) of the U. S. Army Research and Technology Laboratories (USARTL). A data base was acquired from these tests for validation of the Rotorcraft Systems Integration Simulator (RSIS) developed by the U. S. Army Aviation Systems Command (AVSCOM). Data were acquired for steady trimmed flights and for transient responses to control inputs. A full description of the aircraft, test procedures and conditions, and summary results are presented in Reference (1). Subsequently, Sikorsky Aircraft was contracted to validate the BLACK HAWK Simulation Mathematical Model and to modify it, as required, in those areas where there is unsatisfactory correlation.

Eight magnetic tapes comprising 90 runs of transient responses and one tape with 16 sets of steady flight test data were supplied by the Army to Sikorsky. These data were made available, under a joint Army/Sikorsky Cooperation Program, for comparison with the BLACK HAWK version of the Sikorsky General Helicopter Flight Dynamics Simulation Program (GEN HEL). The simulation model is programmed on the PDP-KL10 computer system. It is identical to the mathematical model, Reference (2), provided to the Army under Contract NAS2-10626 and installed on the NASA Ames Simulation Facility. Computer programs were developed to process the test data and convert them into Sikorsky's Internal Record Acquisition (IRA) format and to edit the resulting data files. An existing program (RAPID) was then utilized to drive the BLACK HAWK simulation model with the flight test cockpit control inputs. The resulting computer generated variables were then stored in data files by means of another program, SAVRUN. These variables and corresponding test data were plotted simultaneously, for comparison, by means of the plotting program, MUPLOT. These programs were previously developed under Sikorsky's IRD funding.

In Reference (1) it was pointed out that the intent of the program was to obtain data solely for the purpose of validating the BLACK HAWK mathematical model. Compliance with this objective resulted in flying the aircraft in a highly degraded operating mode. Thus, the test data cannot be considered representative of the UH-60A in a normal operating condition. The object of this study is to determine how well the mathematical model simulates the aircraft and what can be done to improve the model. The mathematical model is solely of interest here. For these reasons, comments on the flying qualities of the UH-60A are inappropriate and scrupulously avoided and no inferences are drawn.

The validation and update of the BLACK HAWK simulation model are presented in the main body of this report and pertinent modified equations are listed in the appendices.

SA 1114

BLACK HAWK SIMULATION MODEL UPDATE

The procedure followed to update the BLACK HAWK engineering simulation model is as follows:

- Validate simulation fidelity by comparing model calculated data with test data.
- Identify unsatisfactory comparison areas.
- Formulate model revisions which have potential for improving correlation.
- Evaluate revised model formulations.
- Identify revisions appropriate for upgrading the simulation model.

Each of these steps is discussed successively in the following sections of this report.

1.0 SIMULATION MODEL VALIDATION

The BLACK HAWK engineering simulation mathematical model is defined in Reference (2). It was validated by comparing model calculated data with flight test data for transient responses to control inputs and for helicopter attitudes and cockpit control positions in trimmed steady flight. Simulation of the flight test runs included the following test conditions:

- Pitch Bias Actuator (PBA) - Disabled and Centered
- Flight Path Stabilization (FPS) - Off
- Trim System - Off
- Stability Augmentation System (SAS)
  - Transient Response - Off
  - Steady Flight - On
- Stabilator Angle - Fixed
  - Transient Response - Flight Test Value
  - Steady Flight - Calculated Trim Value

The locations of the acceleration and velocity sensors are listed in Table I.

The transient responses supplied to Sikorsky consisted primarily of one-half inch and one-inch step and pulse inputs in both directions for each of the four cockpit controls. Some runs also included doublet inputs. The flight conditions included: Forward (351 in.) and Aft (359 in.) CG in hover and 100 knots; and Forward (351) CG at 60 and 120-147 knots. The mechanization of the transient response

SA 1114

comparisons between flight test and the mathematical model was designed to provide the highest possible confidence in the validation. The edited flight test data provided to Sikorsky on magnetic tape were reformatted and stored in the PDP-KL10 computer memory. Test data for the pilot control inputs were separated and used as input drivers to the BLACK HAWK Simulation Model, Reference (2), for the data burst time span. The model was first trimmed to the flight conditions of the test run. The initial condition errors on the controls were then synchronized at T = 0 so that the incremental difference was being utilized to excite the simulation. In this way, initial condition errors in control position did not influence the transient response. Of sole importance, then, is the movements of the controls and these were duplicated precisely. Each simulation transient response was stored in computer memory on a data file for subsequent overlay plotting with the test data. This approach permitted a critical and direct comparison between flight and simulation time histories of up to 32 parameters. These comparison plots were than assessed qualitatively for simulation fidelity. By comparing several input magnitudes and directions of the same control for the same flight condition, the effects of contaminations, such as control hysteresis and gusts, on the assessment were minimized when viewed in terms of the consistency of discrepancies. It should be noted that in order to preserve the flight test data base, no attempt was made to alter the test data. Biases, such as those indicated by steady non-zero accelerations with corresponding zero rates, were left intact. The results of this review are summarized in Table II-1 to II-5 and selected demonstration plots are presented in Figures 1 to 8 for discussion in the next section. A discussion of the steady flight data comparison follows in the subsequent section.

1.1 Transient Response Data Comparison

It is not realistic to critique, in detail, 90 transient response comparisons. The following discussion, then, is an analysis of those which typify the general characteristic responses. From a qualitative assessment of the transient response comparison plots, it is concluded that the BLACK HAWK simulation model is a satisfactory engineering design and evaluation tool. In general, the short term response to control inputs compare well which indicates a good definition of control power. In the long term, errors do build up but the trends compare favorably with test data. This is demonstrated by the comparison data in Figures 1 to 8. All of the responses are considered acceptable. Some, however, are classified as acceptable but unsatisfactory. Those which require further improvement are identified in the following sub-sections which discuss responses to each control input. Note in Figures 1 to 8 that the model calculated data are represented by a solid line with "SAV" identified. Test data "TST" are represented by dotted lines.

SA 1114

1.1.1 Response to Longitudinal Stick Input

The calculated response to a one-inch forward longitudinal stick step input (and recovery) at 100 Kn compares favorably with test data as shown in Figures 1a to 1h. Pitching motions during the step input are acceptable, Figure 1a. The large (4 in.) input during recovery, however, generates a higher nose-up acceleration peak for the model (solid line in the figure). This characteristic - large control inputs produce larger calculated responses - is evident in all of the data reviewed. This discrepancy is attributed to the simplified second-order system simulation of the flight control system dynamic characteristics. The actual control system apparently exhibits non-linear frequency response characteristics which may be characterized by a reduced bandwidth with large amplitude control inputs.

The coupled roll motion also compares favorably with test data, Figure 1b. Coupled yaw motion agrees well during the step input, up to 4 seconds in Figure 1c. However, during the large input recovery, a short (3 second) period oscillation is induced in aircraft yaw rate and heading. The difference in directional response between model and test is considered acceptable but unsatisfactory. This is also true of: lateral velocity, Figure 1d, the associated sideslip angle, Figure 1e, and lateral translational acceleration, Figures 1f and 1h. Thus, the lateral/directional response (exhibited during the recovery) calculated by the model is acceptable but requires improvement. Model longitudinal and vertical translation motion as well as engine and rotor responses calculated by the model, on the other hand, show good agreement with test, Figures 1d to 1h.

1.1.2 Response to Lateral Stick Input

Comparison of responses to a doublet control input is an effective means of evaluating simulation fidelity. The doublet input profile with control reversals permits evaluation of control power, damping, and free-response. The calculated response to a one-inch lateral cyclic stick doublet, shown in Figures 2a to 2d, agree favorably with flight test data in high speed flight, 144 knots. Roll control power and damping are simulated reasonably well, Figure 2a. The cross-coupling effects of the lateral stick input on pitching motion is weaker on the model, however, for the initial right-stick motion, Figure 2b. The aircraft tends to pitch nose-down, whereas model pitch attitude remains stationary. The nose-up coupling with the left stick segment (which is simulated in magnitude but lagged) causes the model to drift nose-up relative to the aircraft. As a result, the aft-stick recovery action by the pilot is opposite to the model requirement so that the model pitches further nose-up. Typically, the two-inch longitudinal control recovery input generates a comparable, but slightly stronger, pitch response on the model. As with longitudinal coupling, lateral/directional coupling with the

lateral stick doublet is predicted weaker by the model. Although yaw coupling is simulated reasonably well both in period and magnitude, Figure 2c, calculated sideslip is relatively benign, Figure 2d. These small differences in cross-coupling with lateral stick between model and test might be reduced by adding (neglected) product of inertia terms to the equations of motion and thereby improving the model lateral/directional characteristics.

1.1.3 Response to Collective Stick Input

Although some of the test data are "noisy", the calculated response, in hover, to a one-inch down collective step input is considered acceptable, Figures 3a to 3d. In particular, predicted vertical and longitudinal accelerations, Figure 3d, match closely test data. Unsatisfactory responses, however, include blade lag angle in Figure 3b; rotor speed, gas governor speed, fuel flow, and engine torque in Figure 3c; and main rotor torque in Figure 3d. These variables are too responsive compared to flight test data. The simulated fuel flow variation with collective stick input is clearly too strong. This indicates that the frequency response bandwidth of the engine model is evidently too wide. Since the engine and the rotor are coupled, the unsatisfactory engine response will affect the rotor, notably rotor speed and blade lag angle. Coupling of fuel-flow with collective, in the load demand system of the engine, therefore is an area of the simulation model that requires improvement.

1.1.4 Response to Pedal Input

Predicted aircraft response to a one-half inch right pedal step input at 144 knots is acceptable, Figures 4a to 4d. Predicted yaw response trends compare reasonably well with test, Figure 4a, and longitudinal coupling correlates quite closely in spite of the longitudinal stick motion, Figure 4b. Roll coupling with pedals, however, is considered acceptable but unsatisfactory. The aircraft roll response is subdued with virtually no adverse roll with pedals, Figure 4c. The model, on the other hand, predicts more roll coupling and response. This is also true for sideslip angle, Figure 4d. Lateral/directional characteristics of the simulation in high speed flight therefore require improvement.

1.1.5 Additional Responses

Four additional response comparisons are presented in Figures 5 to 8 to demonstrate particular aspects of the simulation model validation. In high speed flight, longitudinal coupling with pedal input was predicted with reasonable accuracy, Figure 4b. In hover, however, model pitching motion is similar to the aircraft but opposite in direction, Figures 5a and 5b. The one-half inch left pedal input

SA 1114

generates an increase in tail rotor thrust. Because of the upward tail rotor tilt, the additional thrust generates a nose-down pitching moment. However, main rotor longitudinal control is coupled with pedals to minimizes this pitching motion tendency. The compensating coupling simulated in the model is apparently stronger than rigged on the aircraft.

In addition to the nonlinear frequency response characteristics discussed earlier, the aircraft control system also exhibits a control free-play nonlinearity which is demonstrated in Figure 6. A quarter-inch longitudinal stick aft-step input did not generate a response from the aircraft whereas the model did respond to the analytical input. Modelling of this control free-play nonlinearity is judged to be beyond the scope of this update effort.

On both the simulator and the aircraft, the BLACK HAWK is generally flown with, at least, SAS engaged. Accordingly, pertinent responses to longitudinal and collective inputs are presented in Figures 7 and 8 to validate model fidelity with SAS engaged. The calculated responses to a half-inch aft longitudinal stick input at 122 knots follow test data closely. A slightly higher pitch damping in the model, however, produces a smaller steady pitch rate. The correlation is good.

Calculated cockpit vertical acceleration in response to a half-inch up-collective step input with SAS-On at 140 knots also agrees with flight test, Figure 8. The apparent lag in the calculated acceleration response as well as the 2.8 HZ frequency are caused by the plotting program. This will be discussed later. In general, then, simulation fidelity in the longitudinal axis with SAS engaged is good.

1.2 Transient Response Comparison Summary

Typical responses to control inputs for various flight conditions were discussed in detail above. A general, qualitative assessment of the BLACK HAWK simulation model fidelity is summarized in Tables II-1 to II-5 for each airspeed which encompasses all the 90 time histories made available to Sikorsky. Control power and damping for each degree of freedom of the model are classifed as weak(er) or strong(er) than the aircraft. Potential areas for improvement are identified as unsatisfactory. These are further summarized as follows:

SA 1114

1. Fuel Flow

   - Response with collective input too strong

2. Blade Lagging Angle

   - Steady and vibratory amplitudes are too small
   - Response to collective inputs are too rapid, 0.3 seconds to steady state calculated versus 1.5 seconds for aircraft

3. Main Rotor Torque

   - Response to collective inputs too rapid, 0.3 seconds vs. 1.5 seconds test
   - Affects yaw and roll adversely with collective inputs

4. Inertia Coupling

   - Inertia cross-coupling is approximate

5. Damping

   - Fuselage damping is ignored which could affect unstable roots

6. Control Cross-Coupling

   - Strong adverse roll with pedals
   - Wrong signs (adverse)
     - Roll with longitudinal stick
     - Roll with collective stick
     - Pitch with lateral stick
     - Pitch with Pedals
     - Yaw with longitudinal stick
     - Yaw with collective

7. Control System Dynamics - Control Free-Play

   - Small control inputs produce a model response but no aircraft response due to control free-play.
   - Large (3 inch) and rapid inputs produce larger calculated response

SA 1114

8. Acceleration Responses

- Evidence of 2.8, 7.8, and 16 Hz frequencies, particularly roll acceleration
- Lag in vertical acceleration with collective input, SAS-On.

1.3 Steady Flight Data Comparison

Steady trimmed flight with SAS engaged was simulated on the computer model for the following flight conditions:

- Airspeed sweep - hover to 160 knots.
- Lateral/directional static stability 60, 100, 140 Kn.
- Longitudinal static stability - 60, 100, 137.5 Kn.
- Climbs and descents - 60, 100, 137.5 Kn.
- Steady left and right turns - 60, 100 Kn.
- Rotor speed sweep - 60, 100, 137.5 Kn.
- Stabilator angle sweep - 60, 100, 137.5 Kn.

The calculated results are compared with flight test data in Figures 9 to 18 and discussed in the following sections.

1.3.1 Airspeed Sweep

Data for level flight static trim for airspeeds from hover to 160 knots are compared in Figure 9. Data for the modified model are also shown. These will be discussed later. The data for the original model (now at NASA) show good agreement with test, except for pedal position and stabilator incidence angle, Figures 9b and 9c. During extensive flight tests of the BLACK HAWK at Sikorsky, stabilator angle never exceeded 40° in low-speed flight. The AEFA flight tests, however, recorded values as high as 45°. Furthermore, since calculated pitch attitude agrees with test, it is concluded that the test values are in error. This is corroborated by the data shown in Figure 10. With tail incidence (stabilator angle) held fixed at the test value, calculated pitch attitude and longitudinal stick position differ considerably from test data. Since the test values for stabilator angle are in suspect, all of the subsequent steady flight trim data were generated using the calculated values. Unless the aircraft tail rotor rigging is not within specifications, the difference in pedal position, Figure 9b, is due to the model. This difference, more than 10%, is unsatisfactory and needs improvement.

SA 1114

1.3.2 Lateral/Directional Static Stability

Comparisons between the predicted and test lateral/directional characteristics for 60, 100, and 140 knots are shown in Figures 11, 12, and 13 respectively. As with the airspeed sweep, pedal position shows least agreement with test. At 60 knots, the aircraft is flying on the back side of the power required curve. It is difficult, therefore, for the pilot to maintain trimmed flight for an extended (data taking) period of time. For this reason predicted roll angles, Figure 11a, and pitch attitudes, Figure 11b are considered acceptable and well within test data accuracy. Although lateral stick, Figure 11a, and collective, Figure 11b, show very good agreement with test, predicted longitudinal stick is about 5% aft relative to test data. This is acceptable and probably due to main rotor downwash impinging on the horizontal tail. The main rotor wake simulation in the model is considered adequate.

At 100 knots, the low horizontal tail is clear of the main rotor wake so that the predicted longitudinal characteristics in sideslip flight agree closely with test, Figure 12b. Also, at this speed flight test roll angle is more definitive with sideslip, Figure 12a. As a result, roll correlation improves with only a slight affect on lateral stick comparison. Pedal position, however, remains acceptable but unsatisfactory. This is also true for sideslip flight at 140 knots, Figure 13. Roll angle prediction agrees well with test but lateral stick compares less favorably than at lower speeds. Lateral/directional characteristics of the model in high speed flight, then, should be improved. This is consistent with the transient roll response with pedal input comparison discussed previously.

1.3.3 Longitudinal Static Stability

Comparison data for collective-fixed longitudinal static stability at 60, 100, and 137.5 knots are presented in Figure 14. Of primary interest here is the slope of the flight variables as speed is varied about the trim point. The data in Figures 14a and 14b show, in that context, that the simulation model will predict the longitudinal static stability characteristics with good accuracy. Although model pedal position is consistently right about 5%, the gradient with speed conforms with flight test. Overall, the correlation is considered good.

1.3.4 Steady Climbs and Descents

Calculated and test comparison data for steady climbs and descents at 60, 100, and 137.5 knots are presented in Figures 15a, b, and c respectively. Stabilator angle is held fixed at the calculated level

SA 1114

flight (no climb) trim value for each speed. At 60 knots, simulation of the main rotor wake impinging on the horizontal tail is approximate. This is evident by the difference between the test and calculated values for pitch attitude and longitudinal stick position, Figure 15a. Correlation of these variables, however, is considered acceptable. Although collective, main rotor power and lateral stick are predicted with better accuracy, pedal position comparison is unsatisfactory.

Typically, at the higher airspeeds, 100 and 137.5 knots, pitch attitude and longitudinal stick correlation improve, Figures 15b and 15c. Collective stick, main rotor power and lateral stick correlations are also good at these speeds within the scatter of the test data.

1.3.5 Steady Turns

Flight test data were supplied by the Army for steady turns at 60 and 100 knots. These data are compared with model calculated data in Figure 16. Flight variables are plotted in parallel for each speed as a function of roll angle, the independent variable. The calculated data for all variables shown, except pitch attitude and longitudinal stick, correlate very well with test data. As has been discussed previously, main rotor downwash and stabilator setting have a strong effect on pitch attitude and longitudinal stick position at low airspeeds. This effect is also evident in the difference between the test and calculated values of these variables. The difference is considered small and acceptable. Model prediction for turning flight, then, is considered quite good.

1.3.6 Rotor Speed Sweep

Main rotor rotational speed (Nr) was varied from 95% to 105% (100% = 27 rad/sec) in the simulation model. The calculated results are compared with flight test data for 60, 100, and 137.5 knots in Figure 17. Stabilator angle was held fixed at the 100% Nr value. As shown in the figure, the simulation model predicts quite well the variation of the flight variables with rotor speed. As in turning flight above, main rotor power, collective stick and lateral stick position calculated data correlate well with test data. Pitch attitude, longitudinal stick and pedal position predicted data are offset from the flight data. At 137.5 knots, however, longitudinal stick position shows good agreement in both magnitude and slope; and pitch attitude is acceptable within test data scatter, Figure 17a. Although calculated main rotor power is slightly higher than test at this speed, Figure 17b, the difference is attributed to the test data. Note that calculated main rotor power correlated quite closely with test data at 137.5 knots during the airspeed sweep, Figure 9c. Overall, then, the simulation model predicts the effects of rotor speed variation with acceptable accuracy.

SA 1114

1.3.7 Stabilator Angle Sweep

Calculated stabilator angle did not agree with the flight test values for the airspeed sweep, Figure 9c. It was demonstrated in Figure 10 that by using the flight test value of stabilator angle, calculated pitch attitude and longitudinal position were in error during a sideslip angle sweep at 60 knots. This is also demonstrated by the stabilator angle sweep data at 60, 100, and 137.5 knots, Figure 18. Stabilator position has a significant effect on only pitch attitude and longitudinal stick position. Accordingly, these variables are plotted in Figures 18a and 18b respectively. At the higher airspeeds, 100 and 137.5 knots, test values of stabilator position have a fixed bias, leading edge up, of about 3 degrees. At 60 knots, main rotor wake effects, actual and simulated, cause a less-uniform difference between the data. This is consistent with the previous flight variable sweeps discussed above. Calculated pitch attitude and longitudinal stick position comparison with test is consistently better in high speed flight than at 60 knots. This is also evident in the data comparison in Figure 18. The slope of these variables compare better with test data at the higher airspeeds. The slope comparison also verifies that aeroelastic deflection (if any) does not have a signficant effect on aircraft pitch attitude and longitudinal control position. At these speeds, at least, a rigid stabilator simulation is acceptable.

1.4 Steady Flight Comparison Summary

In general, the BLACK HAWK simulation model predicts steady flight trim characteristics with good accuracy. Flight test values for stabilator position appear to have a bias of about 3°. The model was therefore validated, with good results, using the predicted stabilator settings. The effects of the rotor wake on the fuselage and stabilator are accounted for by downwash correction terms in the existing model. These terms provided favorable correlation of pitch attitude and longitudinal stick position at the higher airspeeds. Several areas, primarily in lateral/directional static stability, however, could be improved. These, which could also affect transient response, include:

- Pedal variation in forward flight and sideslip.
- Roll angle with sideslip.
- Cyclic stick and pedal position with sideslip.

SA 1114

2.0 SIMULATION MODEL UPDATE

2.1 Potential Approaches

In Sections 1.2 and 1.4, correlation areas that were acceptable but unsatisfactory were delineated. Potential approaches to improve the BLACK HAWK simulation model in these areas have been formulated and include the following with identification figures:

- Revise fuel flow coupling with collective stick to improve engine response, Figure 3c.
- Incorporate updated formulation of cross-coupling inertia terms to improve adverse roll and roll response with pedal input, Figure 4.
- Revise downwash correction terms to improve pedal position correlation in sideslip flight, Figures 11 to 13.
- Incorporate first order lag in rotor simulation to improve main rotor torque and blade lag angle response to collective stick inputs, Figures 3b and 3d.
- Introduce tail rotor downwash lag and fuselage damping to improve high speed transient response, Figure 4.
- Investigate source of 2.8, 7.8, and 16 Hz frequencies in acceleration responses, Figures 1b and 3d, and 0.05 sec lag in vertical acceleration response to collective input, Figure 8.

Evaluations of these approaches, discussed below, are centered on collective/fuel flow coupling in hover and high speed lateral directional characteristics. In Figure 19 through 32, the modified model data are represented by solid lines; existing model data are shown as dashed lines; and test data "TST" are expressed as dotted lines.

2.2 Evaluation of Model Revisions

2.2.1 Collective/Fuel-Flow Coupling In Hover

The frequency response bandwidth of the engine simulation is too wide. This is evident by the engine variables responses to a collective stick step input in hover, Figure 19. In particular, fuel flow response is too rapid. As a result, both rotor speed and yaw acceleration calculated response to the input are opposite to the aircraft response, Figure 19a and 19b.

SA 1114

In the engine simulation, gas governor speed is controlled by fuel flow. In order to anticipate the power changes associated with collective stick motion, fuel flow is coupled with collective through the Load Demand Spindle (LDS). Fuel flow is controlled, in part, by the output of the load demand spindle cam. The cam is rotated, through a static droop compensator, by a bell crank in the collective mechanical flight control system. The aircraft system, however, also includes fuel metering lags and nonlinearities such as hysteresis and control free-play in the LDS system.

In order to account for these effects without undue complexity, a first-order lag was incorporated at the output of the load demand spindle cam.

$$LDS\ (new) = LDS\ (old) * (1/(TS+1))$$

A significant improvement in correlation with test was obtained with a time constant, T = 0.75 seconds, as shown in Figure 20. Some of the improvements include:

- Initial rotor speed and yaw acceleration response to collective are now in the proper direction.
- Main rotor blade lag angle and torque as well as all engine variables have rise times comparable to test data.

The sharp increase in calculated fuel flow at 2 seconds, Figure 20a, is attributed to simplifications in the Electrical Control Unit (ECU) of the linear engine simulation model. Since the fuel flow increase does not significantly affect helicopter response, it is considered acceptable. Therefore, all unsatisfactory areas associated with collective stick inputs will be eliminated by incorporating a first order lag with a 0.75 second time constant at the output of the load demand system spindle cam of the model. To do this, the equation for load demand spindle output on Page 5.6-11 of Reference (2) is changed to read as follows:

$$NGGLDS = f(LDSCAM, XC) * (1/((TXC)S + 1))$$
$$\text{where } TXC = 0.75$$

2.2.2 High Speed Lateral/Directional Response

2.2.2.1 Main Rotor Yaw Moment

In high speed flight (140 knots) main rotor torque is high. It is also a principal contributor to the yaw moment equation. In the rotor module, Page 5.1-36 of Reference (2), yaw moment of the main rotor is defined in terms of engine torque, QHEG. The only torque,

SA 1114

about the vertical axis, reacted by the fuselage is main rotor torque, QHBMR. Therefore, QHEG should be replaced by QHBMR in the transformation matrix. Although this change should be incorporated into the model, its implementation had no substantial effect on helicopter response to a pedal input in high speed flight, Figure 21. A check on response to a collective input in hover, Figure 22, also indicates no substantial effect on helicopter or engine response. In hover and high speed flight, for the conditions tested, the engine governor matches power available (engine torque) with power required (rotor torque) quite closely.

2.2.2.2 Main Rotor Downwash Correction

From analysis of rotor-on wind tunnel data and UH-60A flight test data, Sikorsky developed downwash correction terms to the applied aerodynamic forces to account for main rotor wake swirl impinging on the empennage. These are programmed in the simulation model and are listed on Page 5.10-19 of Reference (2). Some of these terms were modified as an approach to improving the model lateral directional characteristics.

As an initial step, however, formulations for the flight control system and control coupling in the simulation model were verified to ensure that they conform with specified rigging data. Secondly, the tail rotor control simulation and aircraft rigging were compared with Sikorsky specifications. Tail rotor rigging data, Figure 23, verify that the test aircraft was rigged to specifications. Also, the simulation provides an acceptable linear model of tail rotor coupling with main rotor collective.

With the control system validated, the downwash correction equations were then modified to improve correlation of lateral stick and pedals in sideslip flight at 140 knots, Figure 13a. The modified equations are listed in Appendix I. The results obtained by implementing these modifications, as well as incorporating main rotor torque in the yaw equation, are shown on Figure 13 as dashed lines. Introduction of a new yaw moment correction term and revision of the roll moment with sideslip terms were effective in improving correlation of lateral stick and pedals. Since the data were "force-fit" at 140 knots and since the force and moment corrections are functions of dynamic pressure, the modifications were evaluated at the lower airspeeds.

The improved correlation of lateral stick and pedals with test was maintained at 100 knots, Figure 12a. Although the slope of roll angle with sideslip was increased slightly, predicted roll angle is considered acceptable and is within the accuracy of the test data. At 60 knots, Figure 11a, dynamic pressure is low and the effects of the modification on the lateral/directional characteristics are small. This is also true for the two longitudinal parameters, pitch attitude and longitudinal stick, at both speeds, Figures 11b and 12b.

SA 1114

The effect of dynamic pressure is also evident in the level flight static trim data shown in Figures 9a to 9c. Pedal position now compares favorably with the aircraft data at high speeds. Longitudinal stick and pitch attitude comparison are also improved. The associated increase in right stick is not considered significant.

The transient response to a pedal input in high speed flight is also improved by the modified downwash correction terms, Figure 24. Peak roll rate and roll angle are more than halved with no degradation in pitching motion. Yaw motion and sideslip are also reduced and match flight test data in the short term. Introduction of these empirical downwash correction modifications, then, can improve the simulation model fidelity, particularly in high speed flight.

2.2.2.3 Tail Rotor Downwash Lag

Tail rotor thrust is a significant contributor to helicopter lateral/directional characteristics. A potential approach to improving adverse roll and subsequent roll motion following a pedal input is to incorporate aerodynamic lag in development of tail rotor downwash. Accordingly, a first order lag was introduced into the tail rotor equations similar to the main rotor. The equation for tail rotor downwash on Page 5.4-7 of Reference (3) was modified to read:

$$DWSHTR = f(MUZTR, THETTR, etc) * (1/((TDW)\ S + 1))$$

Where TDW = tail rotor downwash lag time constant. As shown in Figure 25a, a time constant of 0.050 seconds was effective in improving the initial yaw acceleration and rate response to the pedal input. Its effect on the long term response, however, is negligible, Figure 25b. Tail rotor downwash and thrust did not vary appreciably during the roll and yaw motion. The tail rotor, then, did not participate significantly in the helicopter motion associated with the pedal push and hold input at 140 knots. In particular, tail rotor downwash lag has a negligible effect on roll reversal accompanying the initial pedal motion.

2.2.2.4 Tail Rotor Downwash on Vertical Tail

Interaction between the tail rotor and vertical tail is incorporated in the simulation in the form of tail rotor blockage. This is shown on Page 5.4-8 of Reference (2). Below 30 knots (VBVTTR), tail rotor downwash generates a sideforce (download) on the vertical tail opposite to tail rotor thrust. The net effect is an apparent reduction in tail rotor thrust. Above 30 knots, the tail rotor download is considered negligible so that the net force is due entirely to tail rotor thrust.

SA 1114

Since the tail rotor is only 14 inches from the vertical tail, tail rotor downwash could influence the flow field at the vertical tail, even in high speed flight. At the higher airspeeds, a small change in vertical tail angle of attack (sideslip) induced by tail rotor downwash can produce a measurable side force and thereby influence lateral/directional characteristics of the helicopter.

This interactional aerodynamic effect between the vertical tail and tail rotor in forward flight can be incorporated in the model by means of a tail rotor downwash interference velocity on the vertical tail. It is added to the generalized interference velocity term VYIV1 on Page 5.3-11 of Reference (2). It is defined, similar to main rotor downwash interference velocity, as:

$$VYTRV1 = EKTRVT * DWSHTR * OMEGTR * RTR$$

where EKTRVT is the tail-rotor downwash coefficient. A value of 1.2 was selected for evaluation. Thus, the interference velocity at the vertical tail is assumed to be 1.2 times the downwash velocity at the tail rotor center.

As shown in Figure 26, introduction of tail rotor downwash interference on the vertical tail does not appreciably alter the helicopter response to a pedal input. It primarily influences static trim characteristics. Before its introduction, Figure 25, trim pedal position compared closely with test. After its introduction, calculated trim pedal position shifted to the left about one-half inch, Figure 26.

The primary change in tail rotor downwash occurs in the short term during the pedal input. In the first second following this input, tail rotor interference reduced yaw rate response to improve correlation. Pitch rate response, however, was also reduced and correlation was not improved, Figure 26. In the long term, as discussed above, tail rotor downwash does not vary appreciably. Its interaction with the vertical tail, then, will not significantly affect the long term transient response when pedals are held fixed. Sideslip angle is more important than tail rotor downwash on vertical tail angle of attack.

2.2.2.5 Horizontal Tail Roll Damping

The large (30 ft/sec) peak roll rate predicted by the existing model indicates a potential deficiency in roll damping. The rotor, horizontal tail, and vertical tail all contribute to roll damping, with the main contribution coming from the rotor. Although the horizontal tail contribution from conventional tails is small and often neglected, unusually large horizontal tails can provide significant roll damping. Since the UH-60A horizontal tail is relatively large (14.38 ft. span), it might be providing measurable damping on the aircraft.

SA 1114

Roll rate is used to calculate local velocity and angle of attack at the horizontal tail in the simulation model. However, the tail aerodynamic center is located in the plane of symmetry (BLHT = 0) so that roll rate does not directly produce a roll moment. A separate equation for horizontal tail roll moment due to roll rate was developed using the UH-60A geometry and Section 7.1.2.2 of Reference (3). The resulting roll damping derivative was reduced to the following equation:

$$LPLADD = (-1606)*(QFRE/VXB)*p$$

which was programmed in the downwash correction module. The transient response to the pedal input was then calculated and the results are compared in Figure 27. Tail rotor interference was not included in this calculation run. However, the revised main rotor downwash correction terms, which were included, reduced the roll response so that the horizontal tail contribution to roll damping is negligibly small. A comparison of Figure 27 with 25b shows no significant difference. It was reasonable, then, to neglect the horizontal tail roll damping during the simulation model development. Its potential for improving the simulation model is negligible.

2.2.2.6 Updated Product of Inertia Terms

Implicit in the equations of motion in the existing model, Page 5.10-6 of Reference (2), is the assumption that the helicopter center of gravity is in the plane of symmetry. This is a reasonable assumption for a symmetrically loaded UH-60A. On the test aircraft lateral CG offset was less than 0.25 inches. For asymmetrical loads, ejection of an auxiliary tip tank for example, this assumption is invalid.

The existing moment equations permit a tilt of the X-Z principal inertial axes relative to the corresponding body axes by including the product of inertia IXZ. Lateral tilt is ignored by the assumption that IXY and IYZ products of inertia are both zero. This simplification reduces the coupling of the moment equations of motion and reduces simulation computing time with no significant loss of accuracy.

Since the UH-60A is flown, as a minimum, with SAS engaged, the transient responses to gusts and control inputs are mild, Figures 7 and 8. The angular rates are small and their products are not significant. Product of inertia terms, then, have a negligible effect on the transient response, SAS-On. With SAS disengaged, however, large transient rates can be developed so that inertia coupling may be significant.

SA 1114

An updated formulation of the equations of motion which includes all of the product of inertia terms was recently developed by Sikorsky Aircraft. These fully-coupled equations are listed in Appendix II. The simulation was revised to incorporate these equations with the following representative product of inertia values (in slug-ft^2 units):

IXZ = 1882.0	(no change)
IXY = - 213.0	(added)
IYZ = - 66.0	(added)

The transient response to the pedal input was then calculated and the comparative results are shown in Figure 28. All modifications discussed above were retained except for horizontal tail roll damping. The additional products of inertia IXY and IYZ are small (CG offset was assumed zero) and the angular rates are relatively small so that no significant inertial coupling occurs in this transient response. For this symmetrical loading application, then, the existing simulation model is adequate. As a general purpose engineering simulation model, however, it is limited because it cannot be used for asymmetric loading applications.

The revised inertia coupling did not appreciably affect the calculated adverse roll during the pedal input, Figure 28. The benign response measured on the aircraft may be indicative of a steeper tilt of X-Z inertial axes so that the X inertial axis passes closer to the tail rotor. Accordingly, the product inertia IXZ was increased 50% from 1882.0 to 2823.0. Even with this new value, the simulation model consistently predicts an adverse roll, Figure 29. Also, the increased IXZ value did not significantly alter the overall transient response. In this instance, then, tilt of the X-Z principal axes of inertia is not a critical mass-property parameter. The angular acceleration and the products of the associated rates are small enough to minimize inertial coupling effects.

The updated formulation of the moment equations of motion did not significantly influence the calculated transient response to a pedal input in high speed flight. However, the revised euqations, listed in Appendix II, should be incorporated in the UH-60 engineering simulation model for future use. They will permit simulation of lateral CG offsets which cannot be done with the existing model.

2.2.2.7 Updated Model

A complete updated model was assembled. It includes the following modifications:

SA 1114

- Calculated Stabilator Angle
- Collective LDS Lag
- Main Rotor Torque in Yaw Moment Equation
- Revised Downwash Correction
- Updated Equations of Motion
- Tail Rotor Downwash Lag
- Tail Rotor Downwash on Vertical Tail

The predicted response to the pedal input is compared with test and with the existing model in Figure 30. Correlation is improved, in general, by these modifications, particularly initial yaw rate and all of the roll responses. Peak pitch rate, however, is reduced. Although adverse roll is still strong, the overall predicted helicopter response, on the whole, is considered satisfactory.

As an additional check, the response of the updated model to a pedal pulse input at 100 knots was calculated. A comparison of the results are shown in Figure 31. The improvement in simulation fidelity at this speed is similar to the gains obtained at 144 knots. Although the predicted roll motion is reduced, adverse roll is still strong. The strong calculated roll persists even though the initial yaw response is reduced Figure 31a. Tail rotor downwash interference on the vertical tail is apparently too strong at this speed. The net result is that heading (yaw angle) correlation is not improved Figure 31b. The reduced pitch and roll rates, however, result in favorable comparison of pitch and roll attitude. The primary attribute of the updated model, then, is an improved correlation with test for roll response to a pedal input in high speed forward flight.

2.2.3 Variable Frequencies In Model Acceleration Time Histories

Three frequencies (2.8, 7.8, and 16 Hz) appear in the calculated responses of all accelerations. The 2.8 Hz frequency is clearly evident in roll acceleration, Figure 1b for example. The 2.8 and 7.8 Hz frequencies are fictitious and result from aliasing by the plotting program.

At 100% rotor speed, rotor angular velocity is 27.0 rad/sec so that the one-per-rev (1P) frequency is 4.3 Hz and, with four blades, the b-per-rev (bP) frequency is 17.2 Hz. In-plane harmonic forces in the rotating rotor hub are transmitted to the fuselage as harmonic forces with a steady component and components that are integral multiples of the bP frequency (NbP). Thus, the only high frequency that should appear in the time history plots is on the order of 17.2 Hz, depending on actual rotor speed.

SA 1114

The simulation model was run with a duty cycle of 0.010 seconds. For a nine second run time, 900 points were calculated for each variable. The plotting program, however, is limited to storing a maximum of 300 points per variable. Thus, calculated data points were selectively ignored to compress the data file. As a result, the time interval between data points for the stored (plot) file is longer than the calculated duty cycle. The data for these BLACK HAWK runs were stored with 0.03, 0.04, and 0.05 seconds time intervals, depending on the total run time.

The aliasing equation and Figure 2, both of Reference (4), indicate that the 17.2 Hz frequency can appear as follows:

Time Interval (sec)	Aliased Frequency (Hz)
.03	16.1
.04	7.8
.05	2.8

which correspond to the observed frequencies in the figures. For further proof, the run time for the pedal input transient response at 140 knots was reduced to 3 seconds. The time interval in the resulting plot file matched the computing increment of 0.01 seconds. The corresponding time history plots of angular acceleration, Figure 32a, show that the 17.4 Hz (101% rotor speed) frequency is reproduced correctly. At this high frequency, importantly, the correct accelerations integrate into relatively small rates, Figure 32b. A comparison of the angular rates with and without aliasing, Figures 32B and 30A, shows that aliasing has no significant effect on rates. They were calculated by integrating the "true" bP frequency response. Aliasing, then, is introduced only on the small-amplitude, high frequency component of the plotted rate data.

Calculated vertical acceleration response to a collective input at 140 knots with SAS engaged, Figure 8, has a strong 2.8 Hz frequency and lags test by about 0.05 seconds. In hover, Figure 3d, with SAS off and a 7.8 Hz frequency present, there is no lag. This trend was noted in the other collective responses. Calculated vertical acceleration tends to lag test data when a relatively strong 2.8 Hz frequency is present. The lag in Figure 8, then, is considered to be caused by aliasing in the plotted data. It is not related to SAS or to airspeed.

Of importance is the fact that aliasing effects occur only in the output plotted data and are minimal in rate and attitude data. The test runs were simulated using a 10 millisecond duty cycle which is more than adequate for the fundamental, bP, frequency. For these reasons rate and attitude response data (instead of acceleration) were used to assess simulation model fidelity.

SA 1114

3.0 RECOMMENDED MODEL UPDATES

Potential approaches were assessed as means of improving unsatisfactory areas of correlation of the BLACK HAWK simulation model with test data. Although all of the approaches improve the accuracy of the model, some are more effective in improving correlation for the flight conditions investigated. Recommended modifications of the existing model to create a more descriptive and representative simulation for engineering purposes are as follows in their order of priority:

1. Substitute main rotor torque, QHBMR, for engine torque, QHEG, in the main rotor moment matrix.

2. Introduce a first order lag with a 0.75 second time constant at the output of the LDS/collective system of the engine simulation.

3. Update the moment equations of motion to include additional product of inertia terms and lateral CG offset.

4. Introduce a first order lag with a 0.05 second time constant at the calculation of tail rotor downwash, DWSHTR.

5. Modify downwash correction terms.

6. Introduce tail rotor downwash interaction with the vertical tail in forward flight.

Substitution of main rotor torque for engine torque, Item 1, is important for accuracy with the engine engaged (powered flight). With the engine simulation disengaged (autorotation) the existing model correctly uses main rotor torque in the main rotor moment matrix. Introduction of the LDS/collective lag, Item 2, significantly improved the correlation of transient response to collective inputs. These two modifications are simple but important.

The existing equations of motion which use only the IXZ product of inertia are adequate for simulation of symmetrical loading conditions with trivial helicopter CG offsets from the plane of symmetry. The updated equations in Appendix II, Item 3, are applicable to any helicopter and will permit simulation of any loading condition.

The first order lag on tail rotor downwash, Item 4, will improve the short term yaw motion response correlation. For the conditions investigated, tail rotor downwash did not vary appreciably so that the long term (pedals fixed) effects were minimal. This lag is therefore more important in maneuvering flight.

SA 1114

The existing correction terms for main rotor downwash interaction with the empennage were developed from correlation studies with UH-60A BLACK HAWK flight tests conducted at Sikorsky. Correlation of the existing model with the AEFA test data was improved (lateral/directional stability at 140 knots) by modifying some of the terms. Since the correlation forces and moments are functions of dynamic pressure, the improvement gains are small at 60 knots. In high speed flight, 140 knots, the roll response to a pedal input was significantly reduced and improved correlation. The modifications to the downwash correction terms, however, are empirical and are based on the limited AEFA data. For this reason incorporation of Item 5 is given a low priority.

Tail rotor downwash interaction with the vertical tail is simulated in the existing model at low airspeeds (0-30 knots). It can be incorporated for higher airspeeds, Item 6, by introducing an interference velocity on the vertical tail in terms of tail rotor downwash. In high speed flight, 140 knots, trim pedal position, at least, is changed on introduction of this modification. The change in control position indicates that the adequacy of the downwash correction terms, existing and modified, have to be verified. Also, the downwash ratio factor, EKTRVT = 1.2, implies a strong deflection or entrainment of the flow field at the vertical tail. Additional studies are required to substantiate this value as well as this method of simulating tail-rotor/vertical-tail interactional effects. For this reason, implementation of this modification, Item 6, is placed last in order of priority.

SA 1114

TABLE I

ACCELERATION AND VELOCITY SENSOR LOCATIONS

USAAEFA Project No. 79-24 Black Hawk S/N 77-22716

Nose Accelerometer (PS2)

FS	178	
BL	- 10	(Port)
WL	215	

CG Accelerometer (PS3)

FS	389	
BL	- 31	(Port)
WL	207.7	

Translation Velocity (PS4)

FS	248	
BL	70	(St'b'd)
WL	265	

TABLE II.
BLACK HAWK SIMULATION MODEL
COMPARISON WITH FLIGHT TEST

AEFA TAPE BHAWK 2&8

HOVER

DEGREE OF FREEDOM	CONTROL POWER				DAMPING	
	LATERAL CYCLIC	LONG. CYCLIC	PEDALS	COLLECTIVE	PITCH	ROLL
ROLL		US ADVERSE		STRONG		US WEAK
PITCH	US ADVERSE		US ADVERSE	US STRONG	US WEAK	
YAW			WEAK	US ADVERSE		
LONG.		STRONG	WEAK	STRONG		
LATERAL	WEAK		WEAK			
VERTICAL	STRONG		WEAK			

NOTE: US = UNSATISFACTORY AND NEEDS IMPROVEMENT

TABLE II-
BLACK HAWK SIMULATION MODEL
COMPARISON WITH FLIGHT TEST

AEFA TAPE BHAWK 5

60 KNOTS

DEGREE OF FREEDOM	CONTROL POWER				DAMPING	
	LATERAL CYCLIC	LONG. CYCLIC	PEDALS	COLLECTIVE	PITCH	ROLL
ROLL		US STRONG	US STRONG			
PITCH	US STRONG RECOVERY	US STRONG	US STRONG RECOVERY	US STRONG RECOVERY		
YAW	WEAK	US ADVERSE		ADVERSE		
LONG.		STRONG	STRONG	WEAK		
LATERAL	WEAK		WEAK			
VERTICAL				STRONG		

NOTE: US = UNSATISFACTORY AND NEEDS IMPROVEMENT

SA 29 REV. H

TABLE II-
BLACK HAWK SIMULATION MODEL
COMPARISON WITH FLIGHT TEST

AEFA TAPE BHAWK 4&7

100 KNOTS

DEGREE OF FREEDOM	CONTROL POWER				DAMPING	
	LATERAL CYCLIC	LONG. CYCLIC	PEDALS	COLLECTIVE	PITCH	ROLL
ROLL		STRONG	US STRONG			
PITCH	US ADVERSE	STRONG	US STRONG			
YAW				ADVERSE		
LONG.			STRONG			
LATERAL	WEAK	STRONG				
VERTICAL	US PITCH COUPLING		STRONG			

NOTE: US = UNSATISFACTORY AND NEEDS IMPROVEMENT

SA 29 REV. H

TABLE II-
BLACK HAWK SIMULATION MODEL
COMPARISON WITH FLIGHT TEST

AEFA TAPE BHAWK 3

120 - 140 KNOTS

DEGREE OF FREEDOM	CONTROL POWER				DAMPING	
	LATERAL CYCLIC	LONG. CYCLIC	PEDALS	COLLECTIVE	PITCH	ROLL
ROLL	STRONG LARGE INPUTS	US STRONG	US STRONG ADVERSE - ROLL	US ADVERSE (QMR)		WEAK
PITCH	ADVERSE	STRONG		US WEAK	STRONG	
YAW	WEAK	US ADVERSE	US WEAK @120 STRONG @140	US ADVERSE (QMR)		
LONG.		STRONG RECOVERY		WEAK		
LATERAL	WEAK					
VERTICAL		WEAK				

NOTE : US = UNSATISFACTORY AND NEEDS IMPROVEMENT

TABLE II-
BLACK HAWK SIMULATION MODEL
COMPARISON WITH FLIGHT TEST

AEFA TAPE BHAWK 6

145-150 KNOTS

DEGREE OF FREEDOM	CONTROL POWER				DAMPING	
	LATERAL CYCLIC	LONG. CYCLIC	PEDALS	COLLECTIVE	PITCH	ROLL
ROLL		US STRONG RECOVERY	US STRONG ADVERSE ROLL	STRONG (QMR)		
PITCH	US STRONG	US STRONG ON RETURN		US WEAK		
YAW	WEAK	WEAK	WEAK-LT STRONG-RT	ADVERSE (QMR)		
LONG.				WEAK		
LATERAL	WEAK					
VERTICAL		US WEAK IN PULL				

NOTE: US = UNSATISFACTORY AND NEEDS IMPROVEMENT

ORIGINAL PAGE IS
OF POOR QUALITY

Figure 1a

BLACKHAWK - NASA STUDY 8-DEC-82 13:07 (1/8)

AEFA TEST TAPE BHAWK4 8/18/82
FLT 45A RUN 17 100KTS LONG. INPUT

VKT	99.998644	WEIGHT	16480.000	FSCG	359.59999	IH1	7.8999999
XA	5.2525152	XB	4.1226774	XC	4.8625791	XP	3.07813388
THETAB	.452576E-1	PHIB	0.	OMGRAT	1.0037036	GGRPM	89.872973

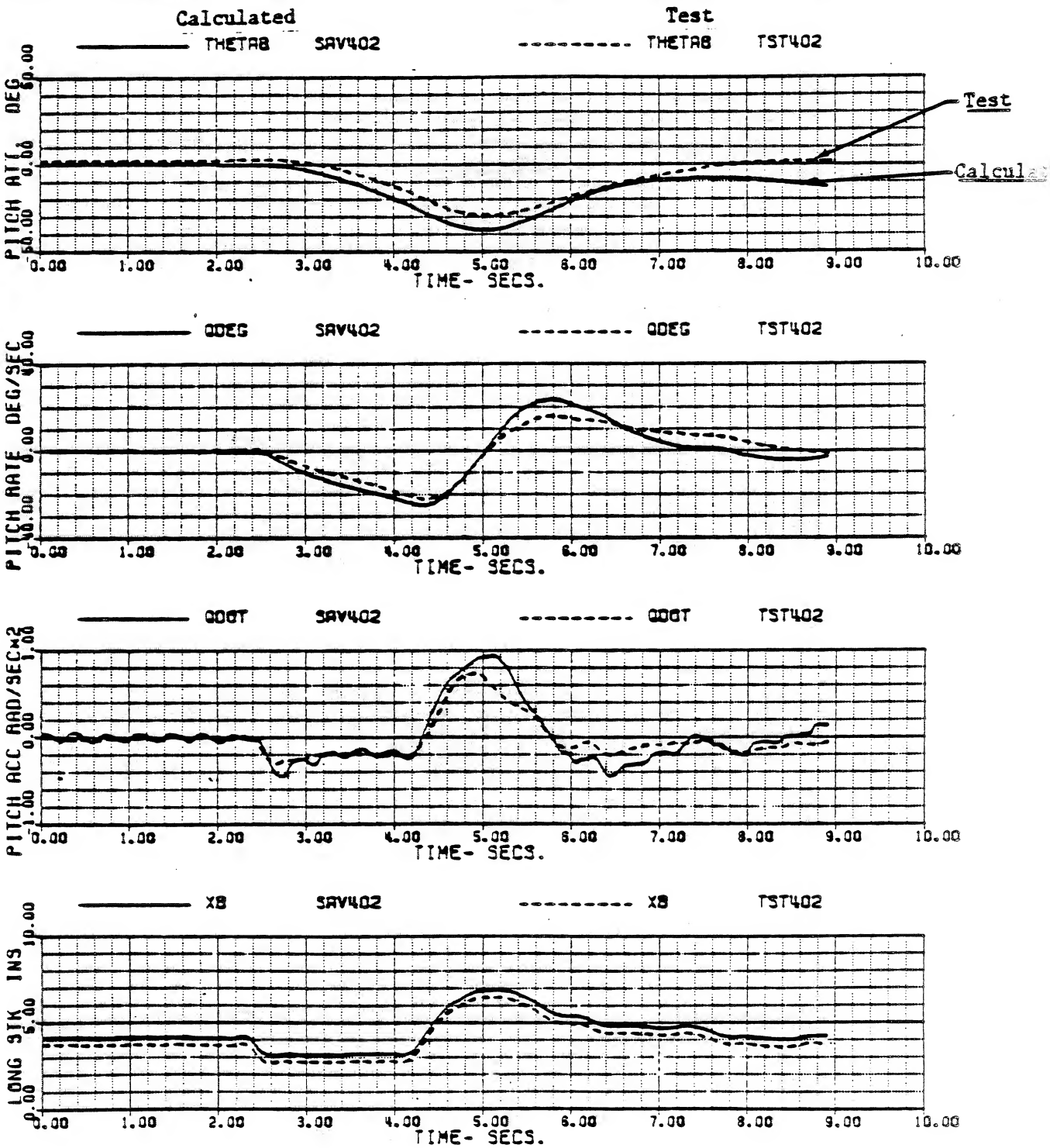

19:19
10-DEC
TST402
.PCD
SAV402
.DAT

Figure 1b

BLACKHAWK - NASA STUDY 8-DEC-82 13:07 (2/8)

AEFA TEST TAPE BHAWK4 8/18/82
FLT 45A RUN 17 100KTS LONG. INPUT

VKT	99.998644	WEIGHT	16480.000	FSCG	359.59999	IH1	7.8999999
XA	5.2525152	XB	4.1226774	XC	4.8625791	XP	3.0781338
THETAB	.452576E-1	PHIB	0.	CMGRAT	1.0037036	GGRPM	89.872973

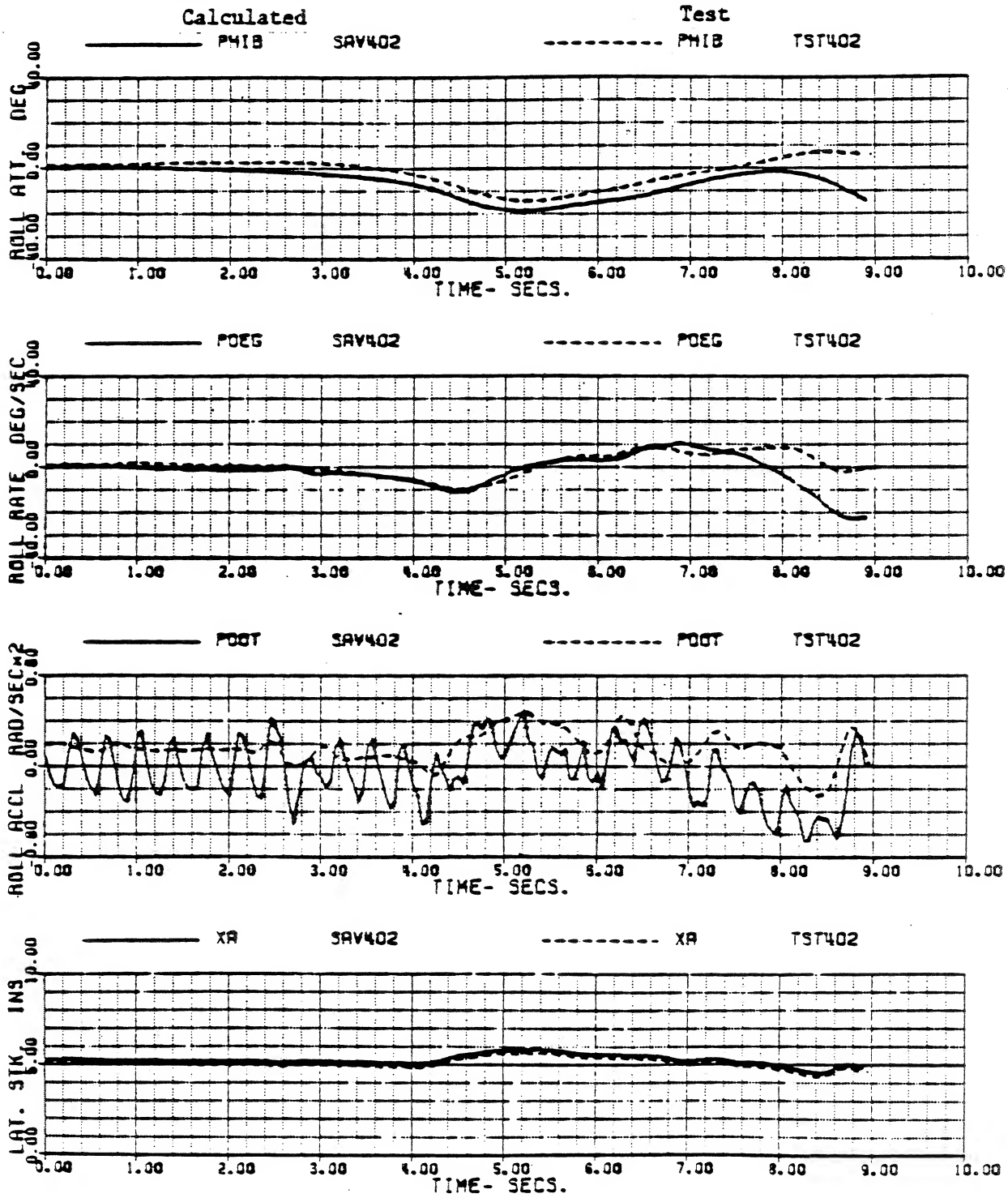

SA 1114

19:13
10-DEC
TST402
.PCD
SAV402
.DAT

Figure 1c

BLACKHAWK - NASA STUDY 8-DEC-82 13:07 (3/8)

AEFA TEST TAPE BHAWK4 8/18/82
FLT 45A RUN 17 100KTS LONG. INPUT

VKT	99.998644	WEIGHT	16480.000	FSCG	359.59999	IH1	7.8999999
XA	5.2525152	XB	4.1226774	XC	4.8625791	XP	3.0781338
THETAB	.4525768-1	PHIB	0.	OMGRAT	1.0037036	GGRPM	89.872973

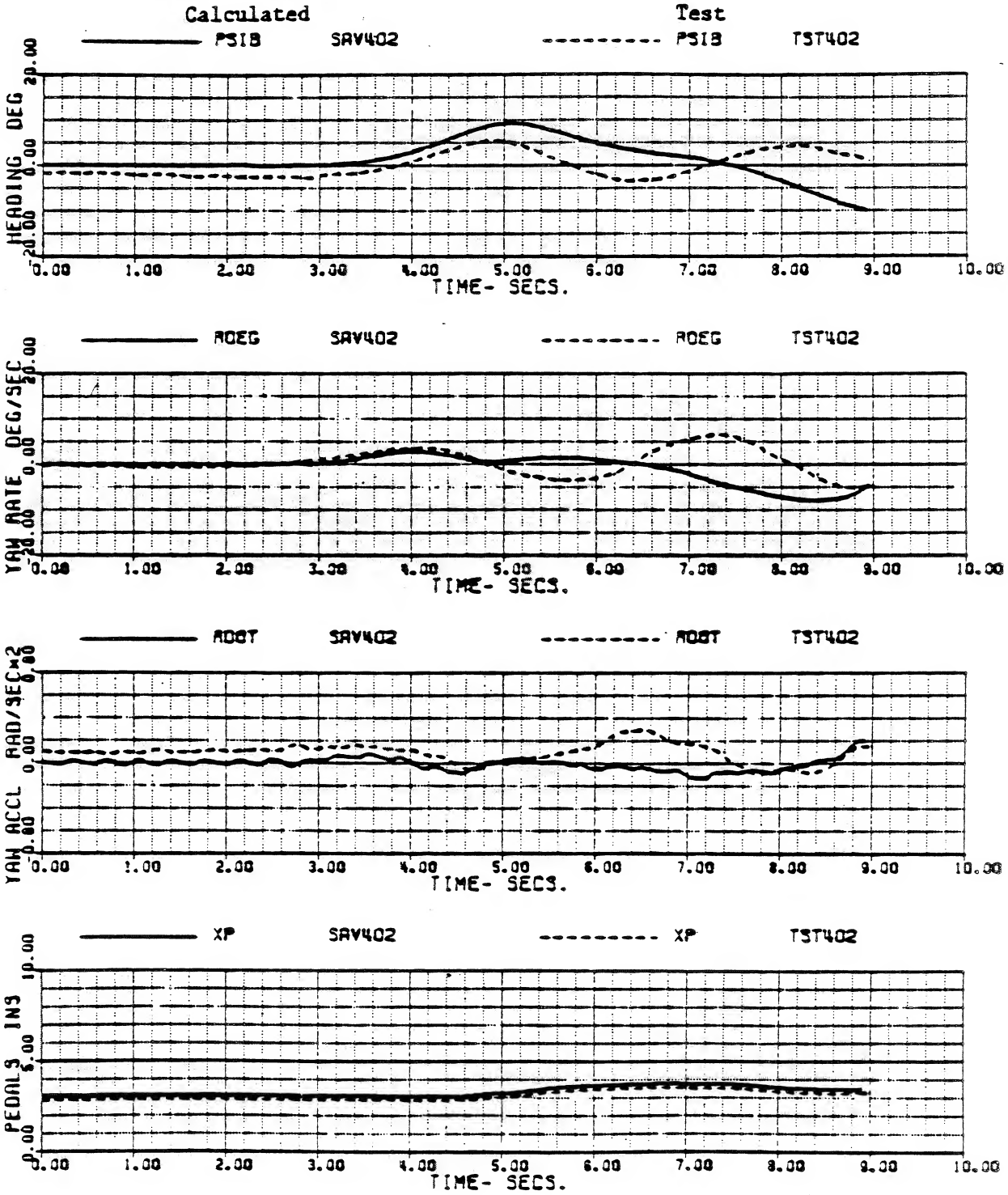

SA 1114

19:13
10-DEC
TST402
.PCD
SAV402
.DAT

Figure 1d

BLACKHAWK - NASA STUDY 8-DEC-82 13:07 (4/8)
AEFA TEST TAPE BHAWK4 3/18/82
FLT 45A RUN 17 100KTS LONG. INPUT

VKT	99.998644	WEIGHT	16480.000	FSCG	359.59999	IH1	7.8999999
XA	5.2525152	XB	4.1226774	XC	4.8625791	XP	3.0781338
THETAB	.452576E-1	PHIB	0.	OMGRAT	1.0037036	GGRPM	89.872973

Calculated Test

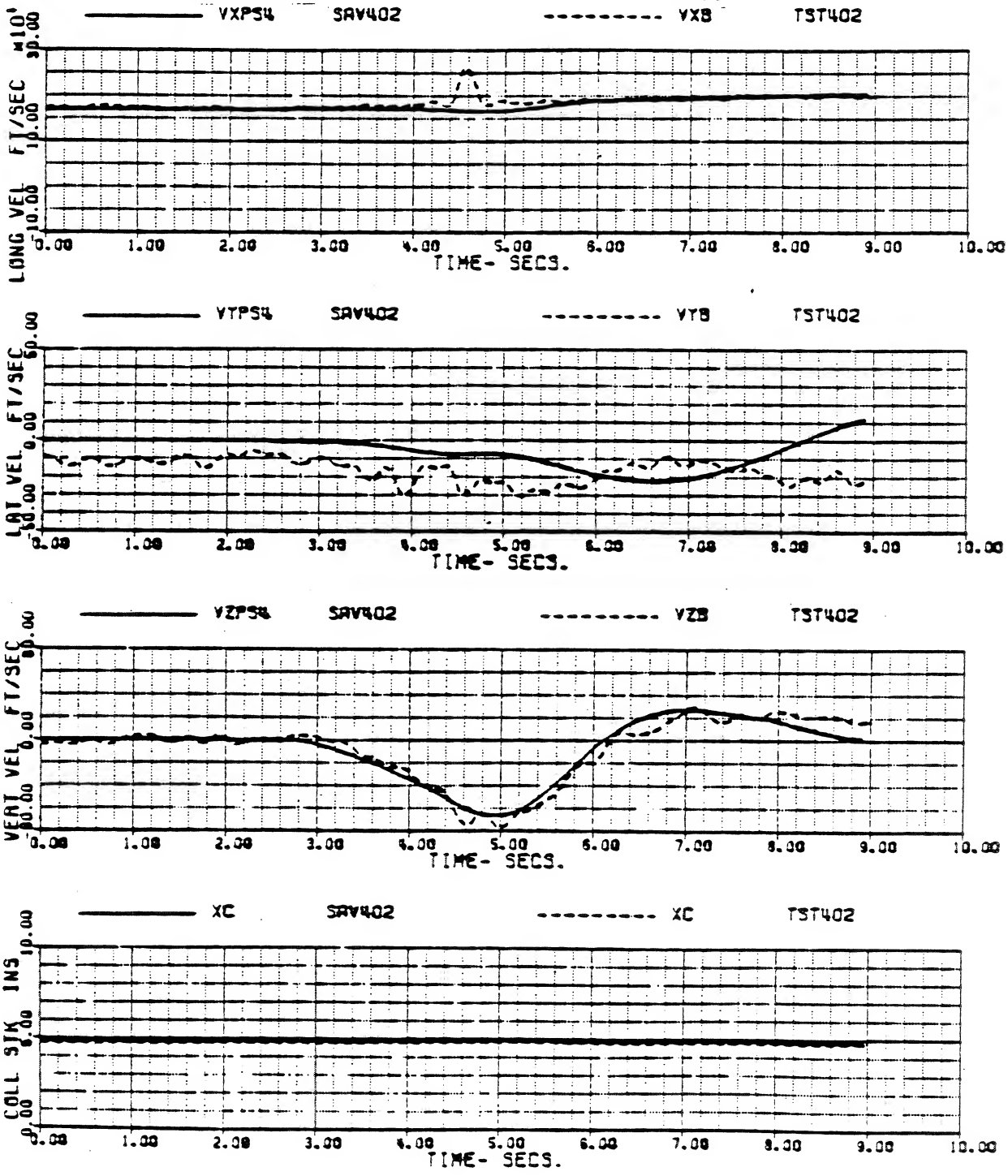

19:13
10-DEC
TST402
.PCD
SAV402
.DAT

Figure 1e

BLACKHAWK - NASA STUDY 8-DEC-82 13:07 (5/8)
AEFA TEST TAPE BHAWK4 8/18/82
FLT 45A RUN 17 100KTS LONG. INPUT

VKT	99.998644	WEIGHT	16480.000	FSCG	359.59999	IH1	7.8999999
XA	5.2525152	XB	4.1226774	XC	4.8625791	XP	3.0781338
THETAB	.4525768-1	PHIB	0.	OMGRAT	1.0037036	GGRPM	89.872973

Calculated Test

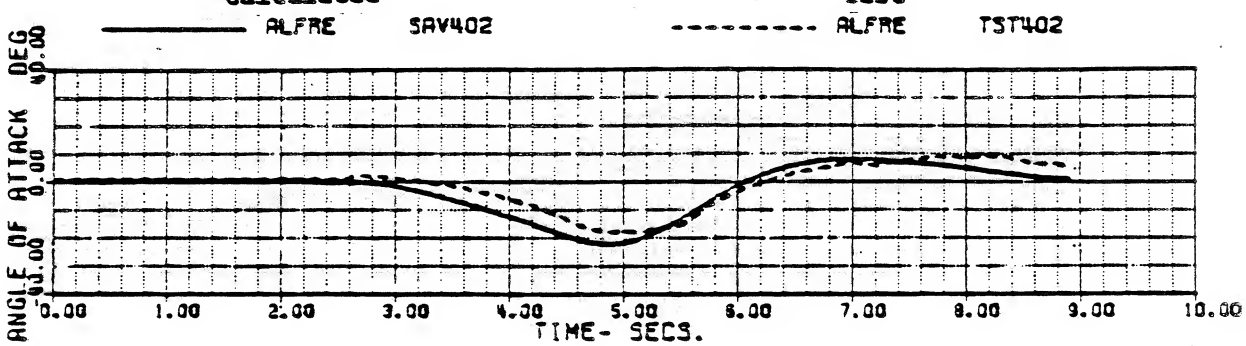

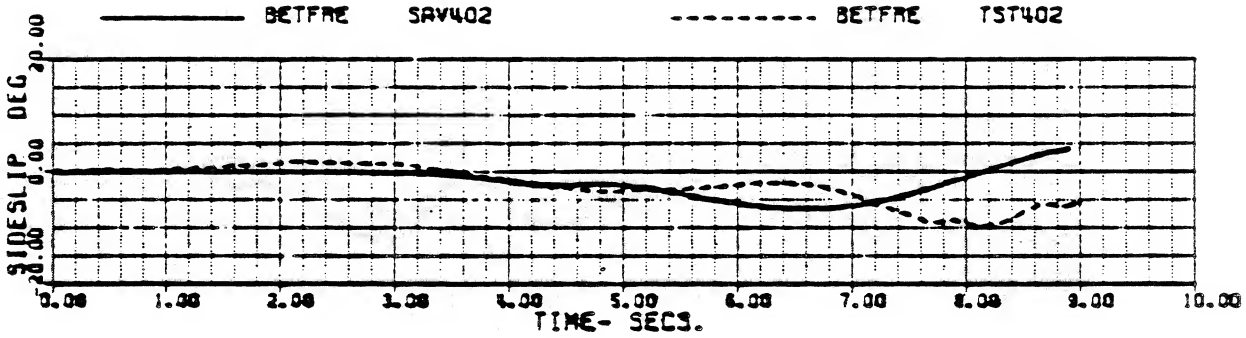

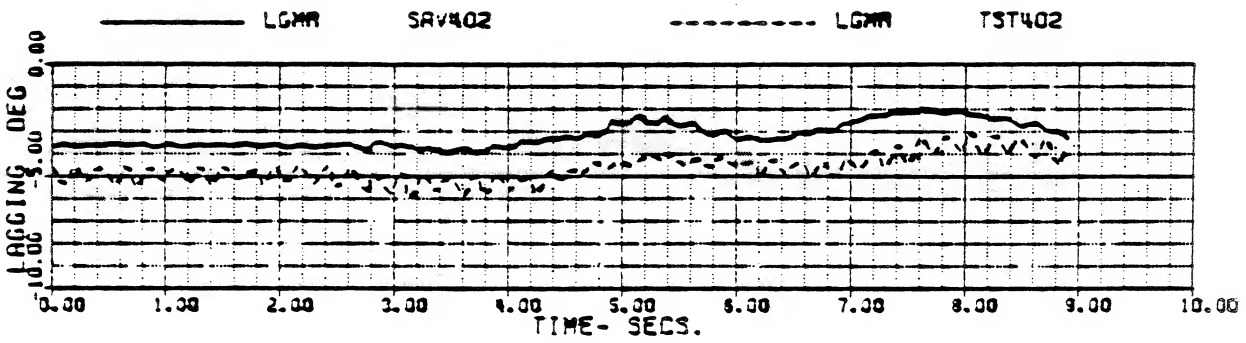

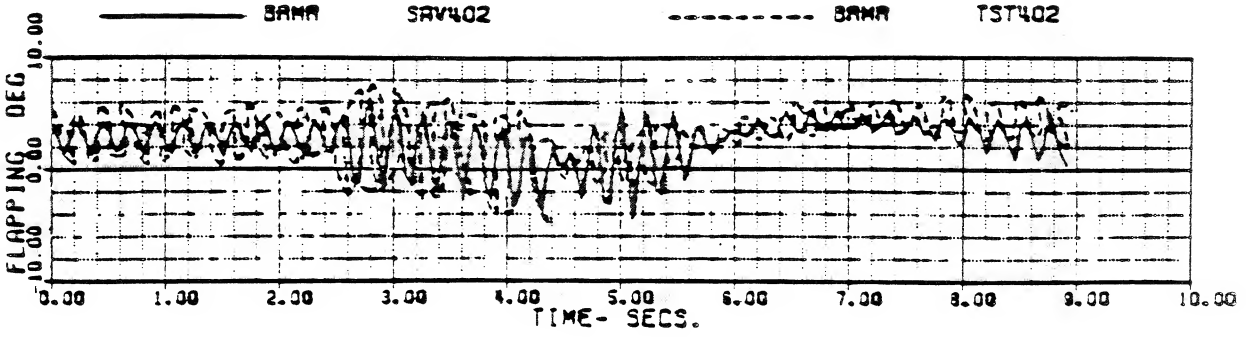

SA 1114

19:13
10-DEC
TST402
.PCD
SAV402
.DAT

Figure 1f

BLACKHAWK - NASA STUDY 8-DEC-82 13:07 (6/8)

AEFA TEST TAPE BHAWK4 8/18/82
FLT 45A RUN 17 100KTS LONG. INPUT

VKT	99.998644	WEIGHT	16480.000	FSCG	359.99999	IM1	7.8999999
XA	5.2525152	XB	4.1226774	XC	4.8625791	XP	3.0781338
THETAB	.452576E-1	PHIB	0.	OMGRAT	1.0037036	GGRPM	89.872973

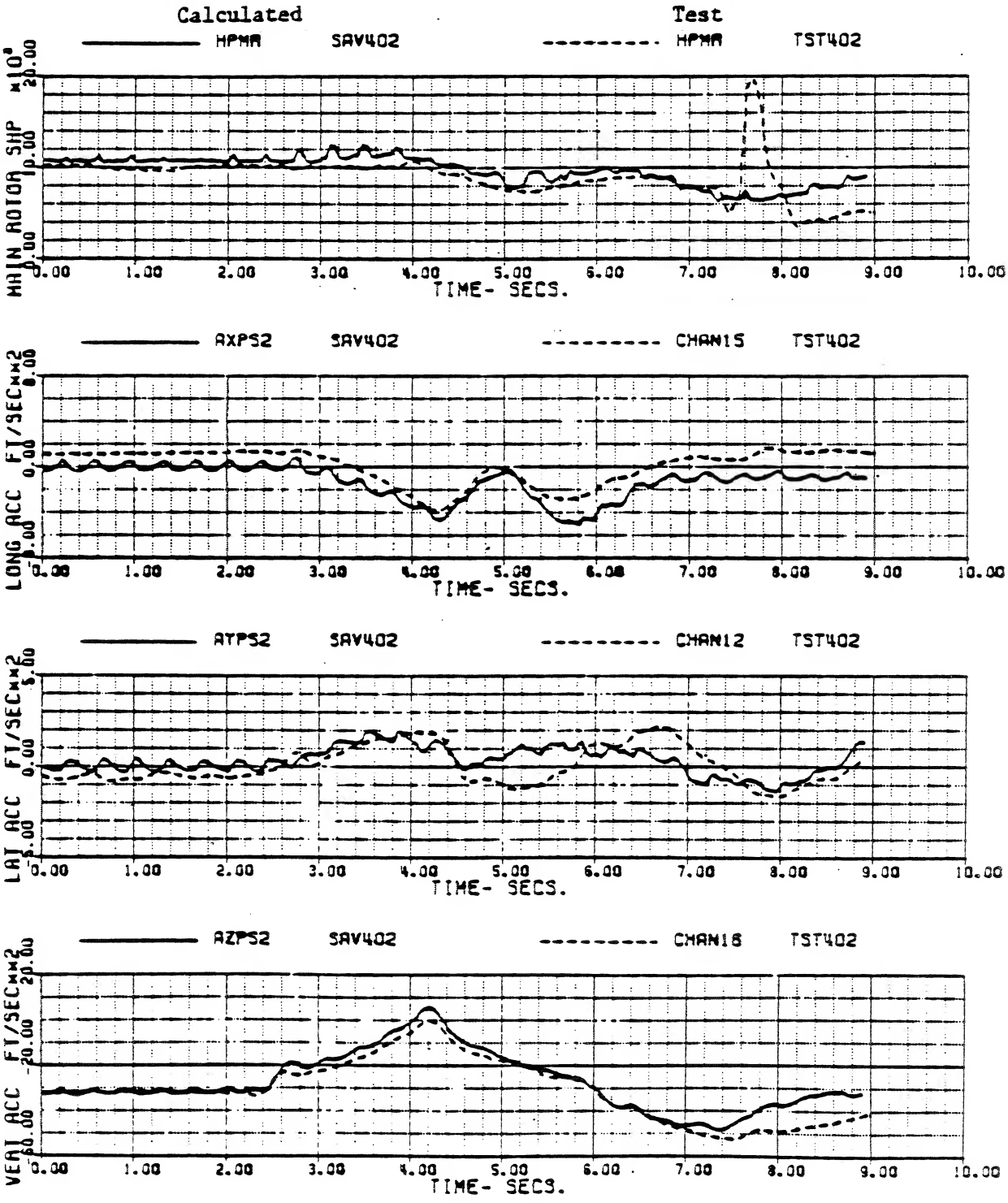

Figure 1g

BLACKHAWK - NASA STUDY 8-DEC-82 13:07 (7/8)

AEFA TEST TAPE BHAWK4 8/18/82
FLT 45A RUN 17 100KTS LONG. INPUT

VKT	99.998644	WEIGHT	16480.000	FSCG	359.59999	IH1	7.8999998
XA	5.2525152	XB	4.1226774	XC	4.8625791	XP	3.0781338
THETAB	.452576E-1	PHIB	0.	OMGRAT	1.0037036	GGRPM	89.872973

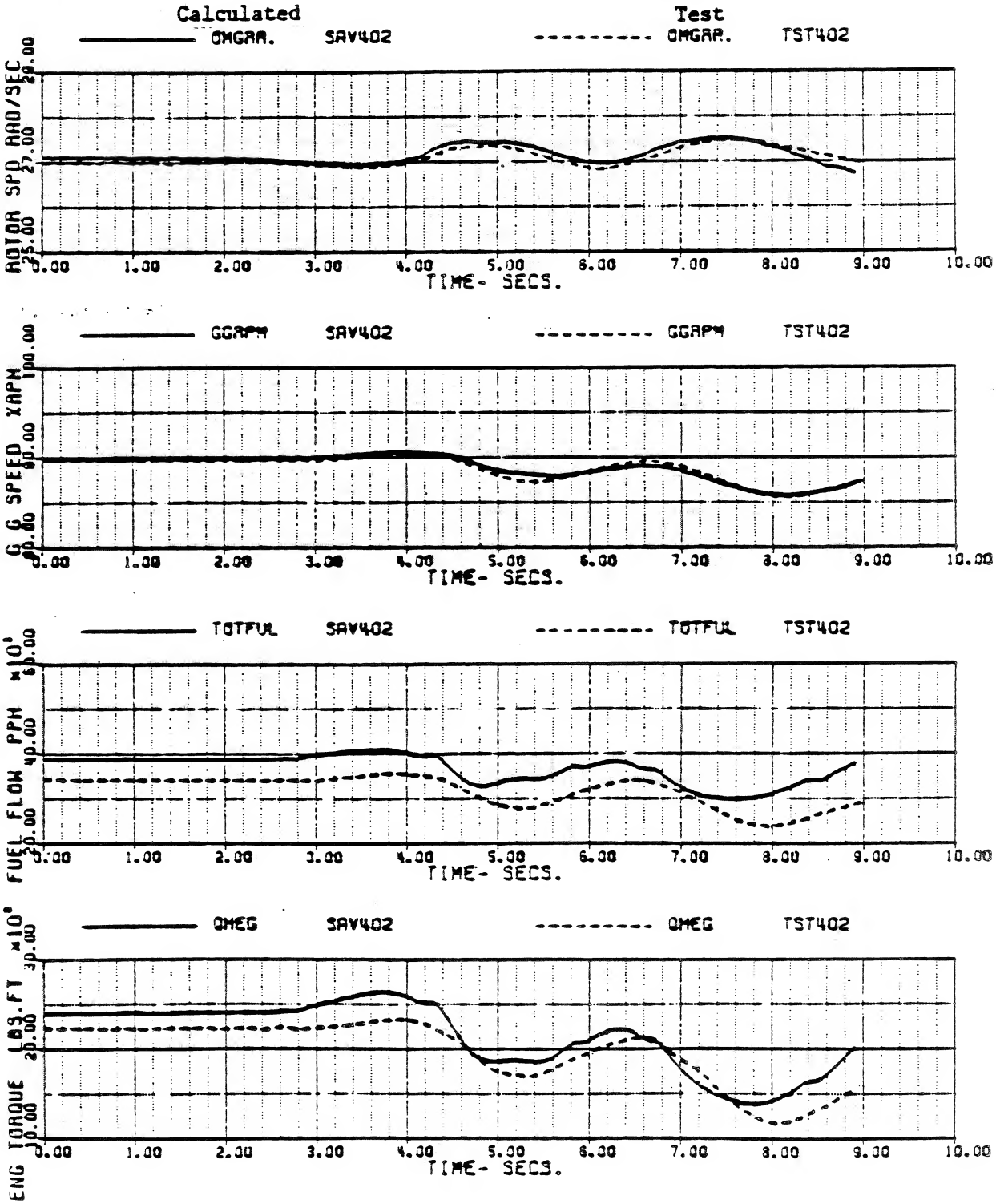

Figure 1h

BLACKHAWK - NASA STUDY 8-DEC-82 13:07 (8/8)

AEFA TEST TAPE BHAWK4 8/18/82
FLT 45A RUN 17 100KTS LONG. INPUT

VKT	99.998644	WEIGHT	16480.000	FSCG	359.59999	IH1	7.8999999
XA	5.2525152	XB	4.1226774	XC	4.8625791	XP	3.0781338
THETAB	.452576E-1	PHIB	0.	OMGRAT	1.0037036	GGRPM	89.872973

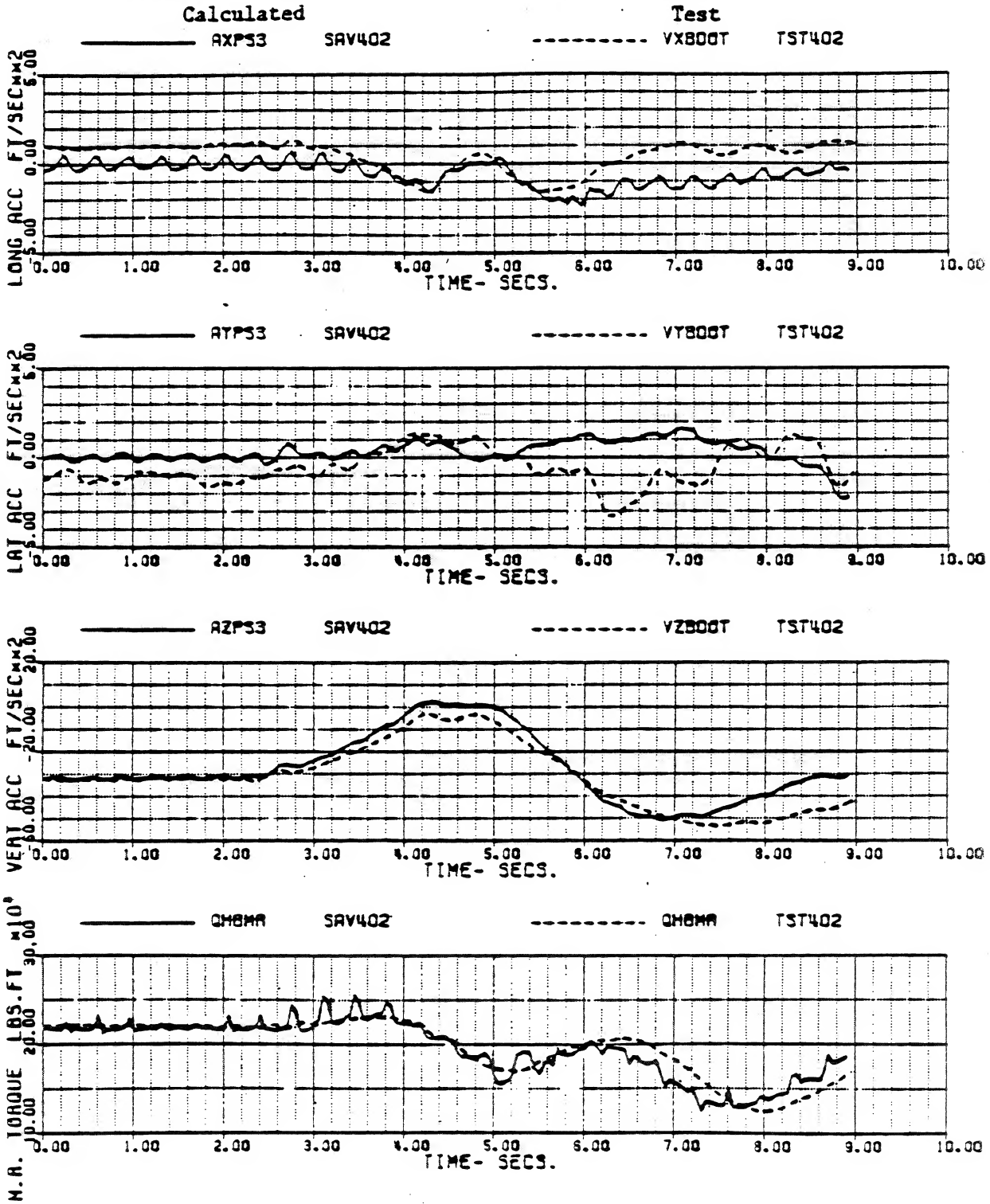

Figure 2a

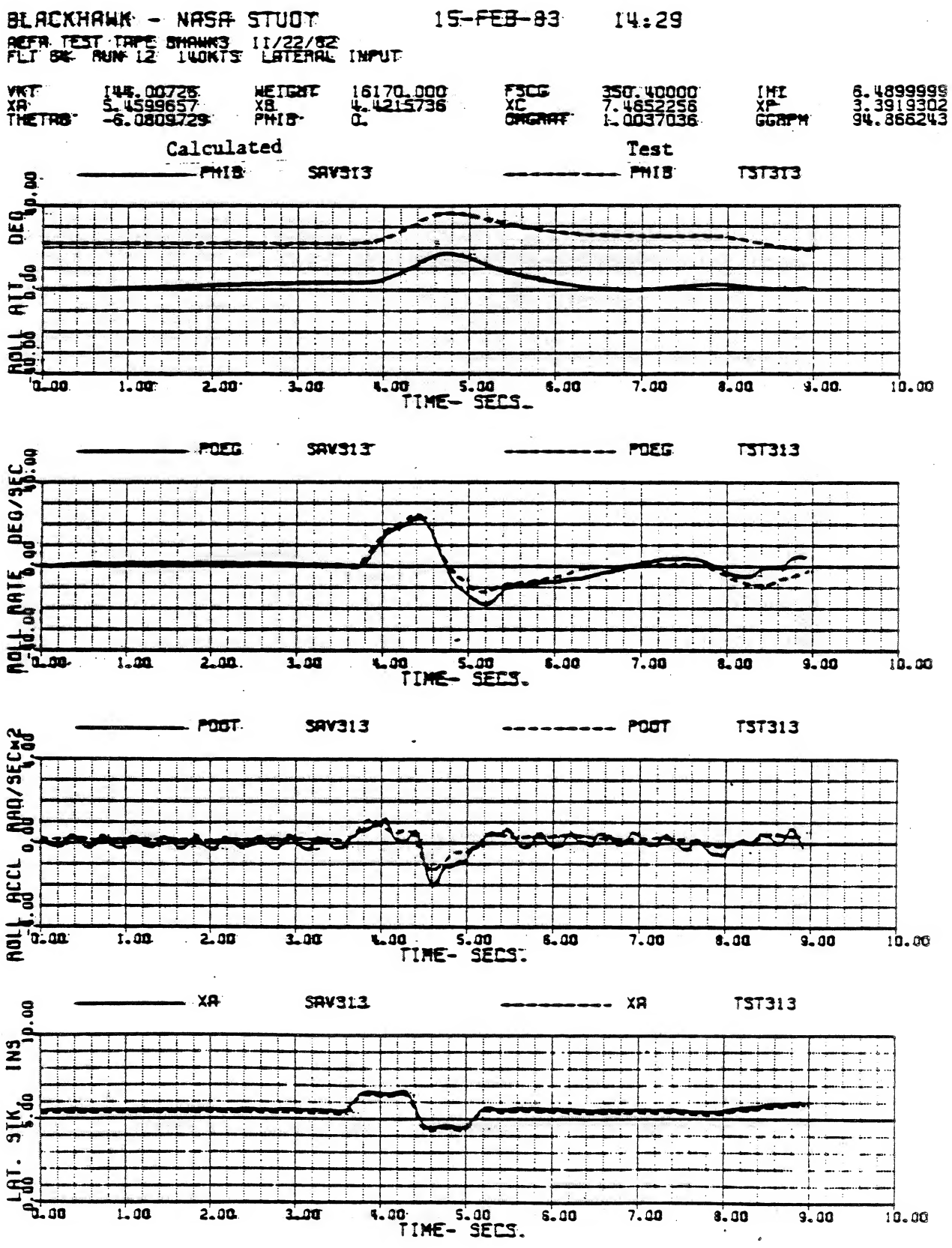

Figure 2b

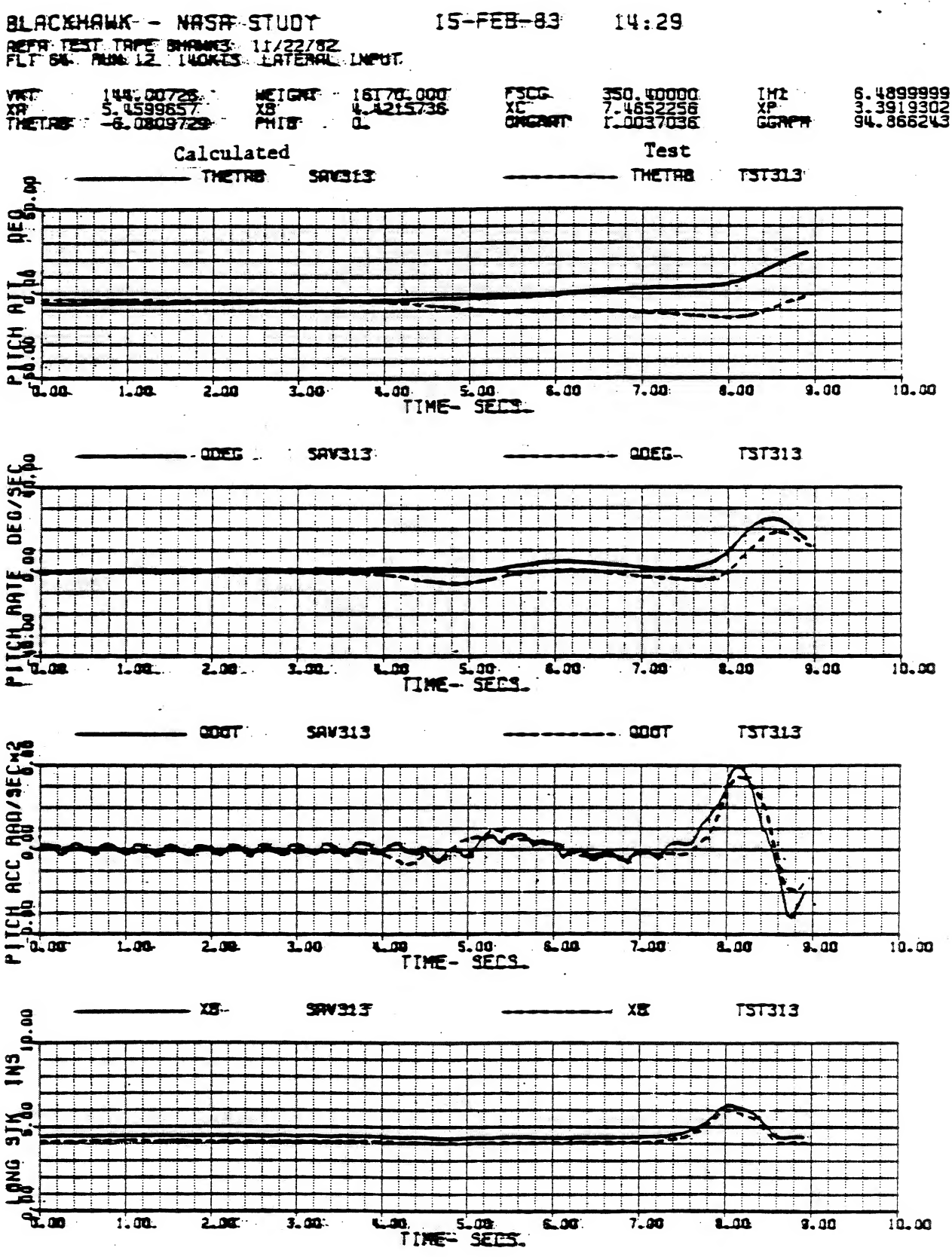
BLACKHAWK - NASA STUDY 15-FEB-83 14:29
REFR TEST TAPE SHRWK3 11/22/82
FLT 64 RUN 12 140KTS LATERAL INPUT
VKT 144.00726 WEIGHT 16170.000 FSCG 350.40000 IMI 6.4899999
XR 5.4599657 XB 4.4215736 XC 7.4652256 XP 3.3919302
THETAR -6.0809729 PHIR 0. ONGART 1.0037036 GGNPR 94.866243
Calculated
Test
THETAR SAV313
THETAR TST313
PITCH ATT DEG
QDEG SAV313
QDEG TST313
PITCH RATE DEG/SEC
QDOT SAV313
QDOT TST313
PITCH ACC RAD/SEC2
XB SAV313
XB TST313
LONG STK INS
TIME- SECS

Figure 2c

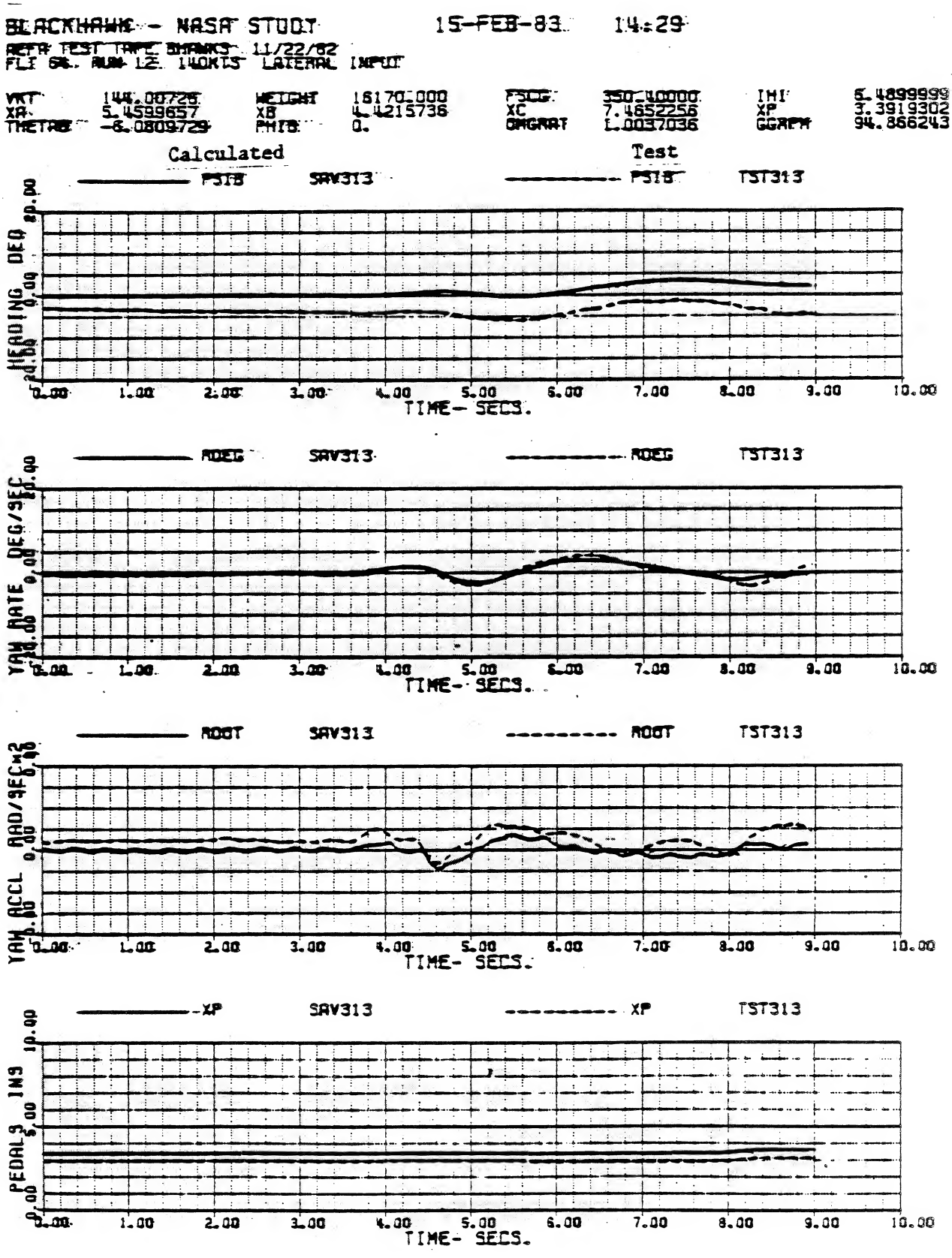

Figure 2d

BLACKHAWK - NASA STUDY 15-FEB-83 14:29

AEFM TEST TAPE BHAWK3 12/22/82
FLT 56, RUN 12 140KTS LATERAL INPUT

VKT	144.00726	WEIGHT	15170.000	FSCG	350.40000	IHt	6.4899999
XR	5.4599657	XB	4.4215738	XC	7.4652258	XP	3.3919302
THETAB	-6.0809729	PHIB	0.	OMGRAT	1.0037036	GGRPM	94.866243

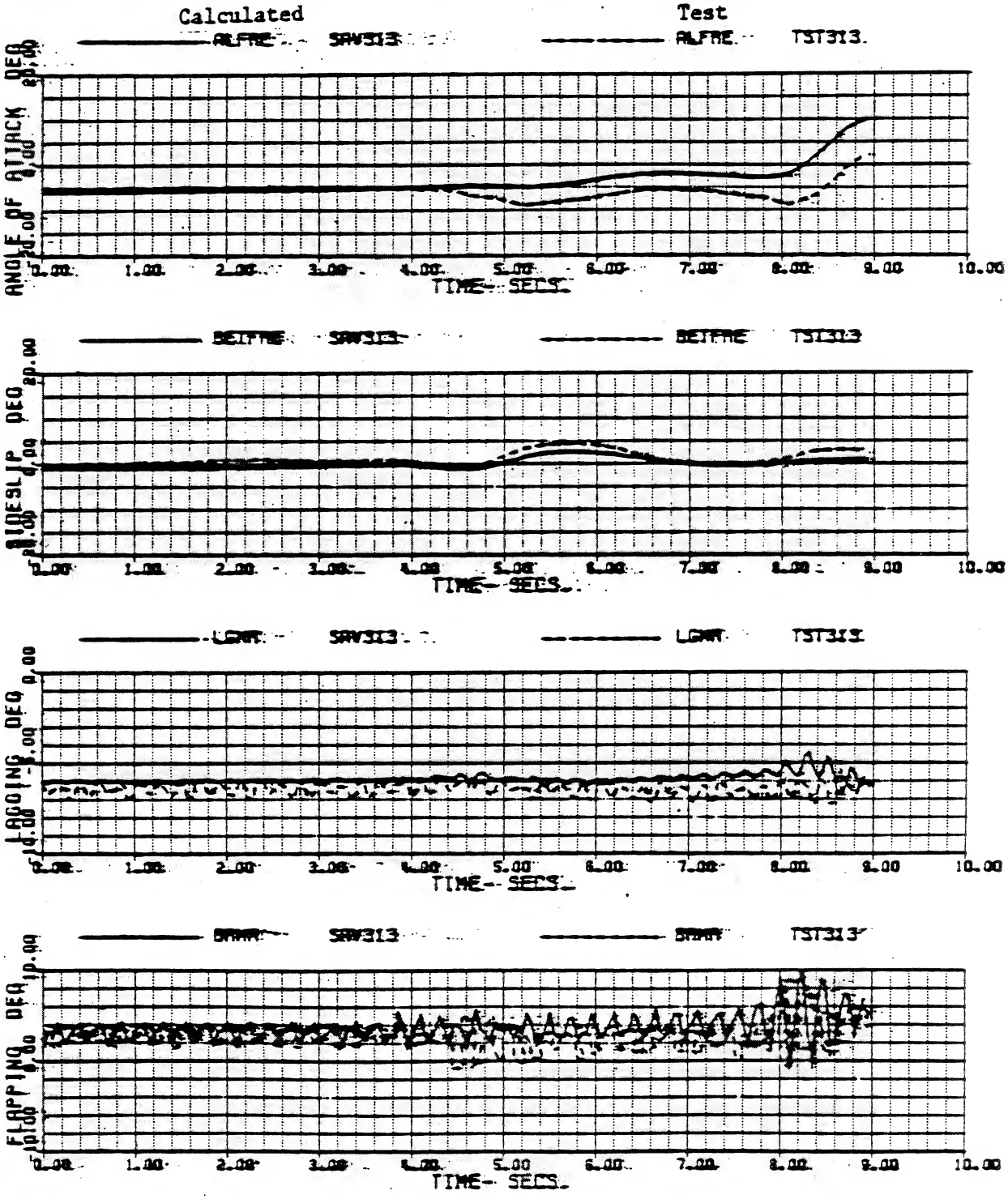

Figure 3a

BLACKHAWK - NASA STUDY 23-NOV-82 10:07 (4/8)
AEFA TEST TAPE BHAWK2 7/28/82
FLT 508 RUN 27 HOVER COLL INPUT

VKT	.3999685E-3	WEIGHT	15940.000	FSCG	359.40000	IH1	44.400000
XA	5.1398469	XB	4.8870671	XC	5.9470320	XP	1.4421845
THETA8	4.4315225	PHI8	-2.8077761	OMGRAT	0.9955555	GGRPM	93.724715

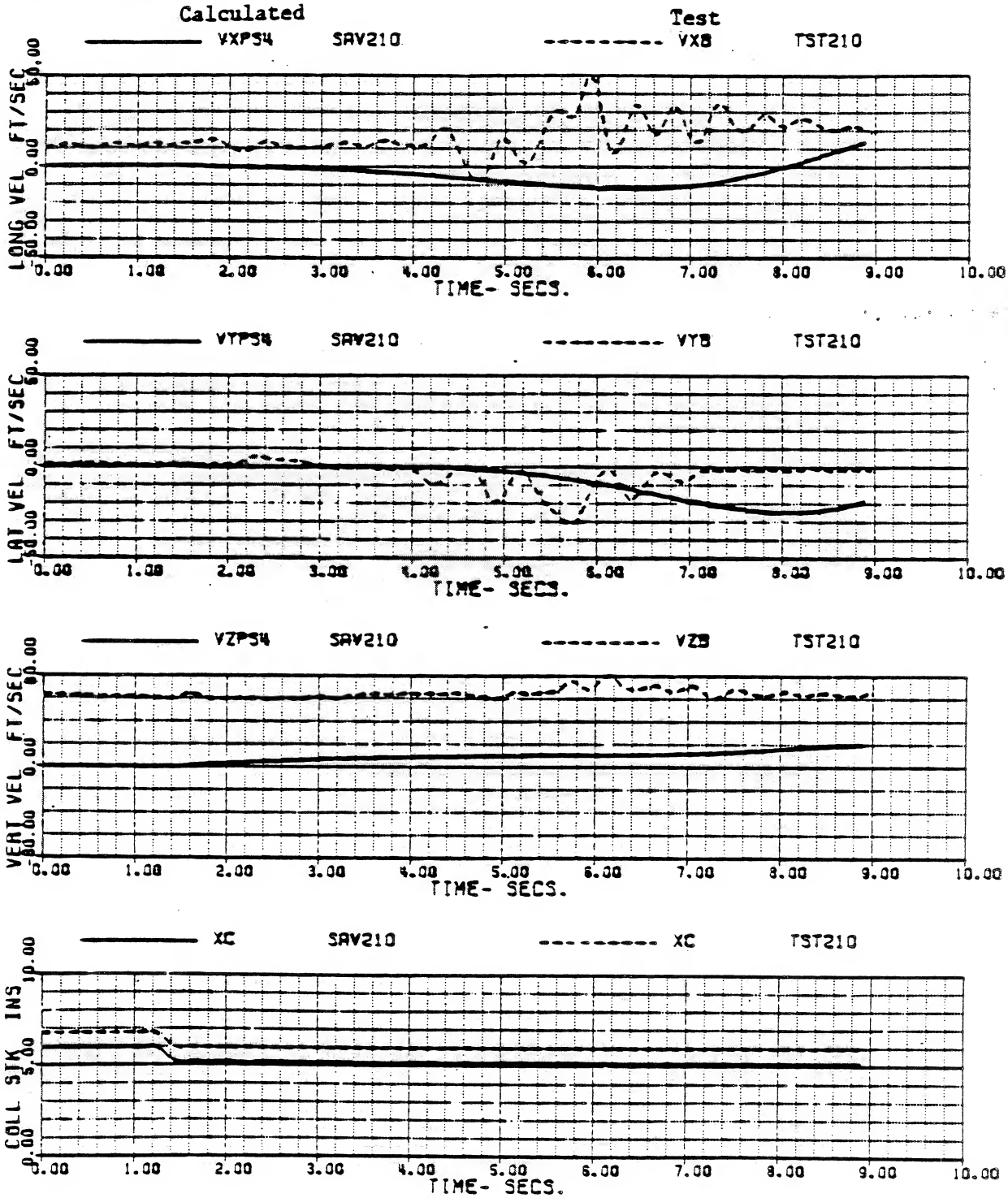

SA 1114

01:49
24-NOV
TST210
.PCD
SAV210
.DAT

Figure 3b

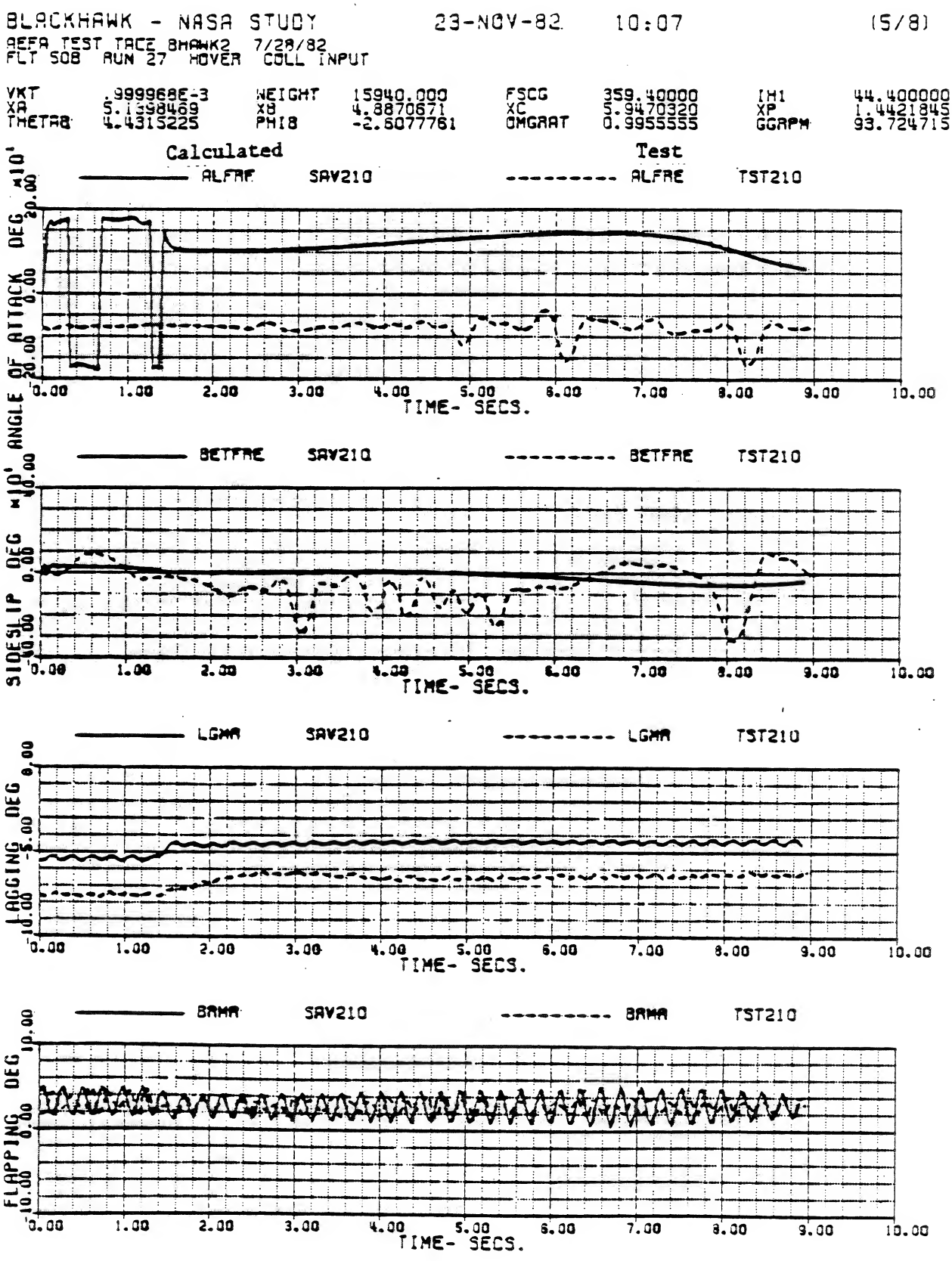

SA 1114

01:49
24-NOV
TST210
.PCO
SAV210
.DAT

Figure 3c

BLACKHAWK - NASA STUDY 23-NOV-82 10:07 (7/8)
AEFA TEST TAPE BHAWK2 7/28/82
FLT 508 RUN 27 HOVER COLL INPUT

VKT	.999968E-3	WEIGHT	15940.000	FSCG	359.40000	IH1	44.400000
XA	5.1398459	XB	4.8870671	XC	5.9470320	XP	1.4421845
THETAB	4.4315225	PHIB	-2.6077761	OMGRAT	0.9955555	GGRPM	93.724715

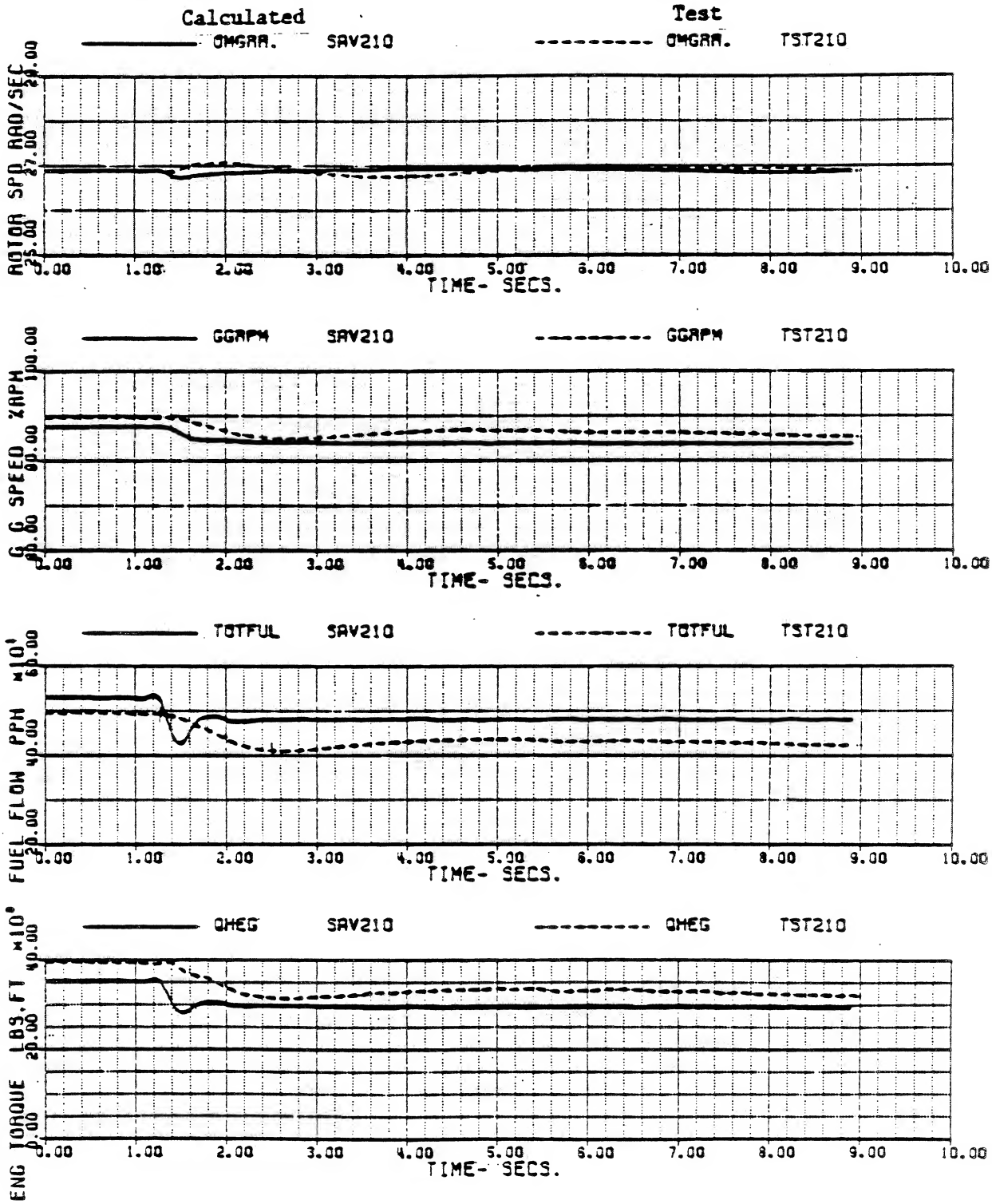

SA 1114

01:49
24-NOV
TST210
.PCD
SAV210
.DAT

Figure 3d

BLACKHAWK - NASA STUDY 23-NOV-82 10:07 (8/8)
AEFA TEST TAPE BHAWK2 7/28/82
FLT 508 RUN 27 HOVER COLL INPUT

VKT	.999968E-3	WEIGHT	15940.000	FSCG	359.40000	IHI	44.400000
XA	5.1398469	X8	4.8870671	XC	5.9470320	XP	1.4421845
THETA8	4.4315225	PHI8	-2.6077761	OMGRAT	0.9955555	GGRPM	93.724715

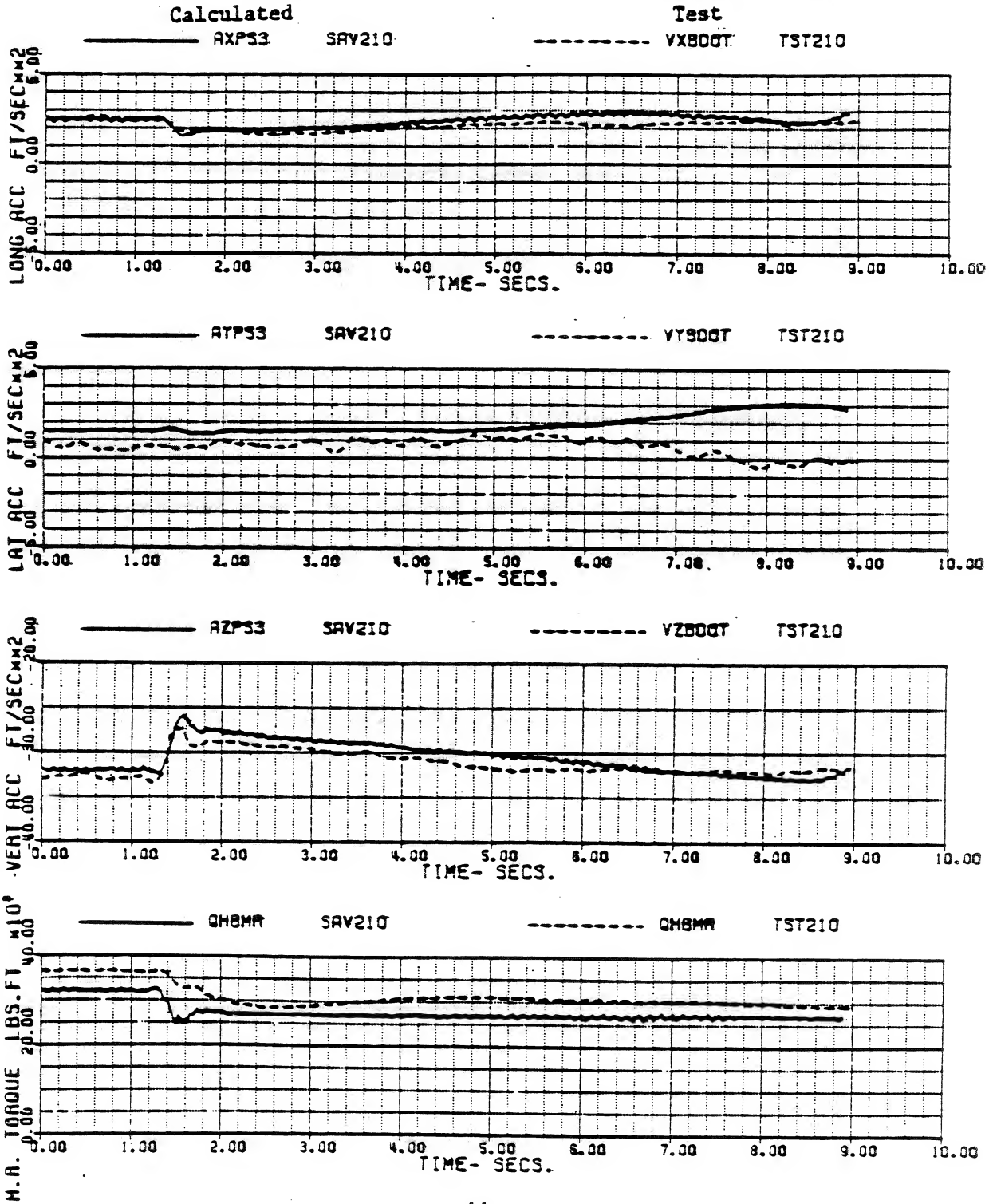

01:49
24-NOV
TST210
.PCD
SAV210
.DAT

Figure 4a

BLACKHAWK – NASA STUDY 15-FEB-83 09:53 (3/8)

REFR TEST TAPE BMARK3 11/22/82
FLT 66 RUN 27 140KTS PEDAL INPUT

VKT	144.00755	WEIGHT	15410.000	FSCG	352.09999	IMI	6.5400000
XR	5.5054389	XB	4.3368436	XC	7.2829869	XP	3.3491829
THETRR	-5.9303845	PHIB	0.	OMGMAT	1.0111110	GGRPM	94.533287

Calculated Test

PSIB SAV308 PSIB TST308

HEADING DEP 10.00 0.00 -10.00

0.00 1.00 2.00 3.00 4.00 5.00 6.00 7.00 8.00 9.00 10.00
TIME- SECS.

RDEG SAV308 RDEG TST308

YAW RATE DEG/SEC 10.00 0.00 -10.00

0.00 1.00 2.00 3.00 4.00 5.00 6.00 7.00 8.00 9.00 10.00
TIME- SECS.

RDDT SAV308 RDDT TST308

YAW ACCL RAD/SEC**2 0.40 0.00 -0.40

0.00 1.00 2.00 3.00 4.00 5.00 6.00 7.00 8.00 9.00 10.00
TIME- SECS.

XP SAV308 XP TST308

PEDALS INS 10.00 5.00 0.00

0.00 1.00 2.00 3.00 4.00 5.00 6.00 7.00 8.00 9.00 10.00
TIME- SECS.

Figure 4b

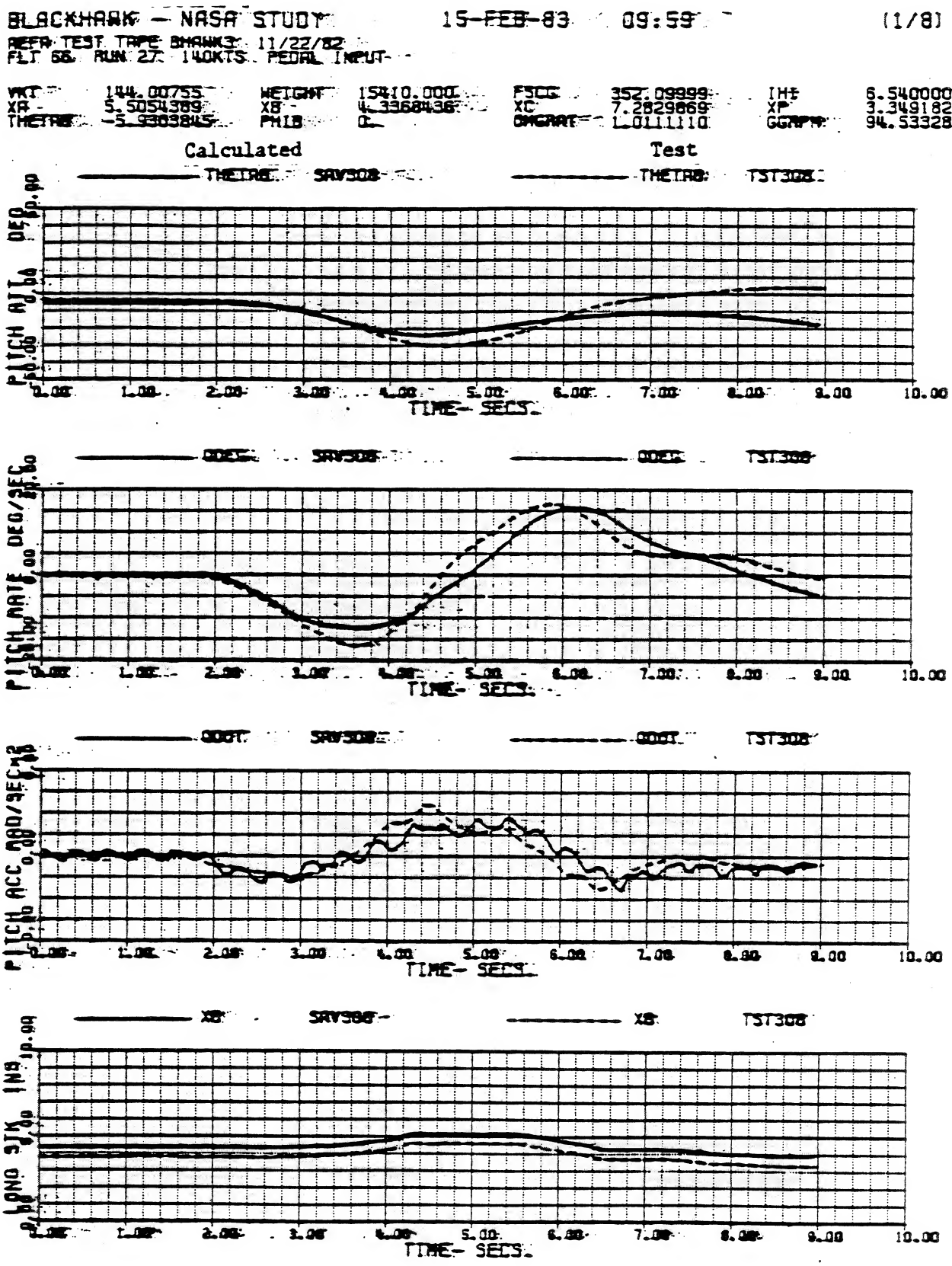

Figure 4c

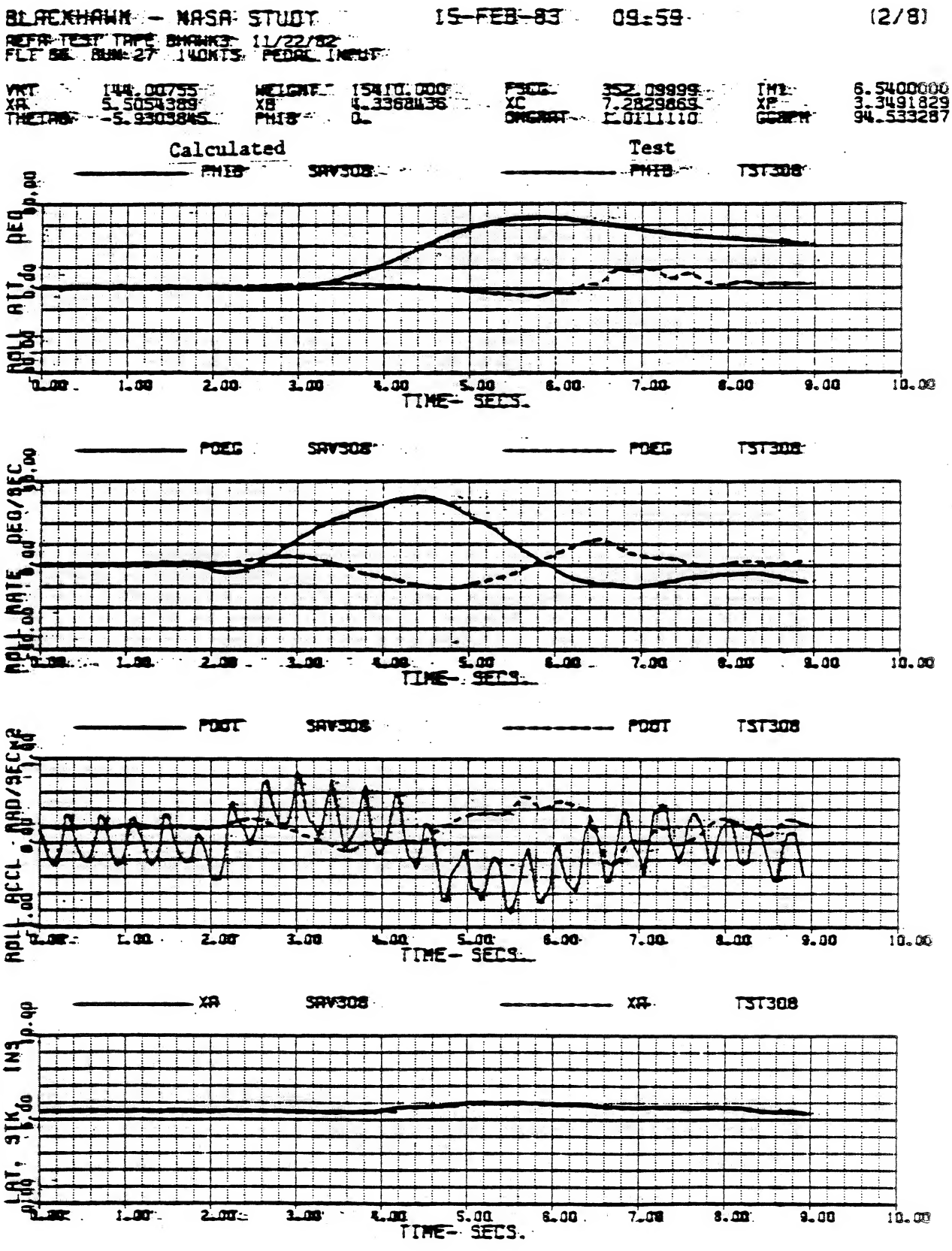

Figure 4d

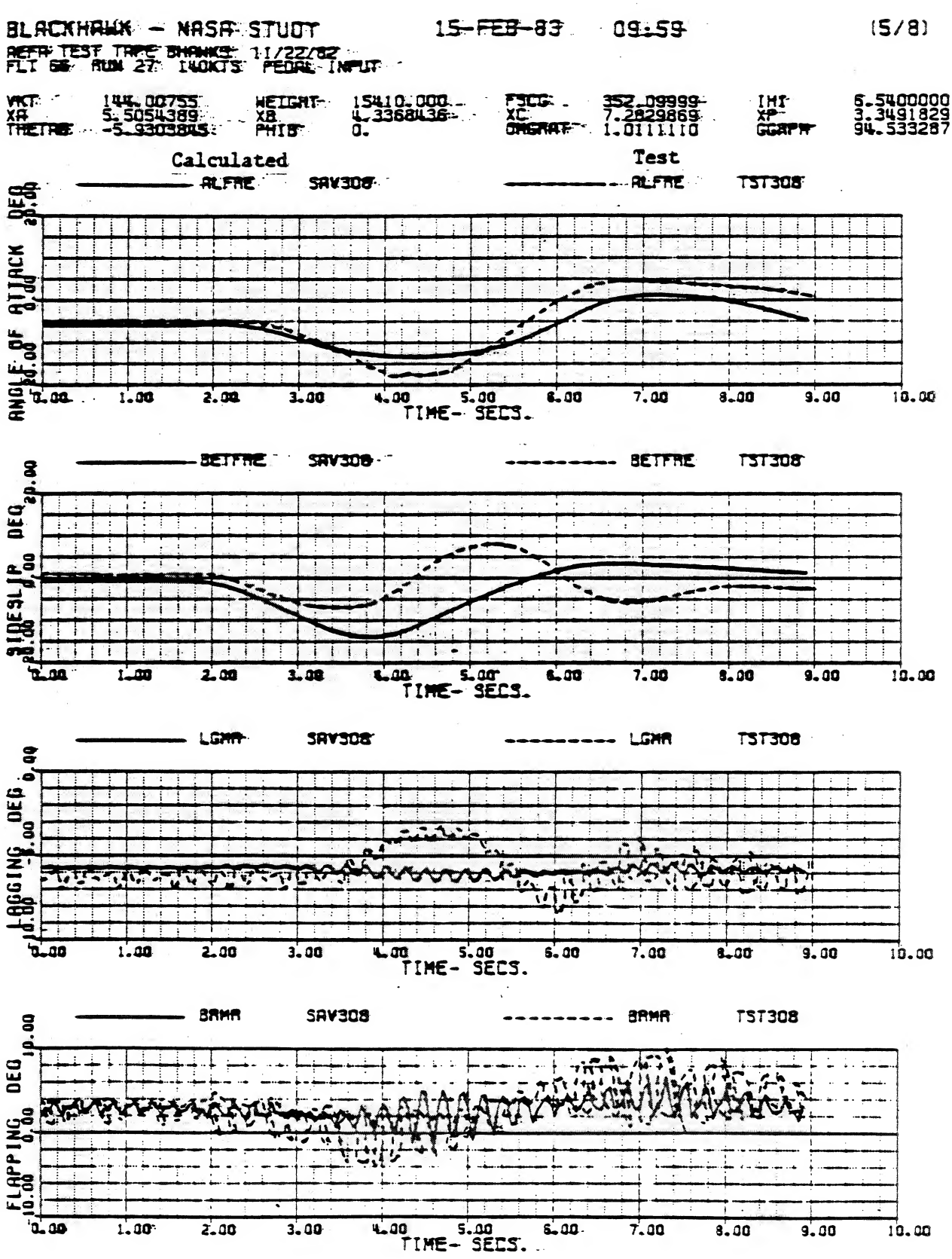
BLACKHAWK - NASA STUDY 15-FEB-83 09:59 (5/8)
REFR TEST TAPE BHANK: 11/22/82
FLT 66 RUN 27 INOKTS PEDAL INPUT
VKT 144.00755 WEIGHT 15410.000 FSCG 352.09999 IHI 6.5400000
XA 5.5054389 XB 4.3368436 XC 7.2829869 XP 3.3491829
THETRR -5.9303845 PHIR 0. OMGRAT 1.0111110 GGRPM 94.533287
Calculated
Test
ALFRE SAV308
ALFRE TST308
ANGLE OF ATTACK DEG
TIME- SECS.
BETFRE SAV308
BETFRE TST308
SIDESLIP DEG
TIME- SECS.
LGMR SAV308
LGMR TST308
LAGGING DEG
TIME- SECS.
BRMR SAV308
BRMR TST308
FLAPPING DEG
TIME- SECS.

Figure 5a

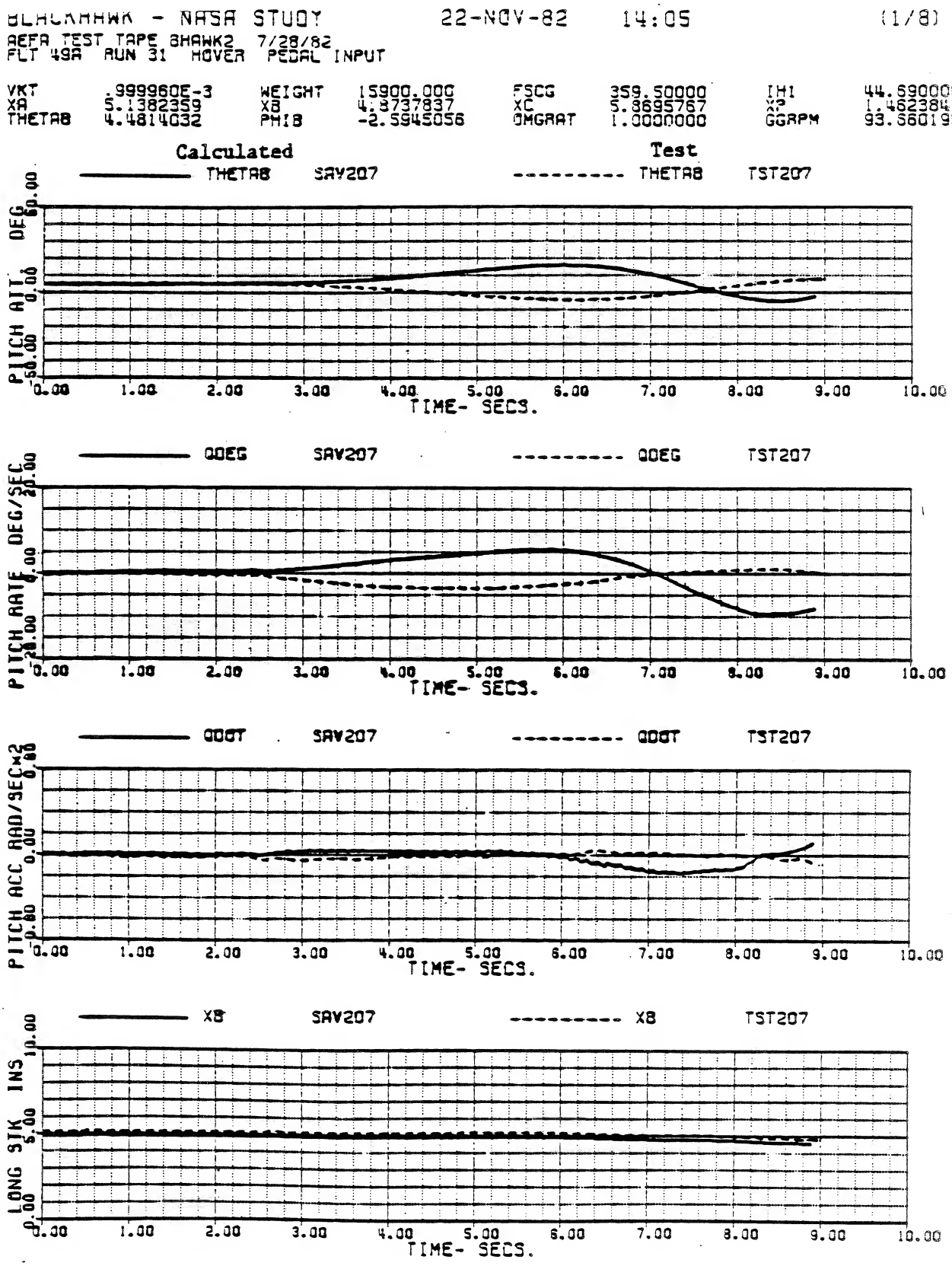

19:41
25-NOV
TST207
.PCD
SAV207
.DAT

Figure 5b

BLACKHAWK - NASA STUDY 22-NOV-82 14:05 (3/8)
AEFA TEST TAPE BHAWK2 7/28/82
FLT 49A RUN 31 HOVER PEDAL INPUT

VKT	.9999605E-3	WEIGHT	15900.000	FSCG	359.50000	IH1	44.690000
XB	5.1382359	XB	4.8737937	XC	5.8695767	XP	1.4523847
THETAB	4.4814032	PHIB	-2.5945056	OMGRAT	1.0000000	GGRPM	93.660199

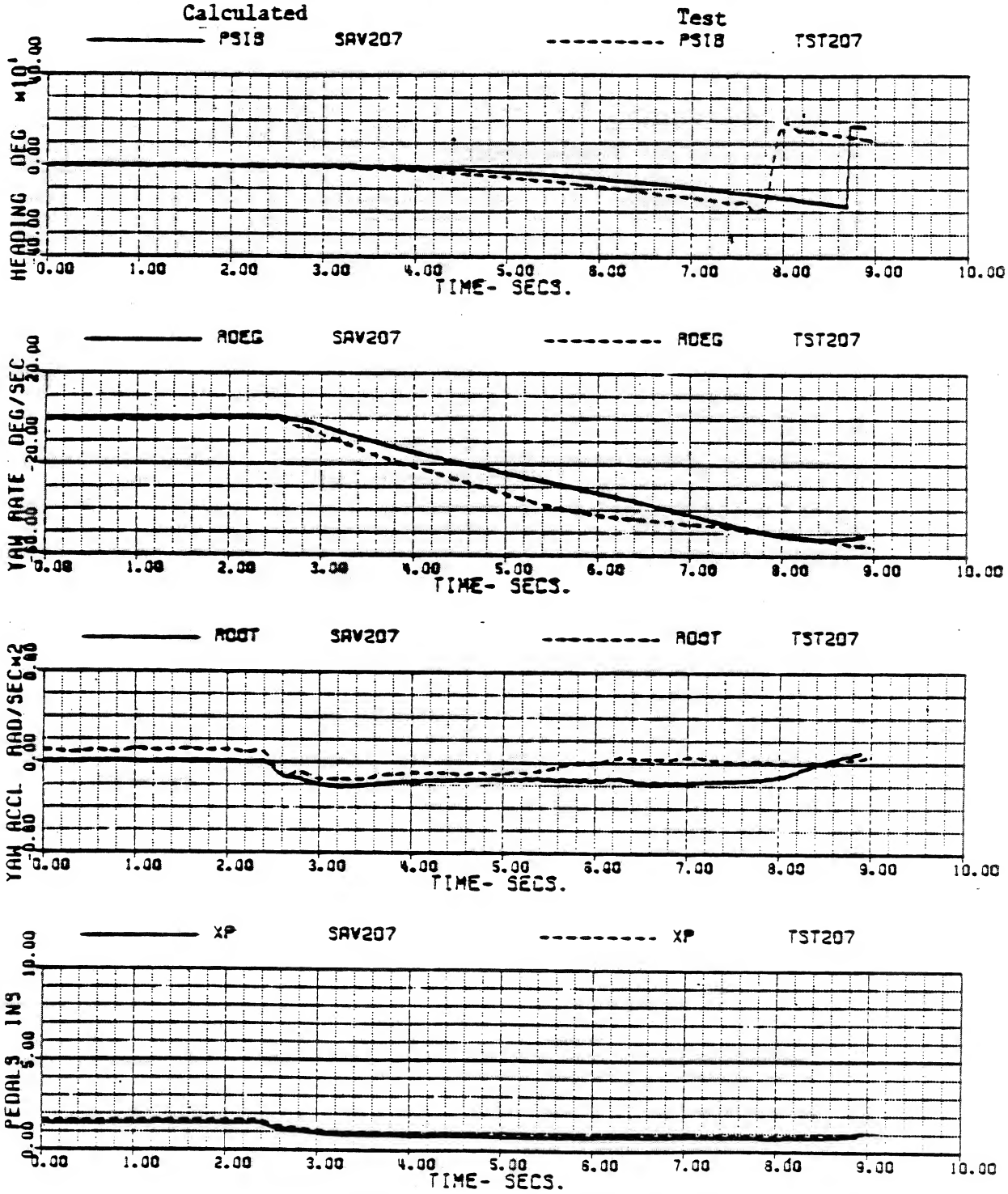

19:41
23-NOV
TST207
.PCD
SAV207
.DAT

Figure 6

BLACKHAWK - NASA STUDY 29-NOV-82 15:12 (1/8)
AEFA TEST TAPE BHAWKS 11/1/82
FLT 25 RUN 30 60KTS LONGITUDINAL INPUT

VKT	59.996385	WEIGHT	15810.000	FSCG	351.29999	IH1	31.599999
XA	4.8413347	XB	5.8241637	XC	4.4628078	XP	2.6382460
THETAB	-2.6528021	PHIB	0.	OMGRAT	0.9925925	GGRPM	88.431324

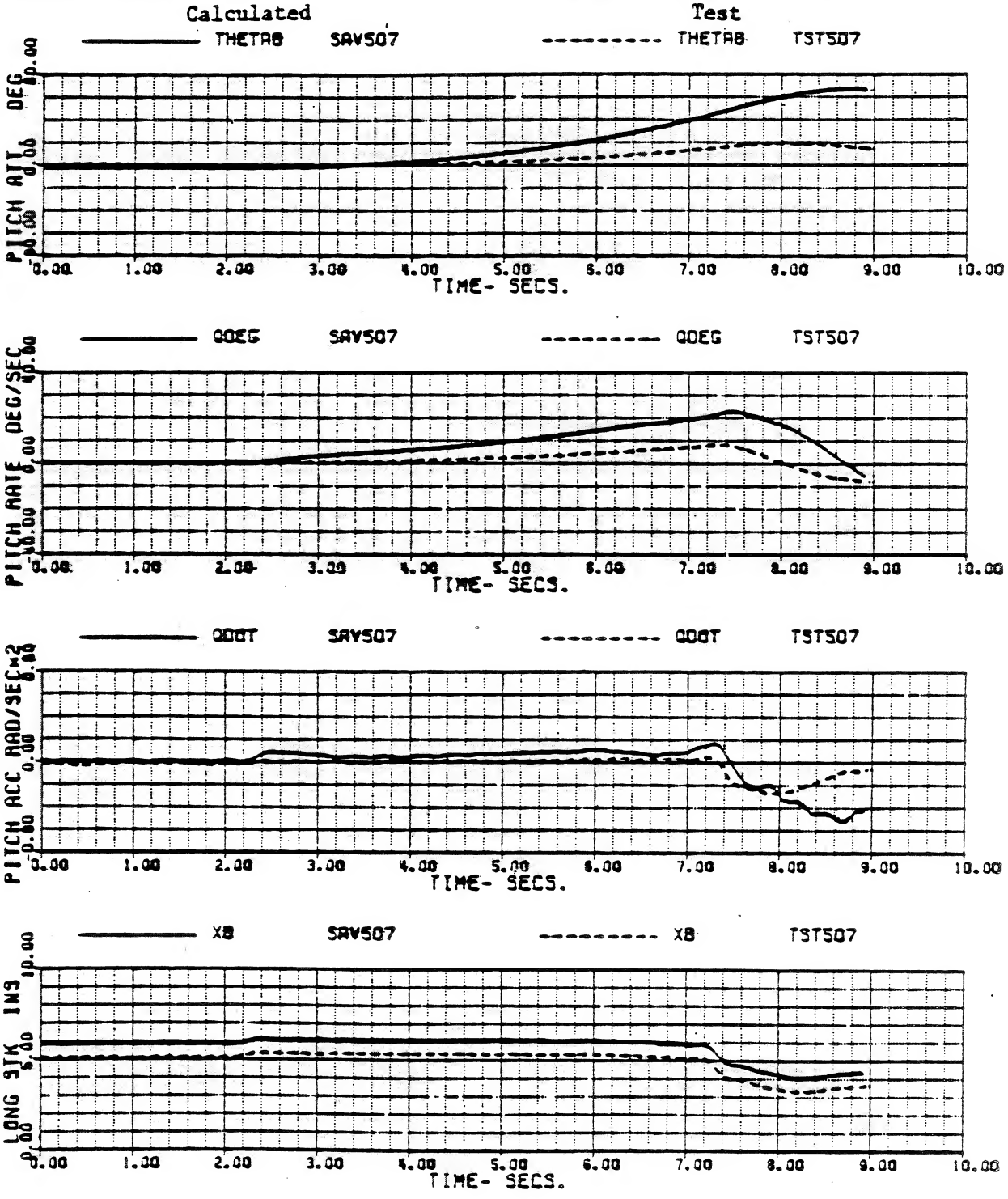

Figure 7

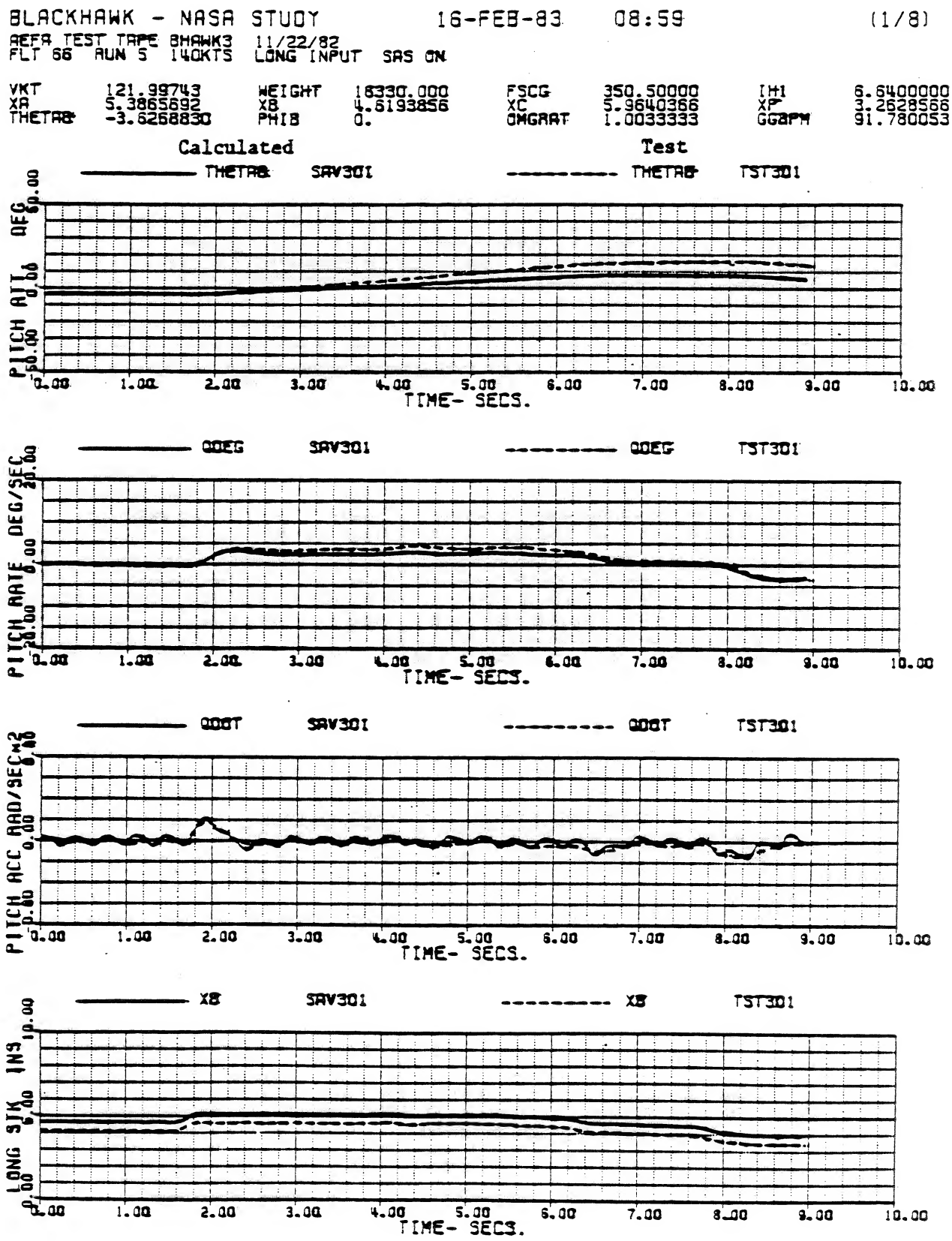

SA 1114

19:12
22-FEB
TST301
.PCB
SAV301
.DAT

Figure 8

BLACKHAWK – NASA STUDY 16-FEB-83 09:07 (6/8)
AEFA TEST TAPE BHAWK3 11/22/82
FLT 66 RUN 14 140KTS COLL INPUT SAS-ON

VKT	139.99773	WEIGHT	15940.000	PSCG	350.90000	IHH	6.6999999
XA	5.4814162	XB	4.4619484	XC	7.1526744	XP	3.3640629
THETAB	-5.6468600	PHIB	0.	DNGRAT	1.0018518	GGRPM	94.128872

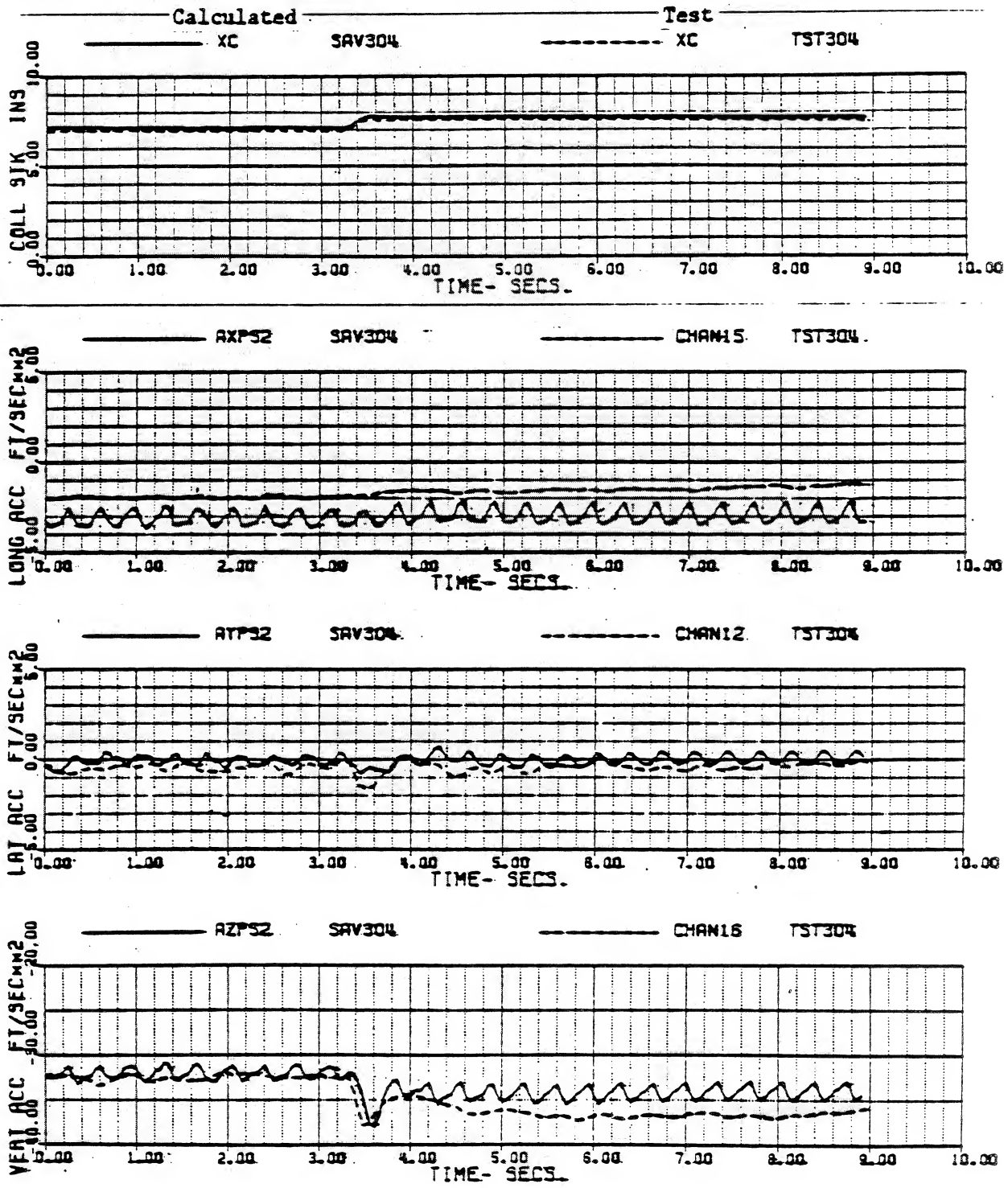

FIGURE 68

FIGURE 3-6

BLACK HAWK SIMULATION MODEL VALIDATION

LEVEL FLIGHT STATIC TRIM

SAS-ON

GW=15000LB FSCG=351.0 WLEG=291.5 hd=5250 FT

UP OL AFEA(19-24)=1.13 RUNS 8-21

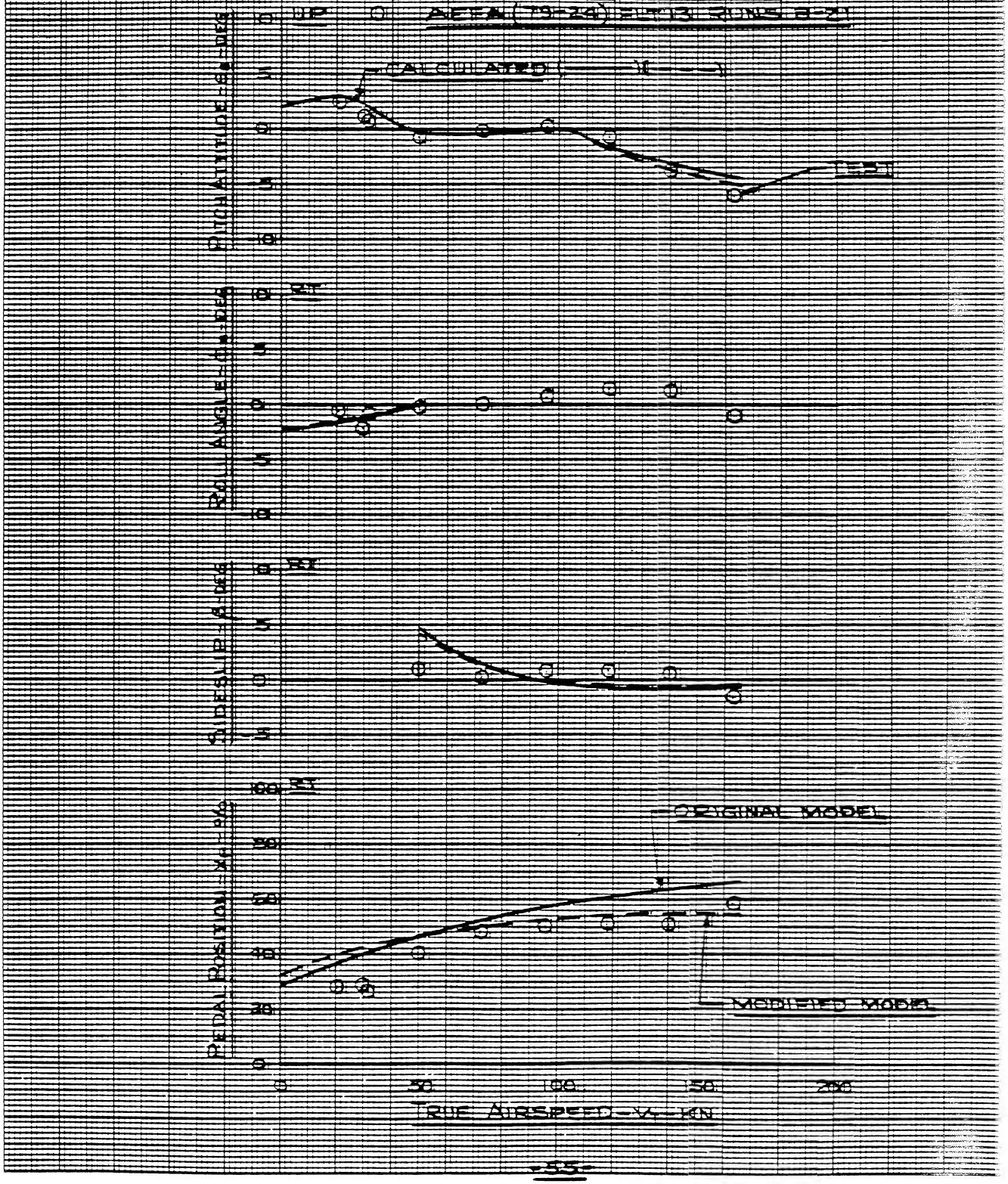

FIGURE 32

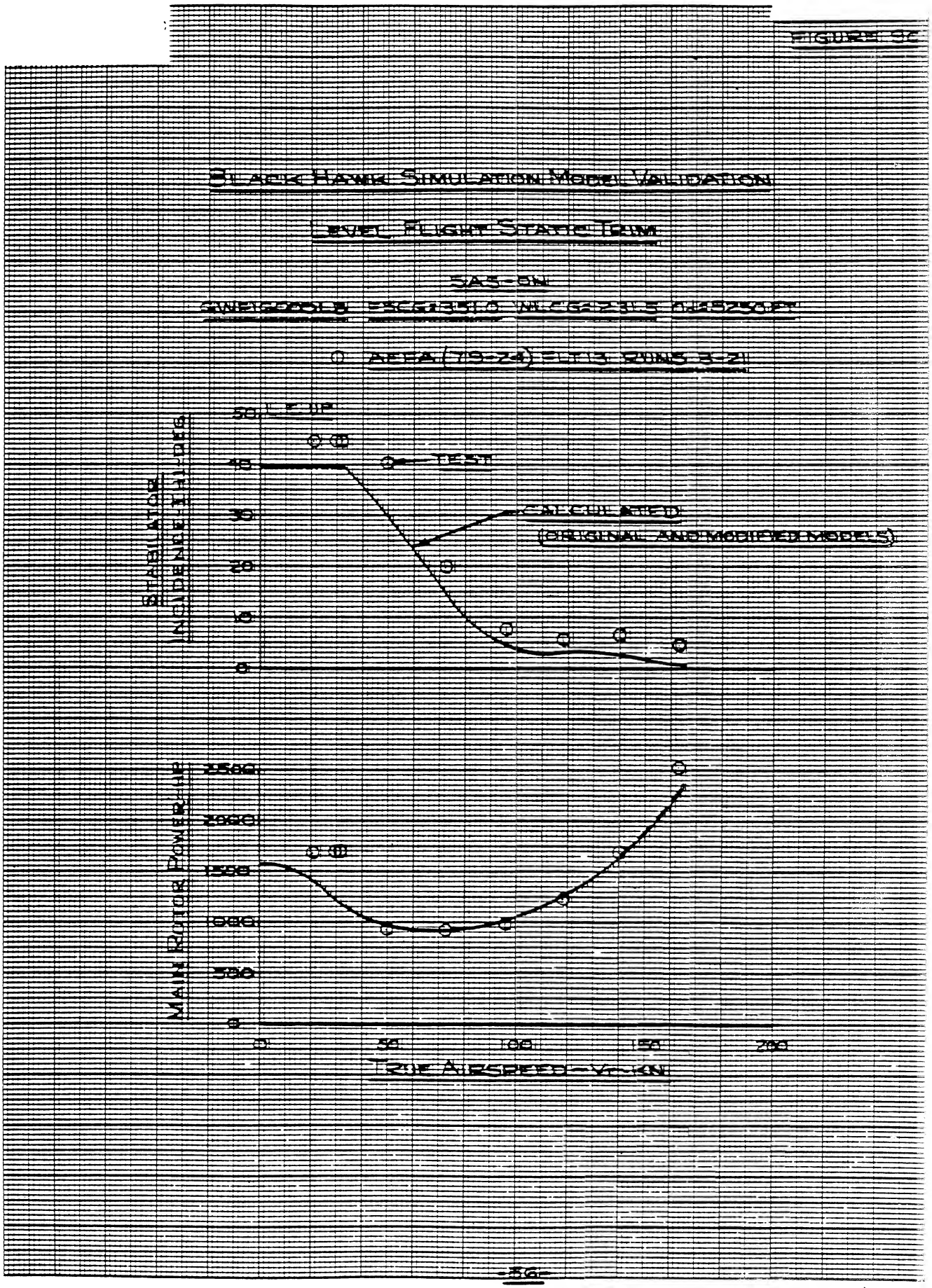

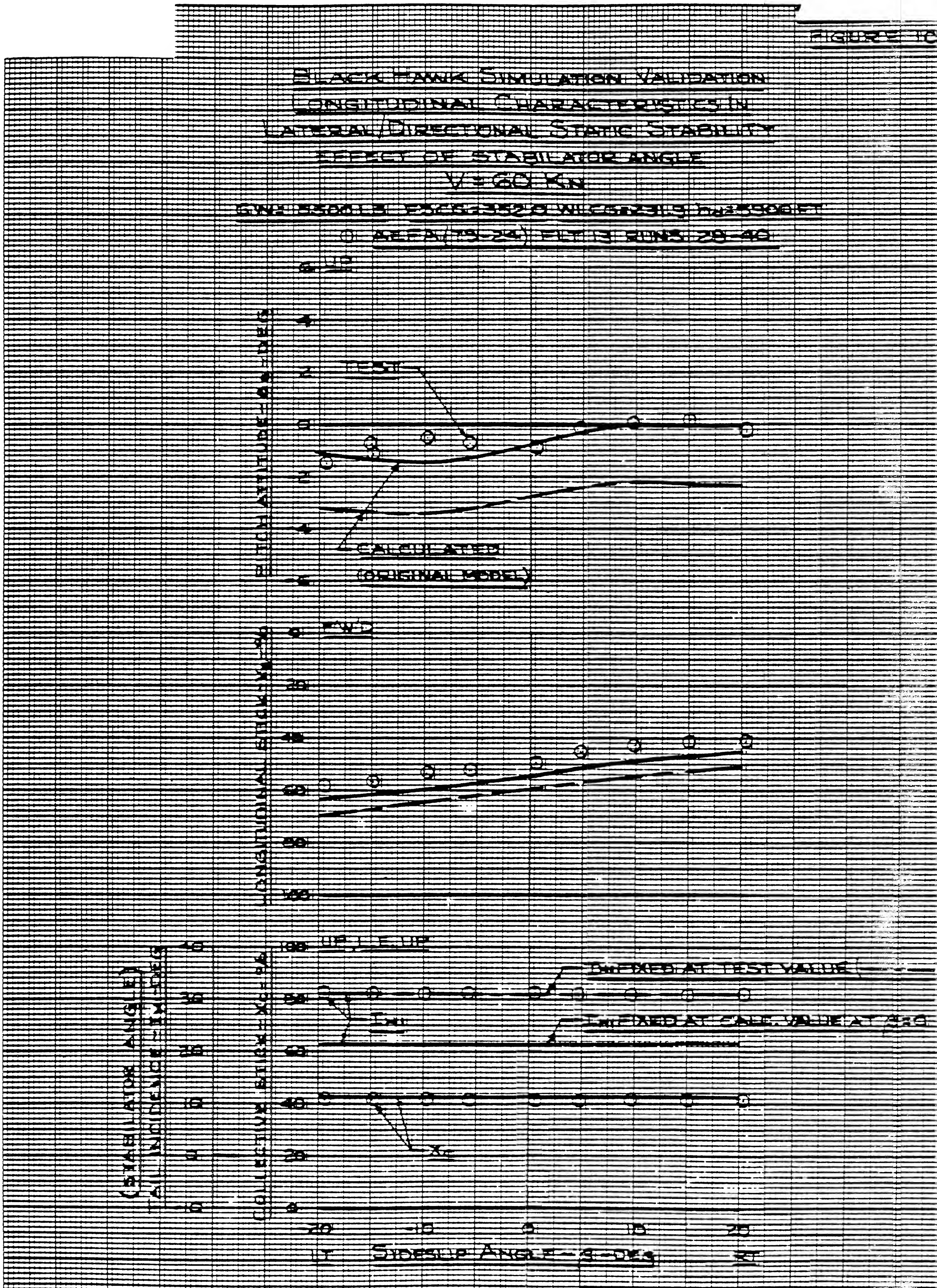

FIGURE 11a

BLACK HAWK SIMULATION MODEL VALIDATION

LATERAL/DIRECTIONAL STATIC STABILITY

V = 60 KN

GW=15500 LB FSCG=352.0 WLCG=235.9 Hp=1500 FT

○ AEFA (79-24) FLT 13 RUNS 28-40

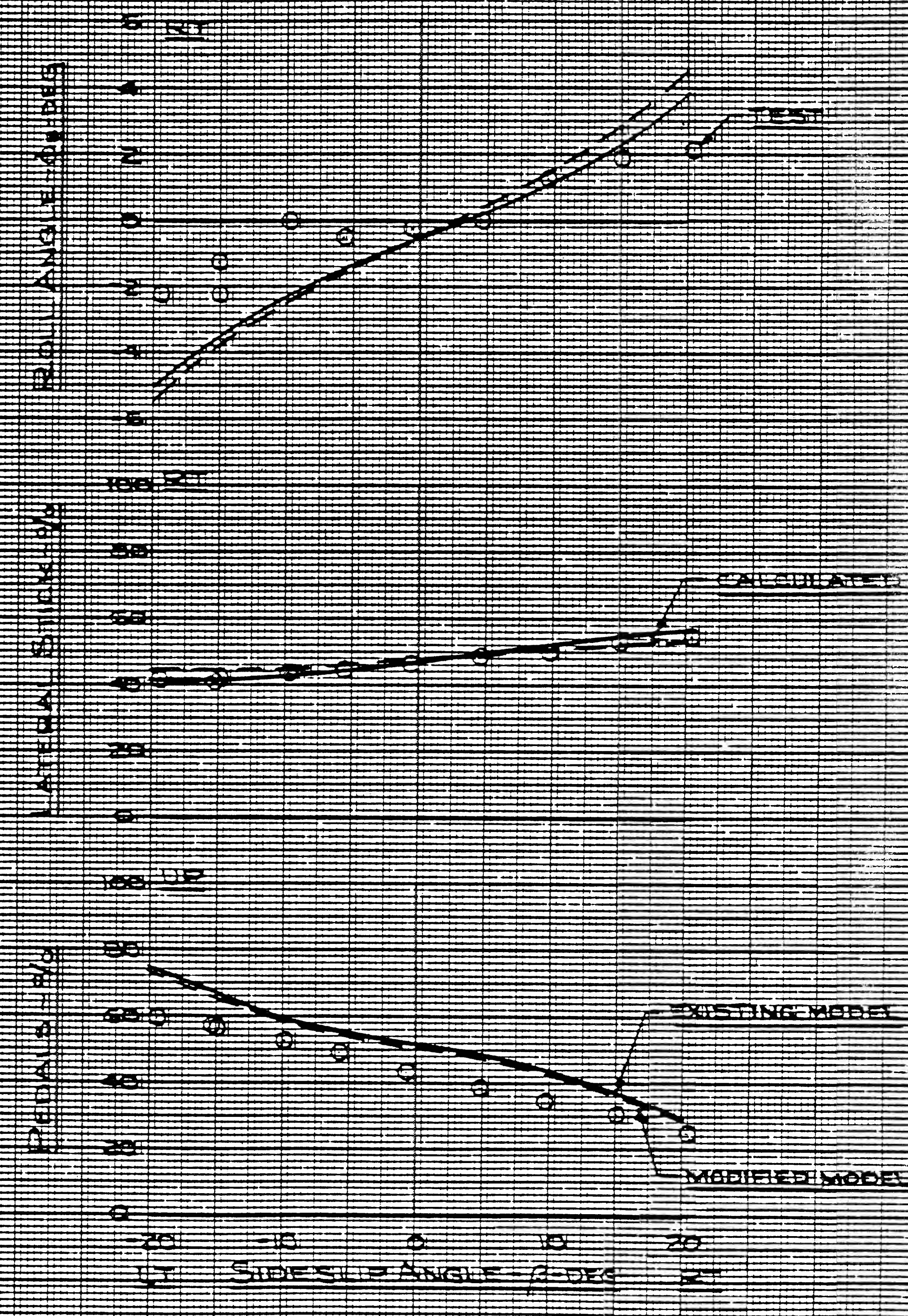

FIGURE 11c

BLACK HAWK SIMULATION MODEL VALIDATION

LATERAL/DIRECTIONAL STATIC STABILITY

V=60 KN

SW=15500 LB; FSCG=352.0 WL CG=231.9; h=3500 FT

○ AEFA (79-24) FLT 13 RUNS 28-40

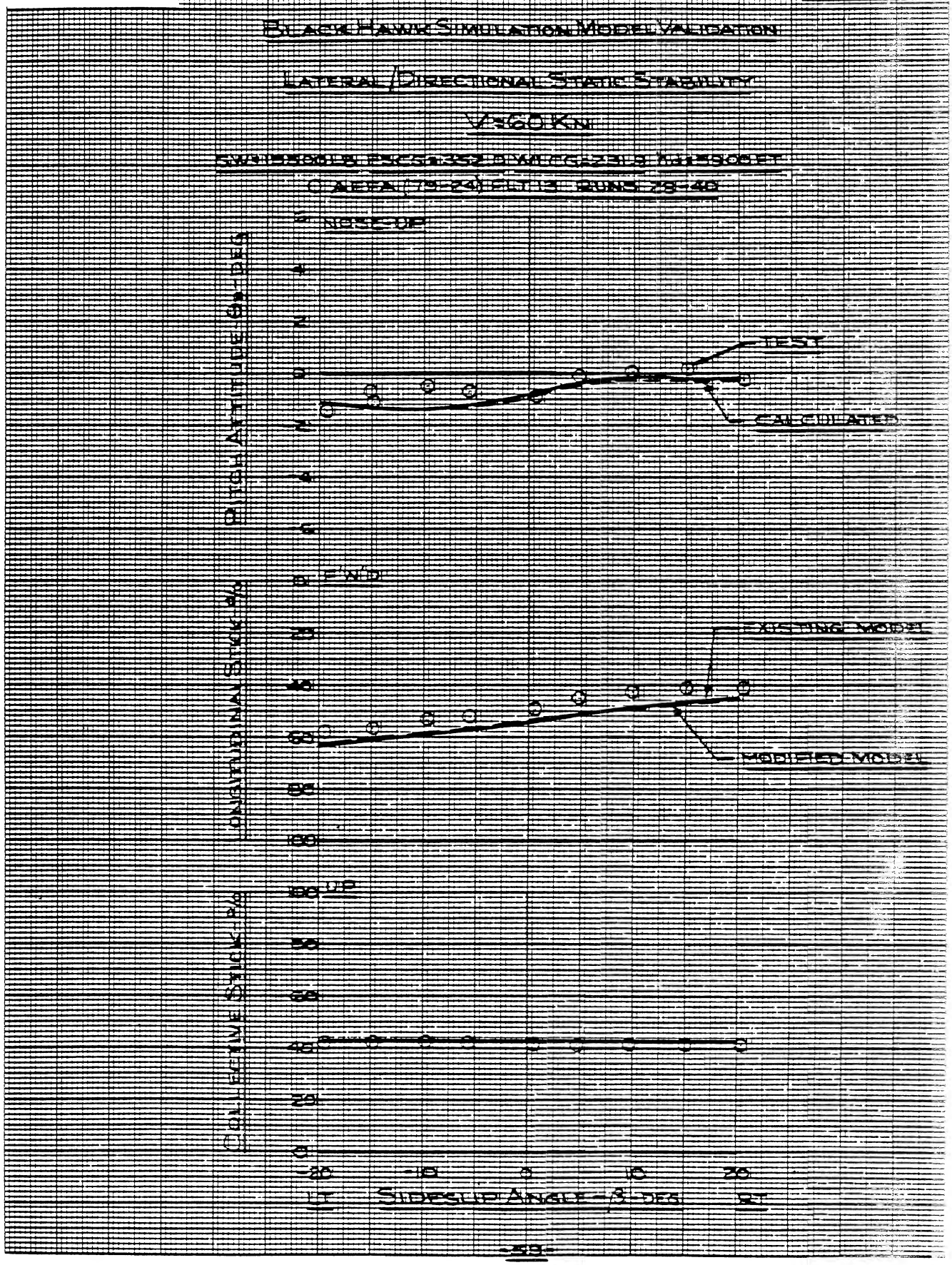

FIGURE 126

BLACK HAWK SIMULATION MODEL VALIDATION

LATERAL/DIRECTIONAL STATIC STABILITY

V=100 KN

GW=16000 LB FSCG=348.7 WLCG=231.6 Hp=5700 FT

○ AEFA(75-25) FLT 17 RUNS 18-27

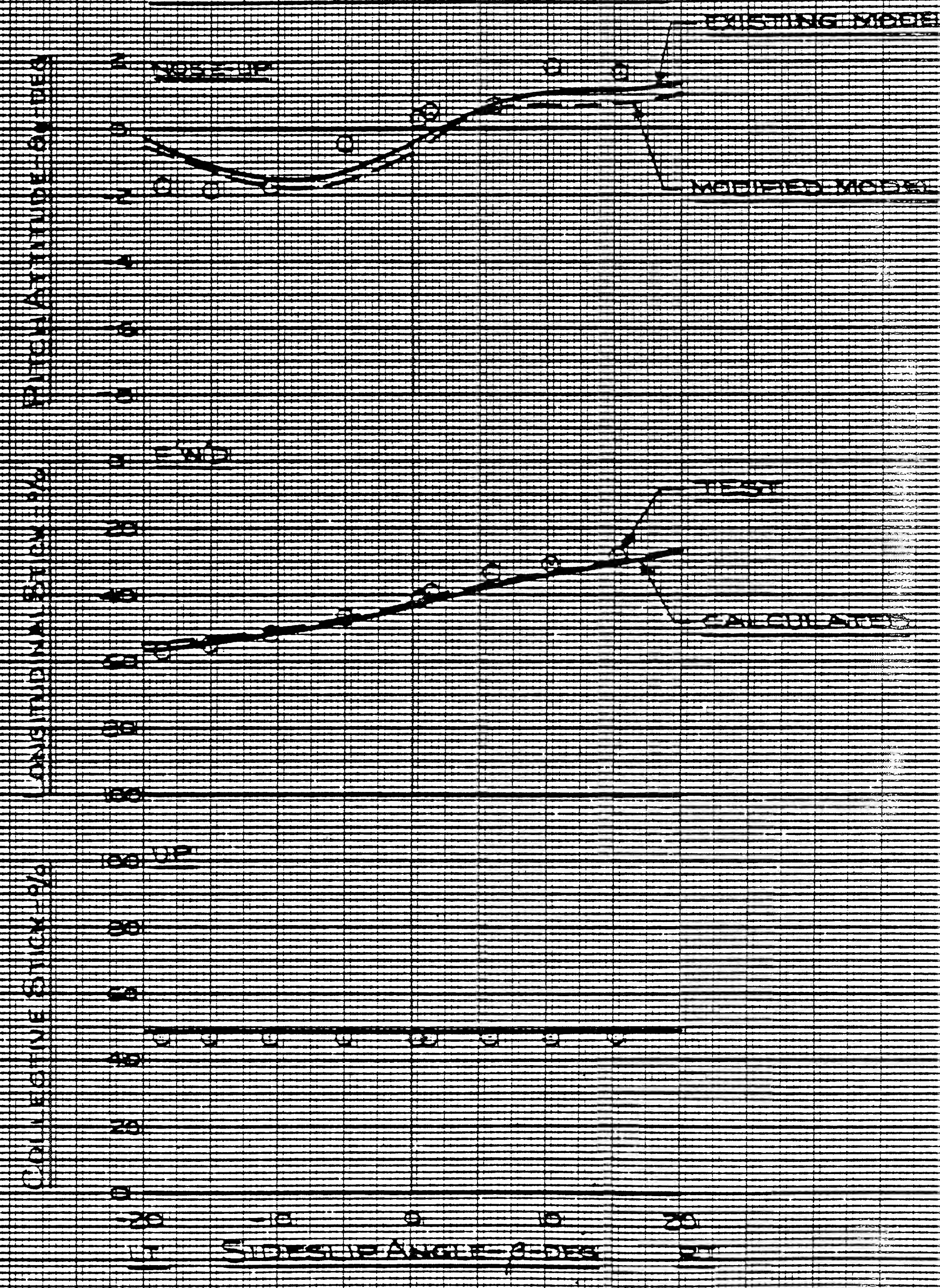

FIGURE 134

BLACK HAWK SIMULATION MODEL VALIDATION

LATERAL/DIRECTIONAL STATIC STABILITY

V=140 KN

GW=15750 LB FSCG=351.2 WLCG=231.8 Hd=5750 FT

O AEFA (79-24) FLT 19 RUNS 21-26

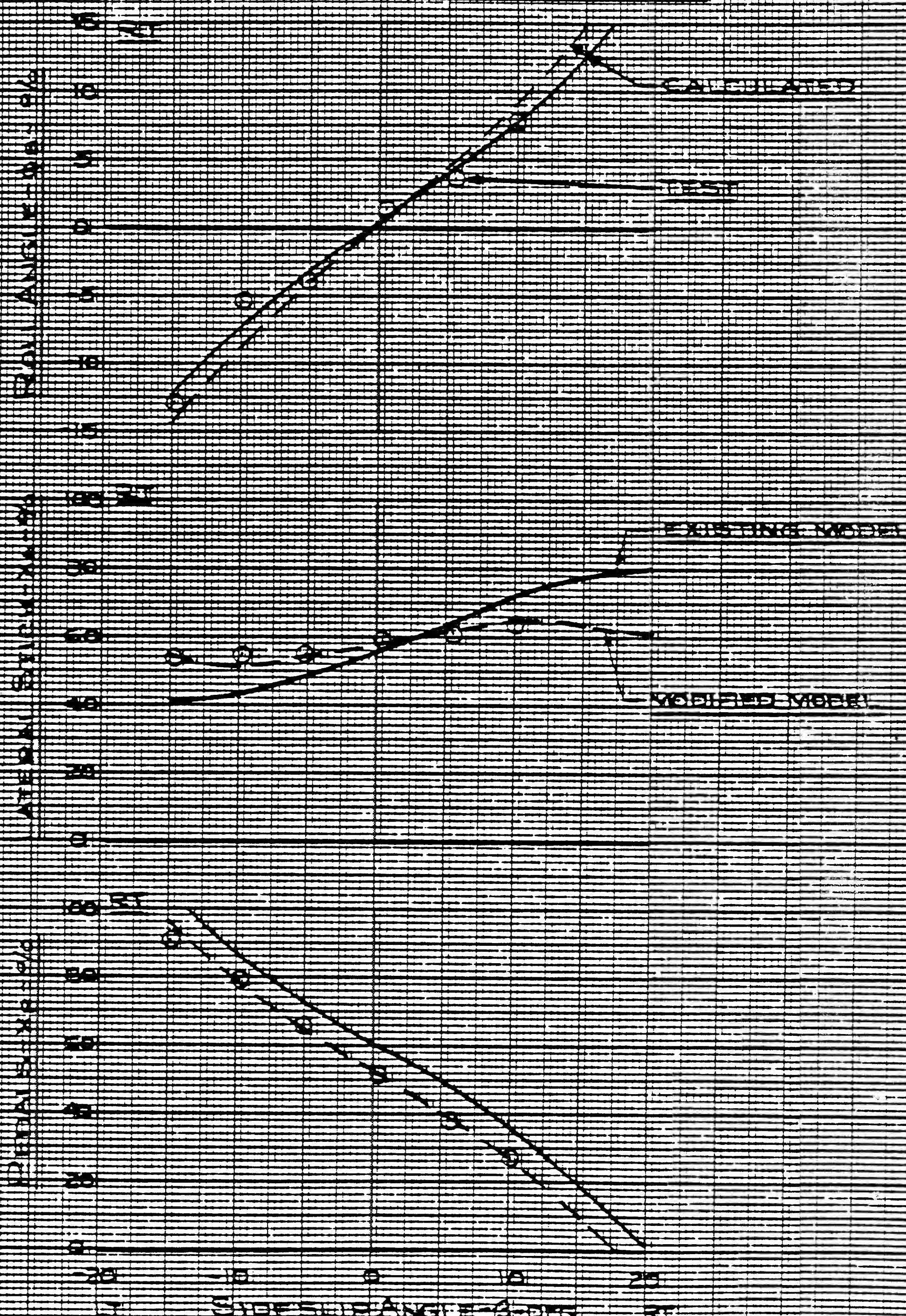

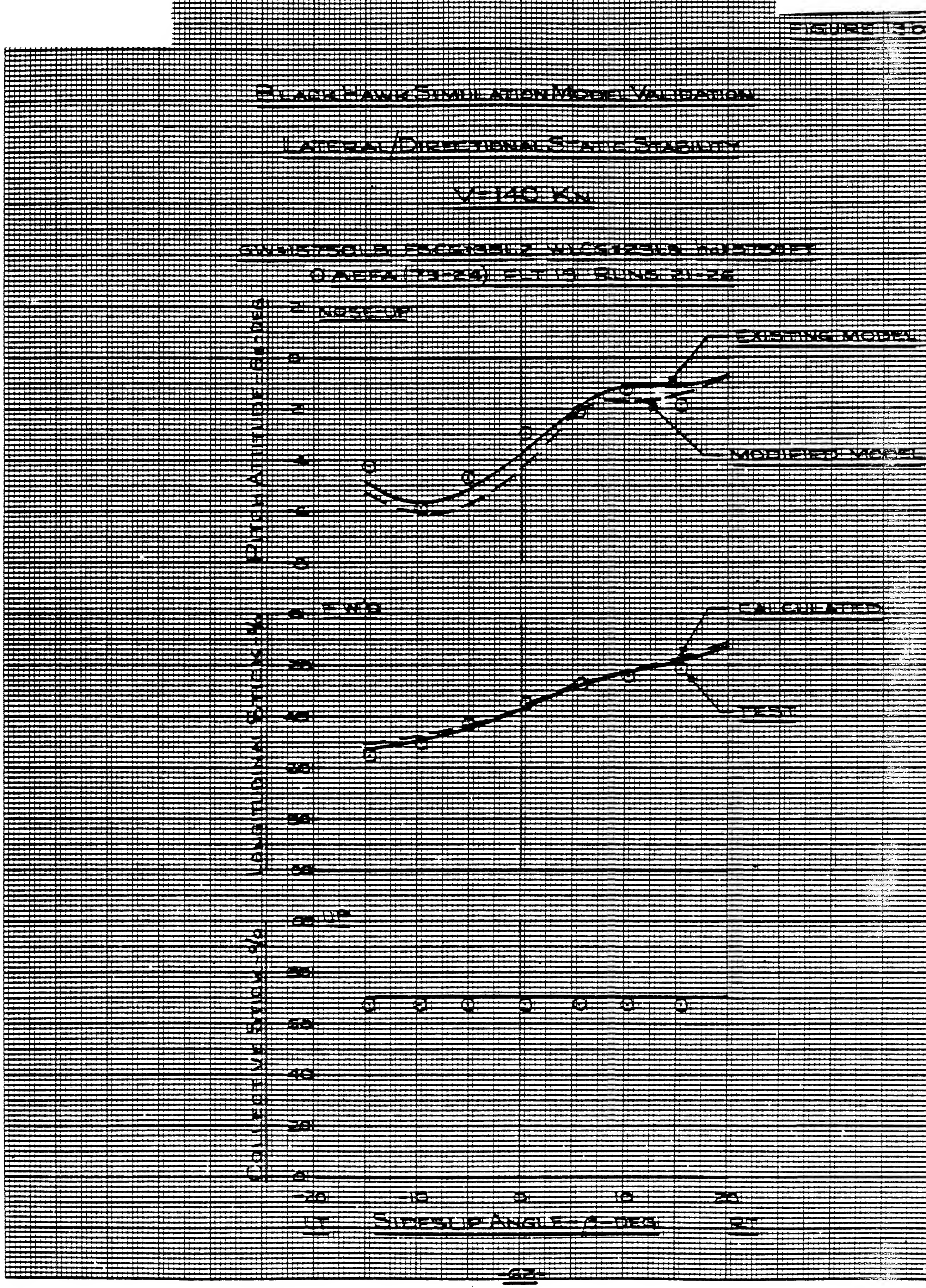

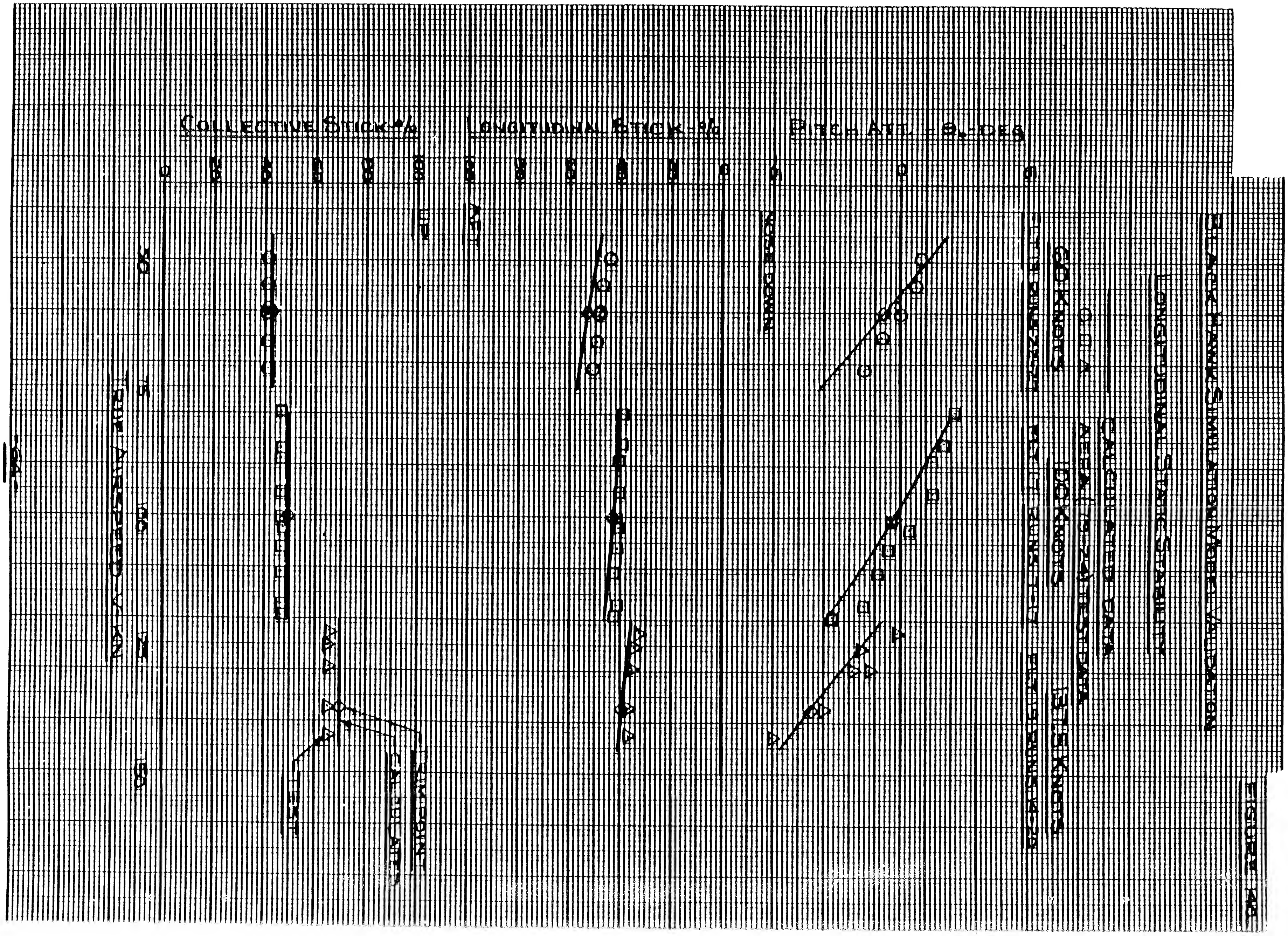

FIGURE 145

BLACK HAWK SIMULATION MODEL VALIDATION

LONGITUDINAL STATIC STABILITY

CALCULATED DATA

○ □ △ AEDC (TS-24) TEST DATA

60 KNOTS 100 KNOTS 137.5 KNOTS

FLT 19 RUNS 23-27 FLT 17 RUNS 7-17 FLT 19 RUNS 4-20

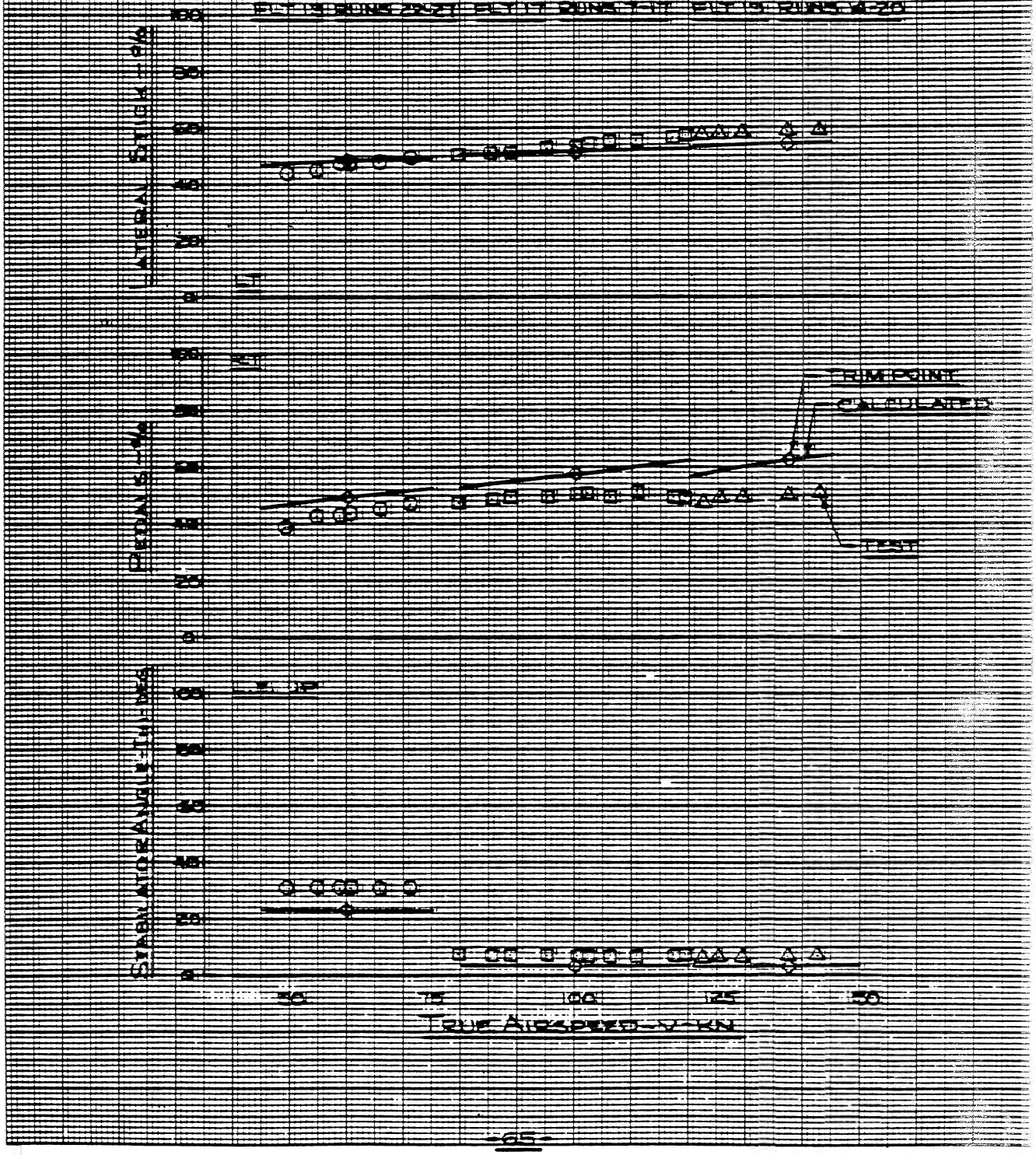

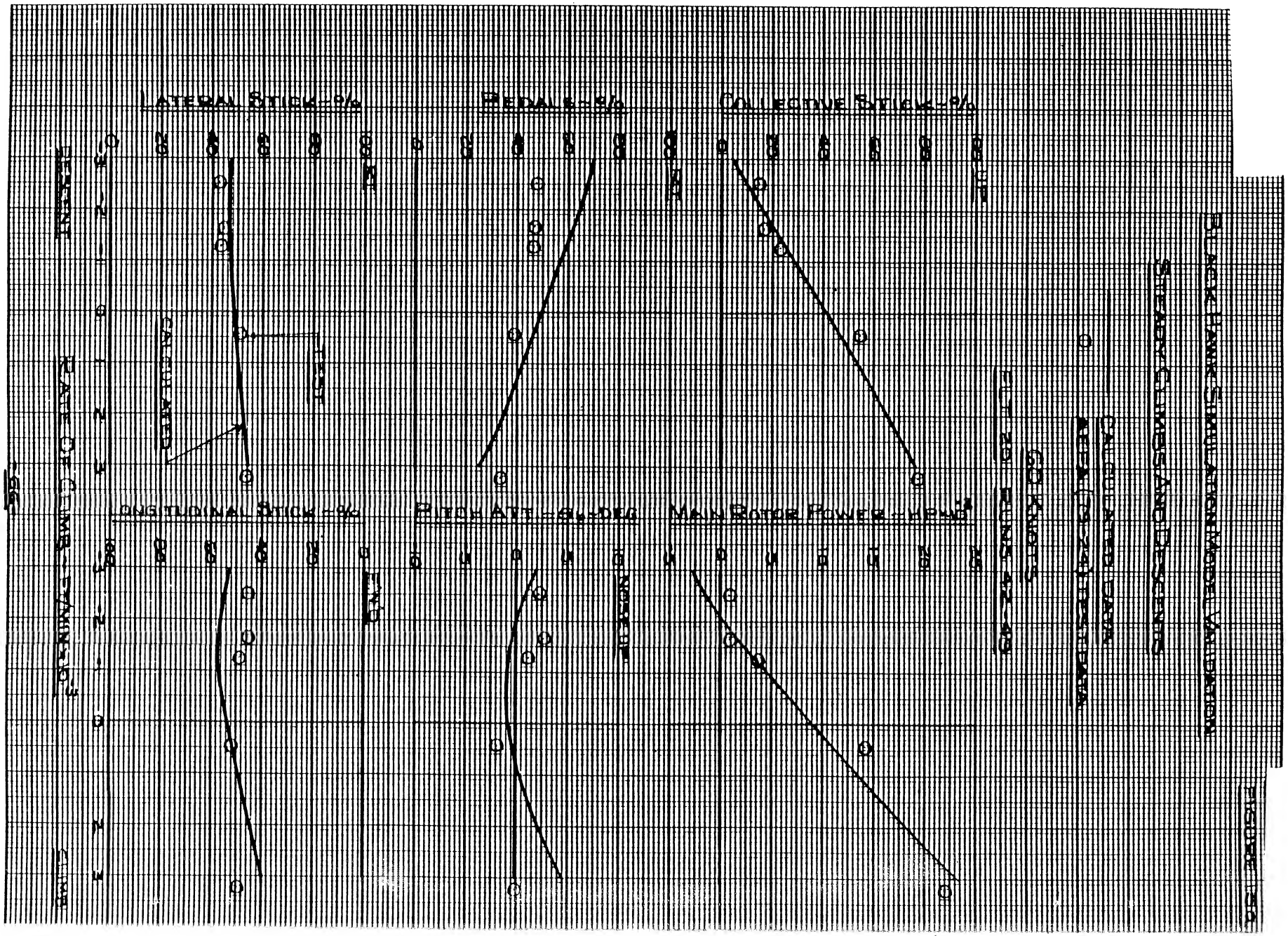

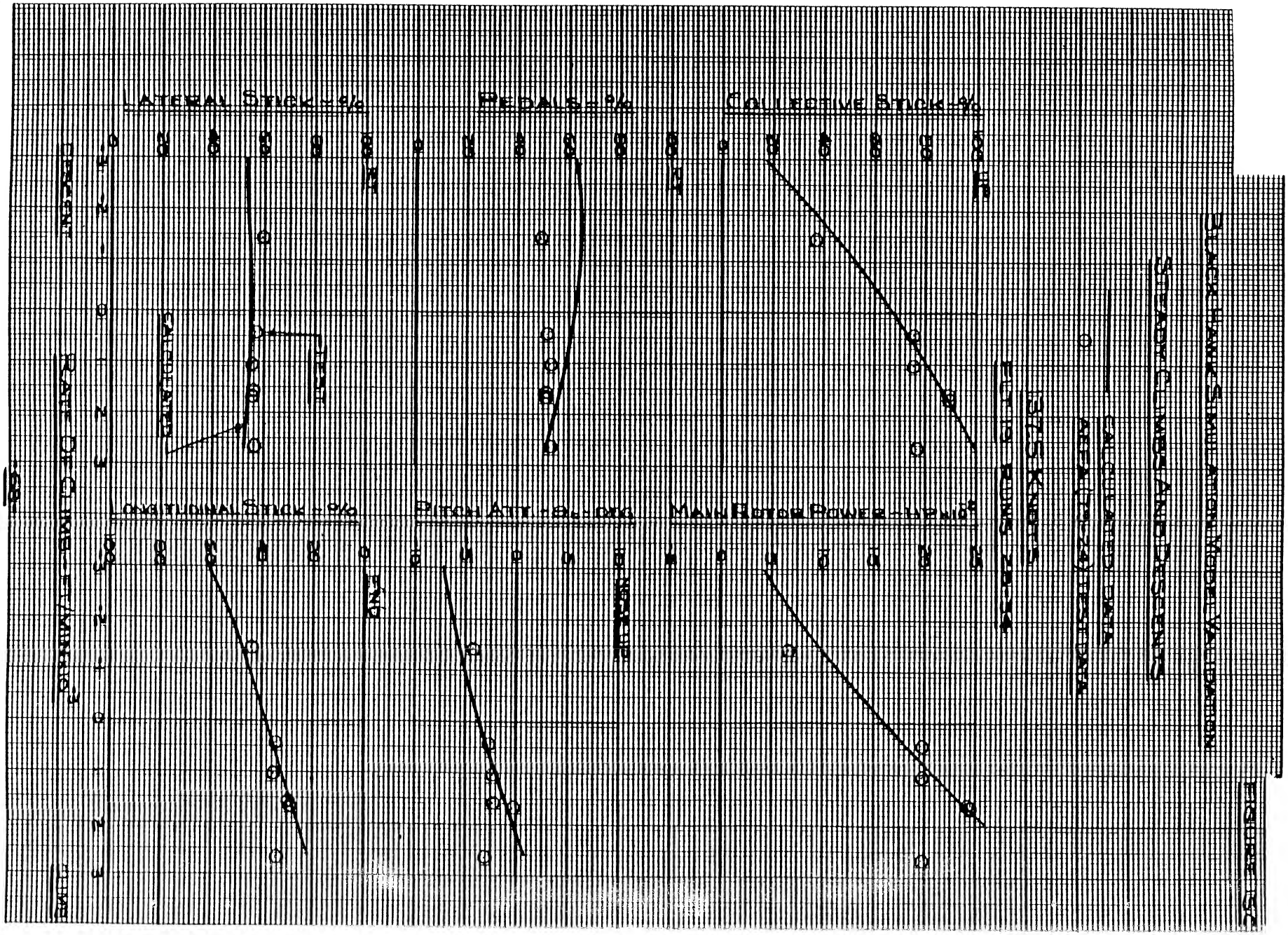

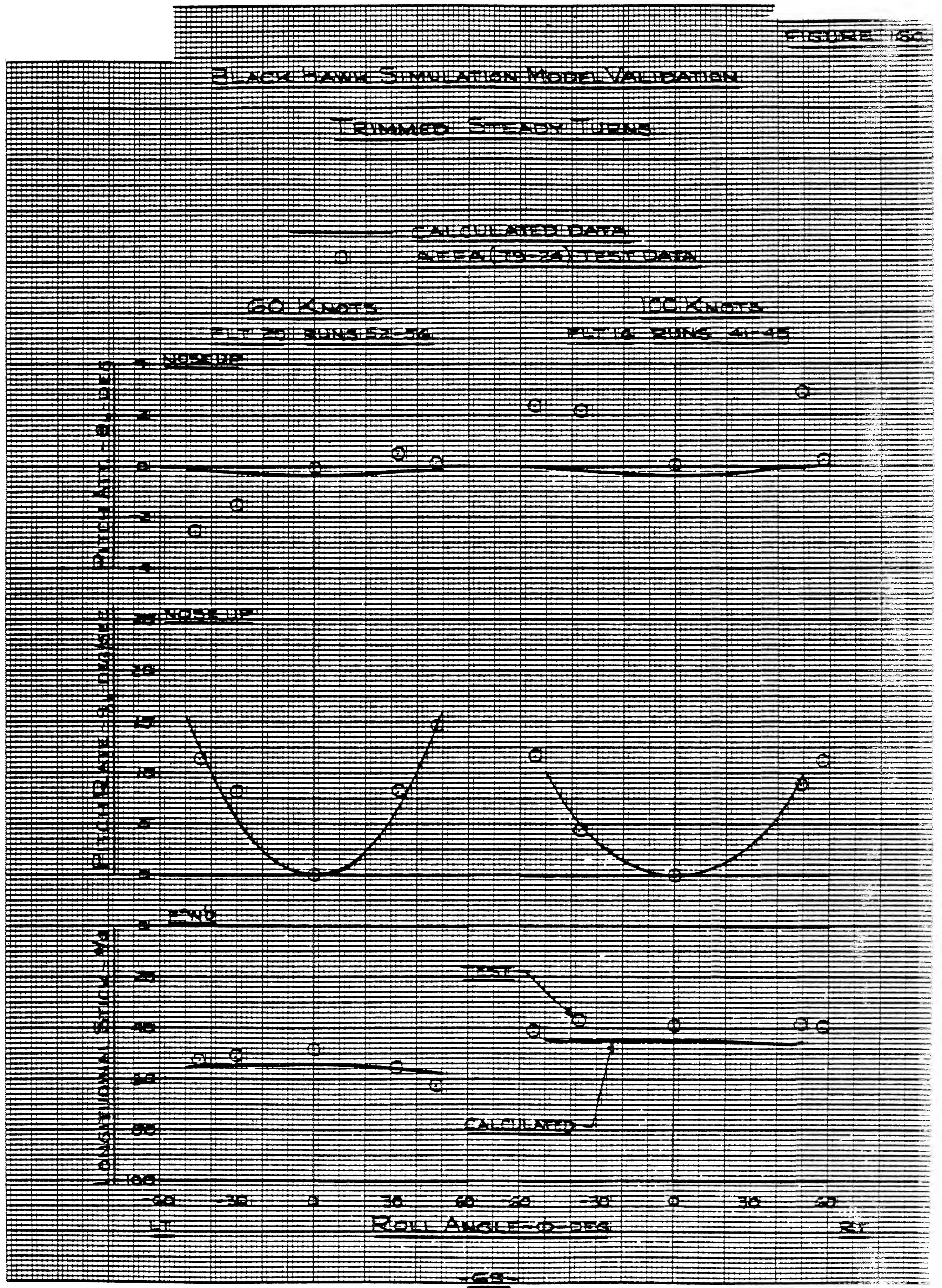

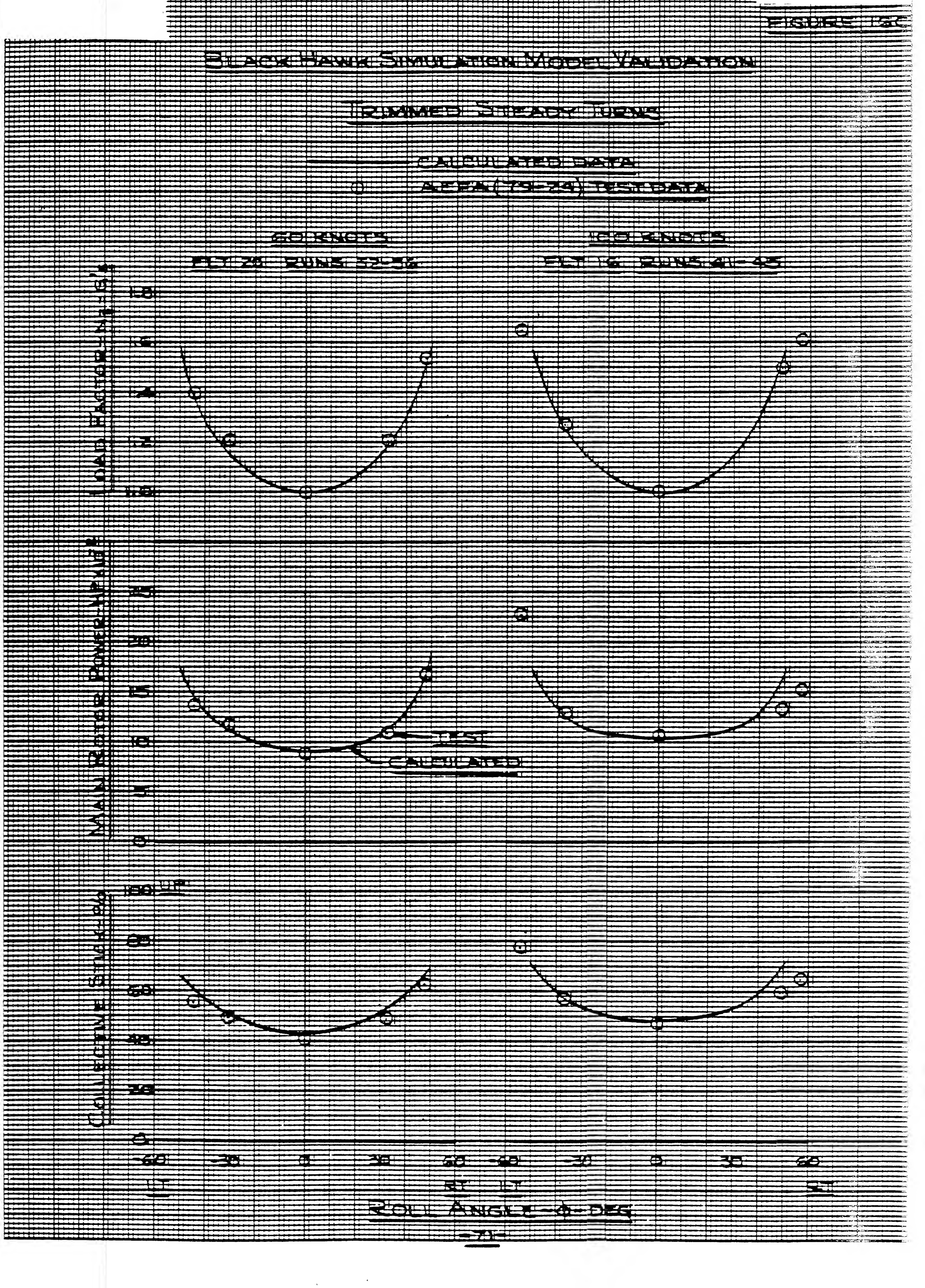

FIGURE 15

BLACK HAWK SIMULATION MODEL VALIDATION

ROTOR SPEED SWEEP

——— CALCULATED DATA

○ □ △ AEFA (79-24) TEST DATA

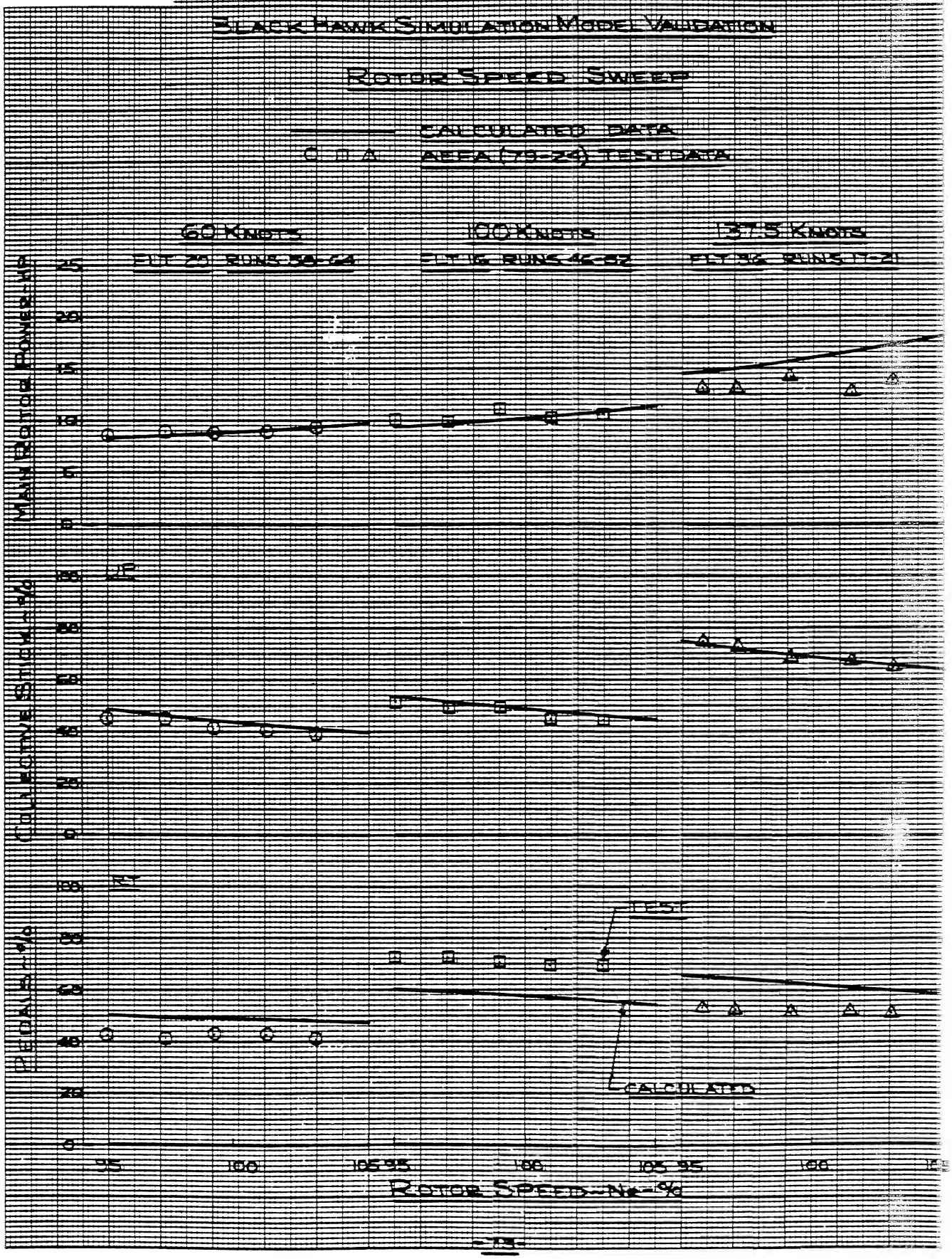

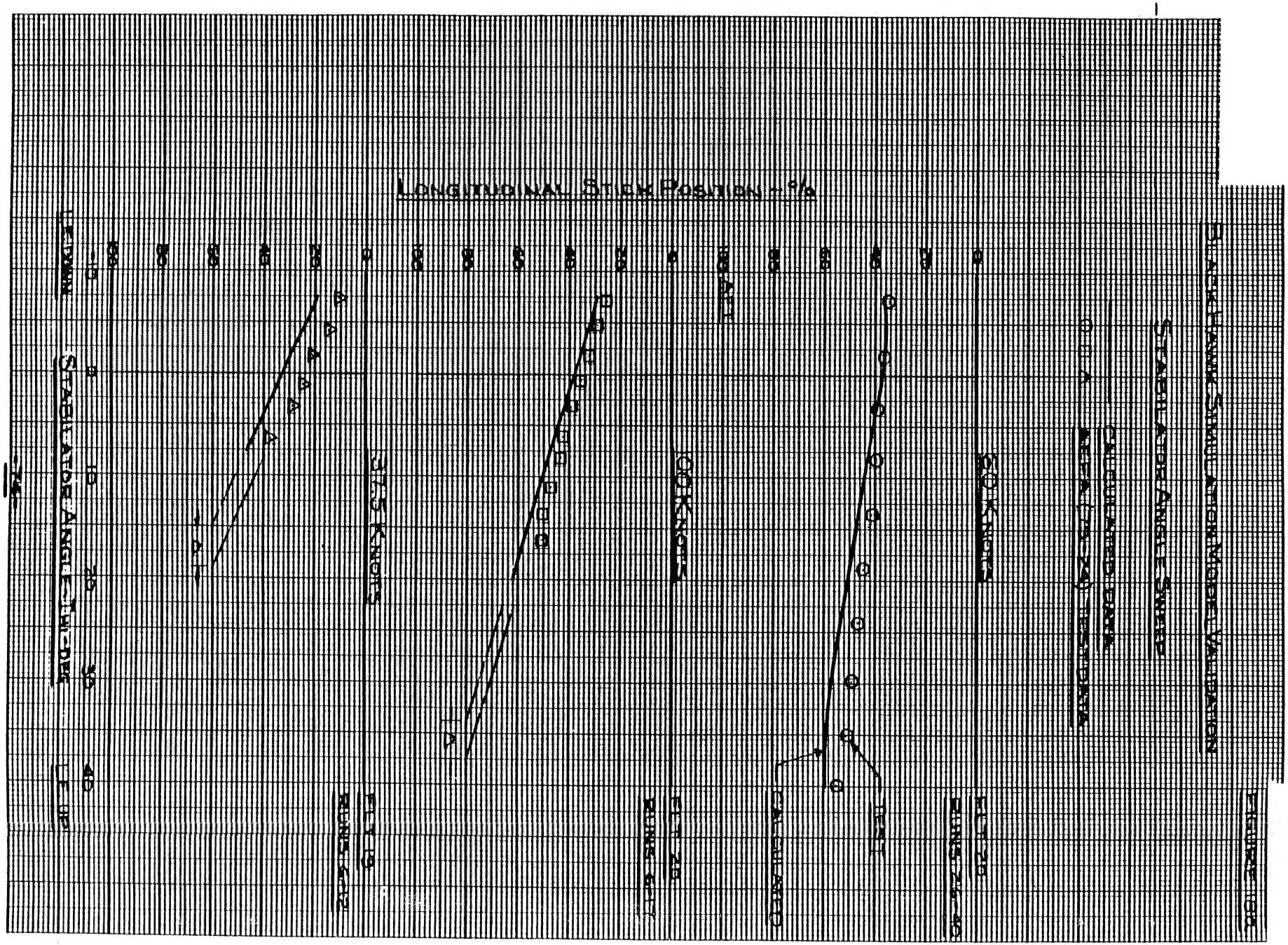

FIGURE 13b

BLACK HAWK SIMULATION MODEL VALIDATION

STABILATOR ANGLE SWEEP

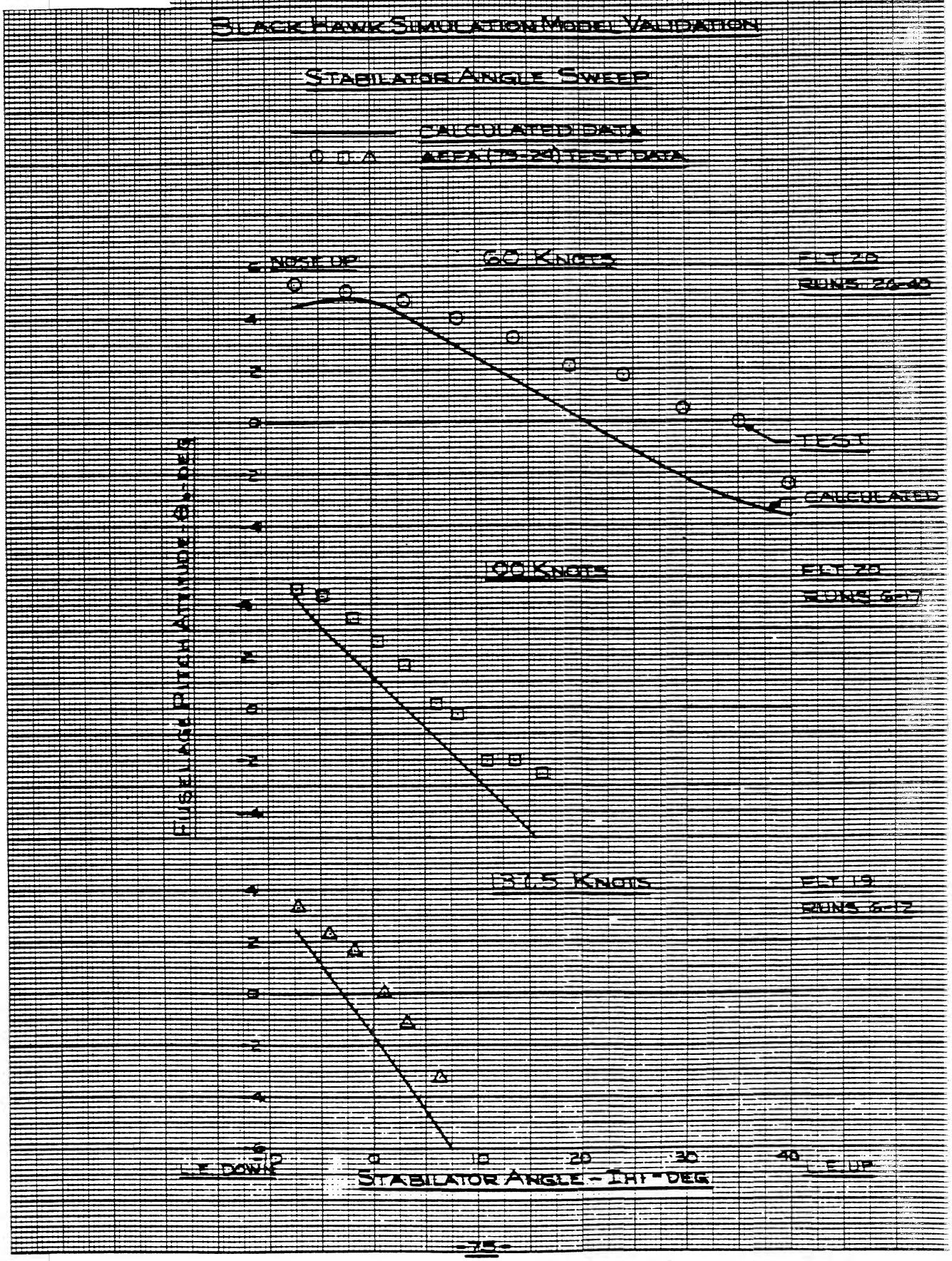

Figure 19a -

BLACKHAWK - NASA STUDY 1-FEB-84 13:23 (1/2)
AEFA TEST TAPE BHAWK2 7/28/82 FLT 508 RUN 27
HOVER COLL INPUT, LDS COLL LAG TAU = 0.0 SEC

VKT	.9999800E-3	WEIGHT	15940.000	FSCG	359.40000	IH1	44.400000
XA	5.1311577	XB	4.8915395	XC	5.9401567	XP	1.4379850
THETAB	4.3629094	PHIB	-2.5790894	OMGRAT	0.9955535	GGRPM	93.737382

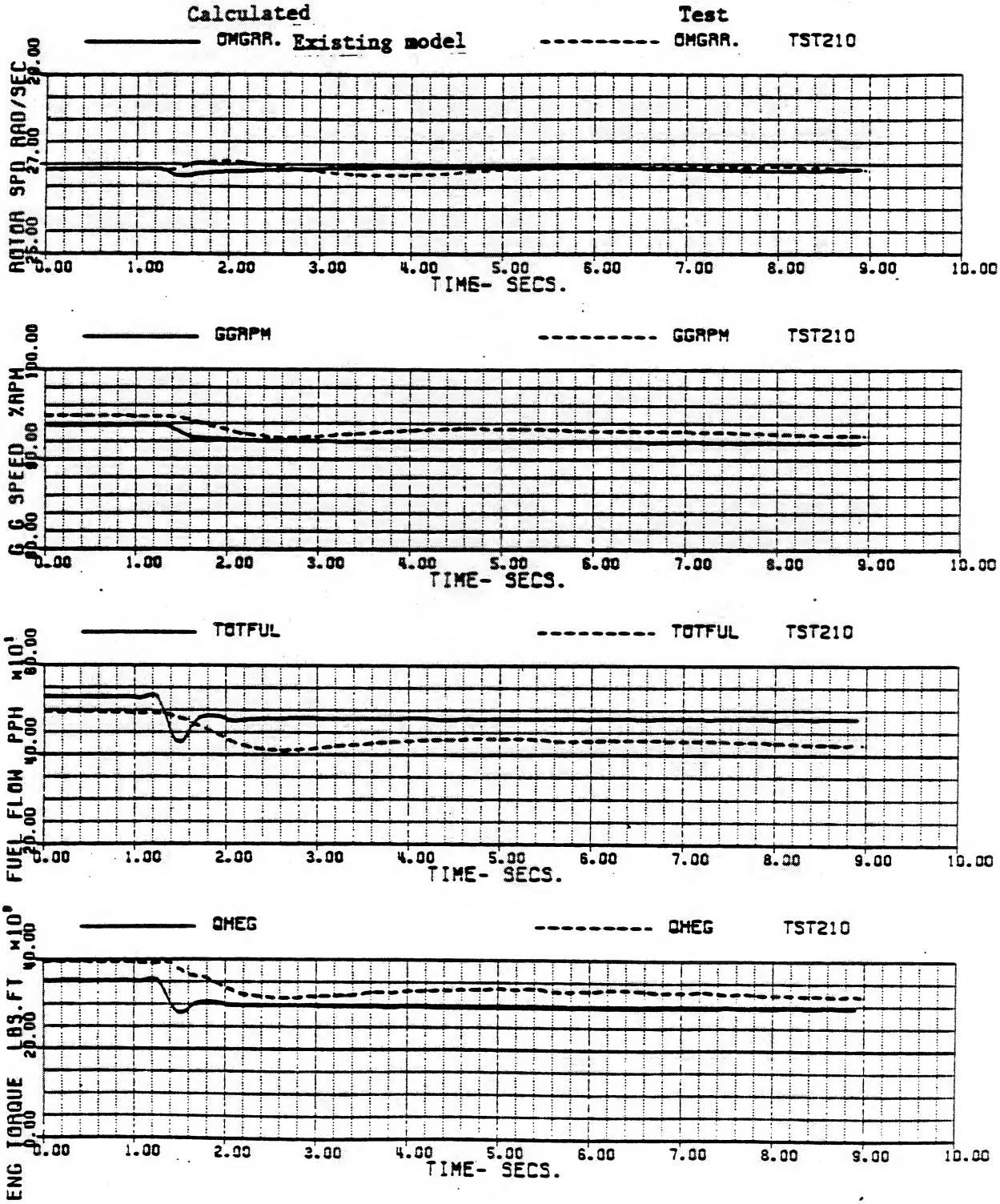

Figure 19b

BLACKHAWK - NASA STUDY 1-FEB-84 13:23 (2/2)

AEFA TEST TAPE BHAWK2 7/28/82 FLT 508 RUN 27
HOVER COLL INPUT, LDS COLL LAG TAU = 0.0 SEC

VKT	.999980E-3	WEIGHT	15940.000	FSCG	359.40000	IH!	44.400000
XA	5.1311577	XB	4.8915395	XC	5.9401567	XP	1.4379850
THETAB	4.3629094	PHIB	-2.5790894	OMGRAT	0.9955555	GGRPM	93.737382

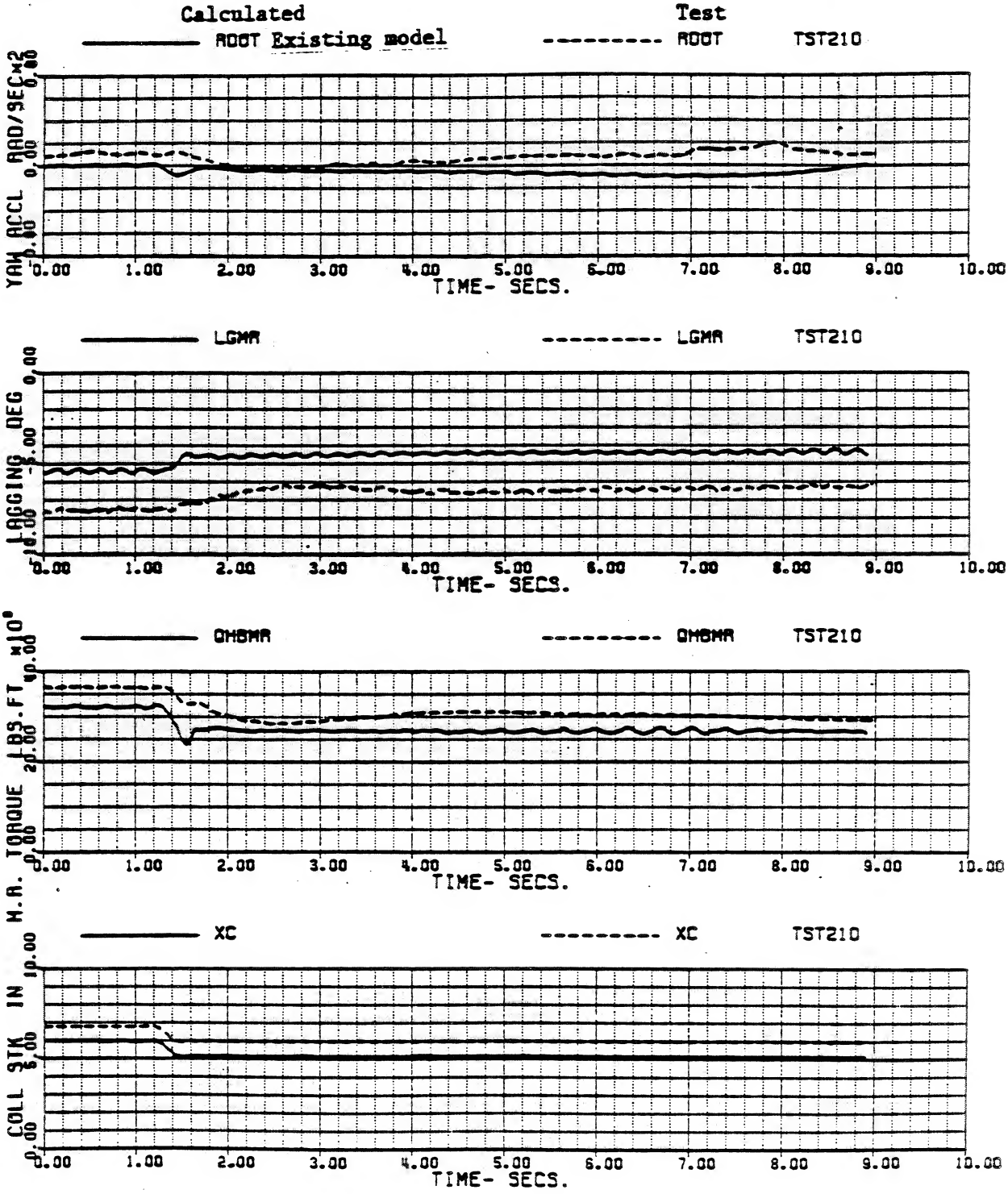

Figure 20a

BLACKHAWK - NASA STUDY 1-FEB-84 13:27 (1/2)

AEFA TEST TAPE BHAWK2 7/28/82 FLT 508 RUN 27
HOVER COLL INPUT. LDS COLL LAG TAU = 0.75 SEC

VKT	.999983E-3	WEIGHT	15940.000	FSCG	359.40000	IH1	44.400000
XA	5.1303934	XB	4.8912170	XC	5.9401001	XP	1.4365065
THETAB	4.3486081	PHIB	-2.6002522	OMGRAT	0.9955555	GGRPM	93.740830

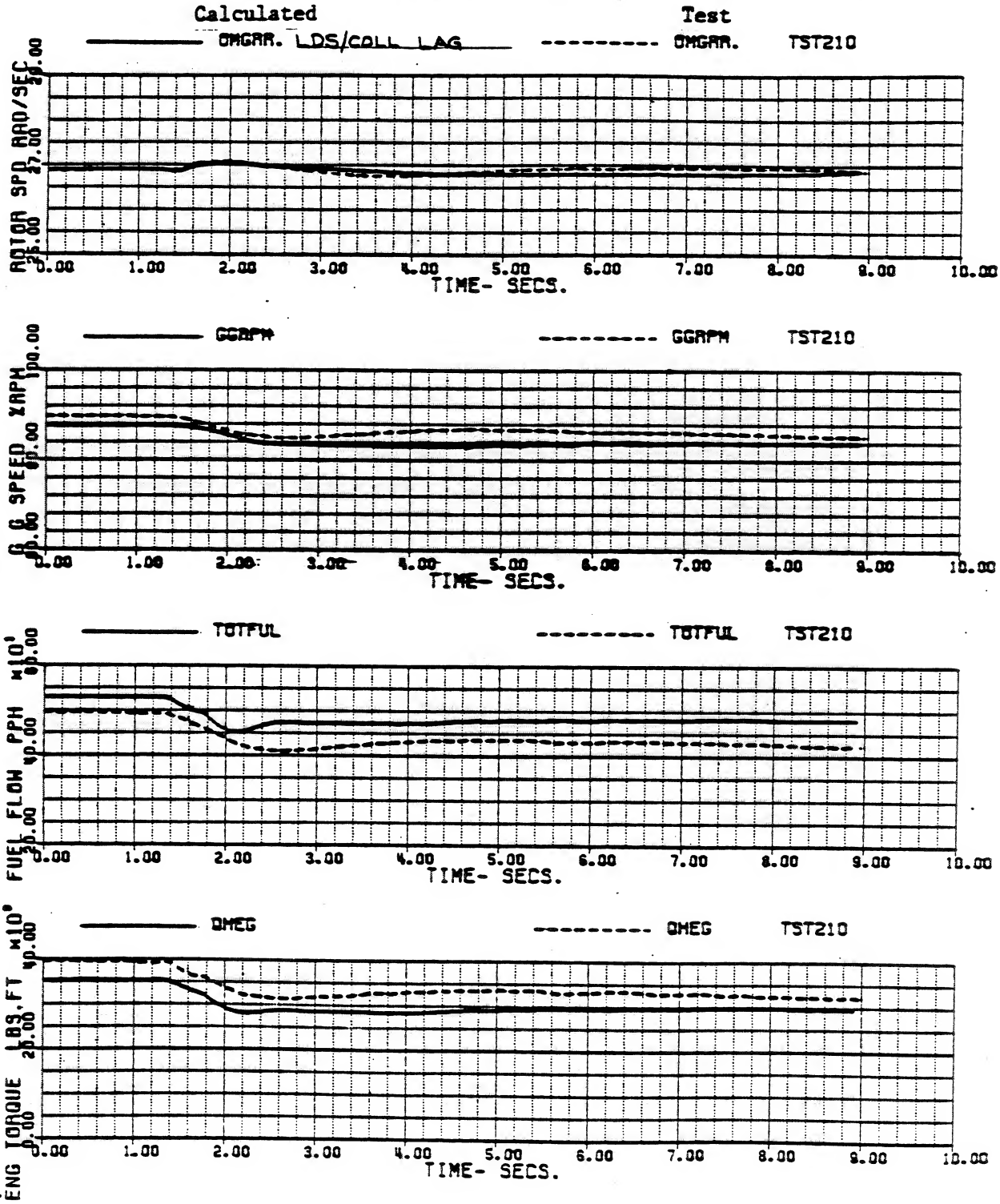

Figure 20b

BLACKHAWK - NASA STUDY 1-FEB-84 13:27 (2/2)

AEFA TEST TAPE BHAWK2 7/28/82 FLT 508 RUN 27
HOVER COLL INPUT, LDS COLL LAG TAU = 0.75 SEC

VKT	.999983E-3	WEIGHT	15940.000	FSCG	359.40000	IH1	44.400000
XA	5.1303934	XB	4.8912170	XC	5.9401001	XP	1.4365065
THETAB	4.3486081	PHIB	-2.6002522	OMGRAT	0.9955555	GGAPM	93.740830

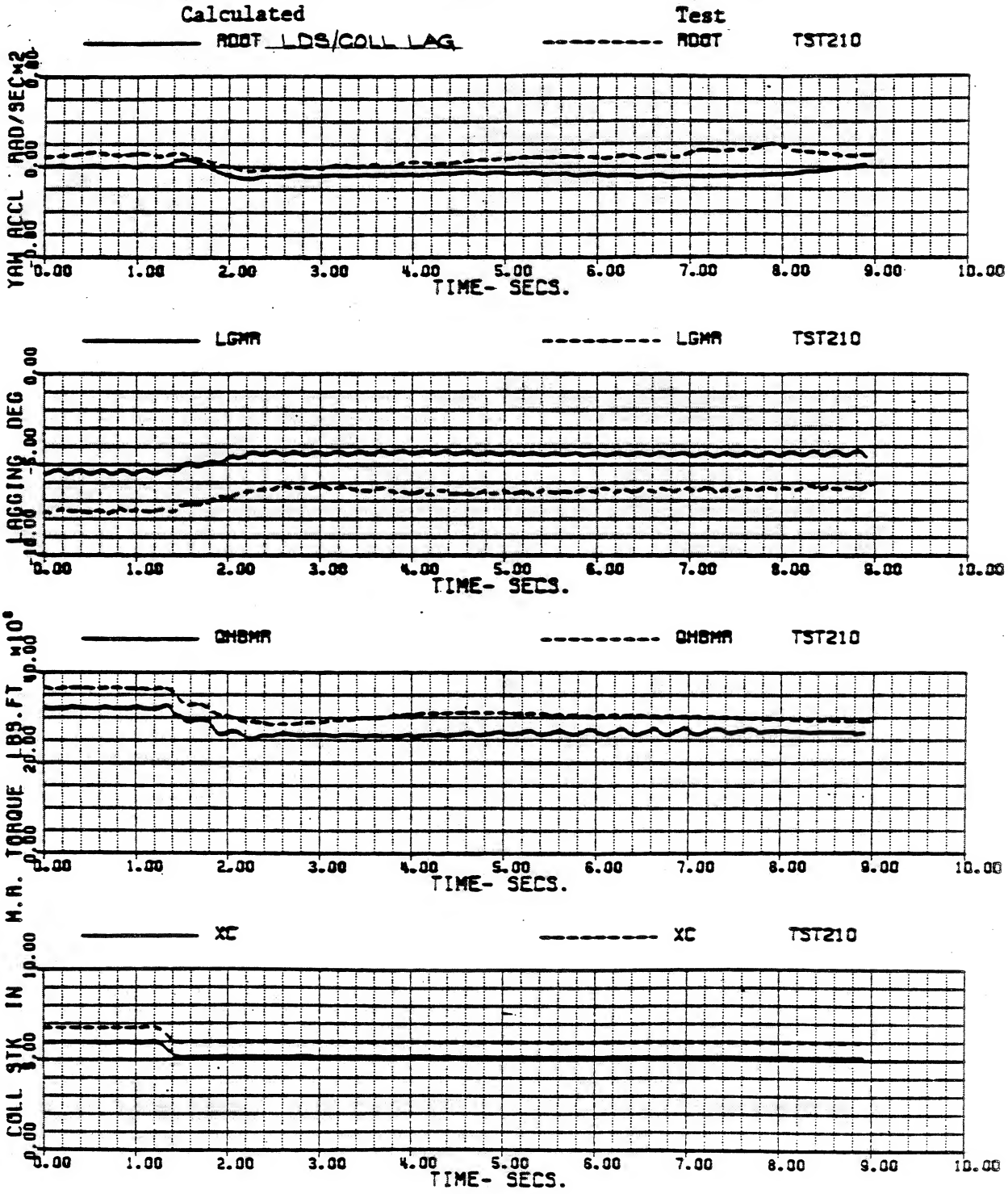

Figure 21

BLACKHAWK - NASA STUDY 13-APR-84 10:22 (1/2)
AEFA TEST TAPE BHAWK3 11/22/82 FLT 66 RUN 27
140 KN PEDAL INPUT, ITCALC + NMA=QHBMA (=2)

VKT	144.00143	WEIGHT	15410.000	FSCG	352.09999	IHL	3.0690999
XA	5.5880285	XB	3.7267280	XC	7.2753286	XP	3.5403678
THETAB	-3.7718707	PHIB	0.	OMGRAT	1.0111110	GGRPM	94.662789

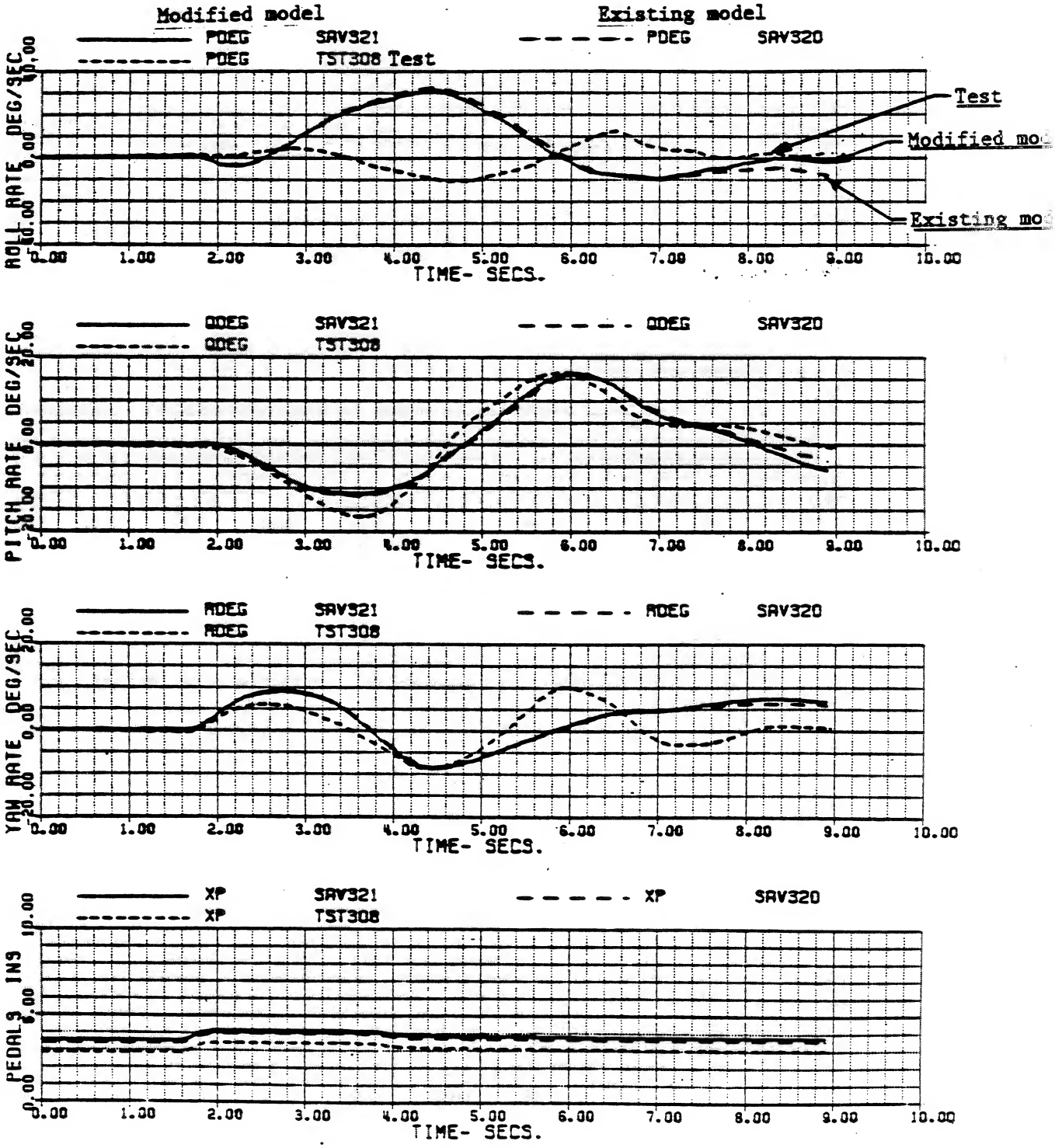

Figure 22a

BLACKHAWK - NASA STUDY 11-APR-84 14:24 (1/2)

AEFA TEST TAPE BHAWK2 7/28/82 FLT 508 RUN 27
HOVER COLL INPUT, LOS LAG 0.75 SEC., UPDATED MODEL

VKT	.9999468E-3	WEIGHT	15940.000	FSCG	359.40000	IH1	39.000000
XA	5.2077971	XB	4.9377300	XC	5.9503980	XP	1.6423207
THETAB	4.5816852	PHIB	-2.4123701	OMGRAT	0.9955555	GGRPM	93.780563

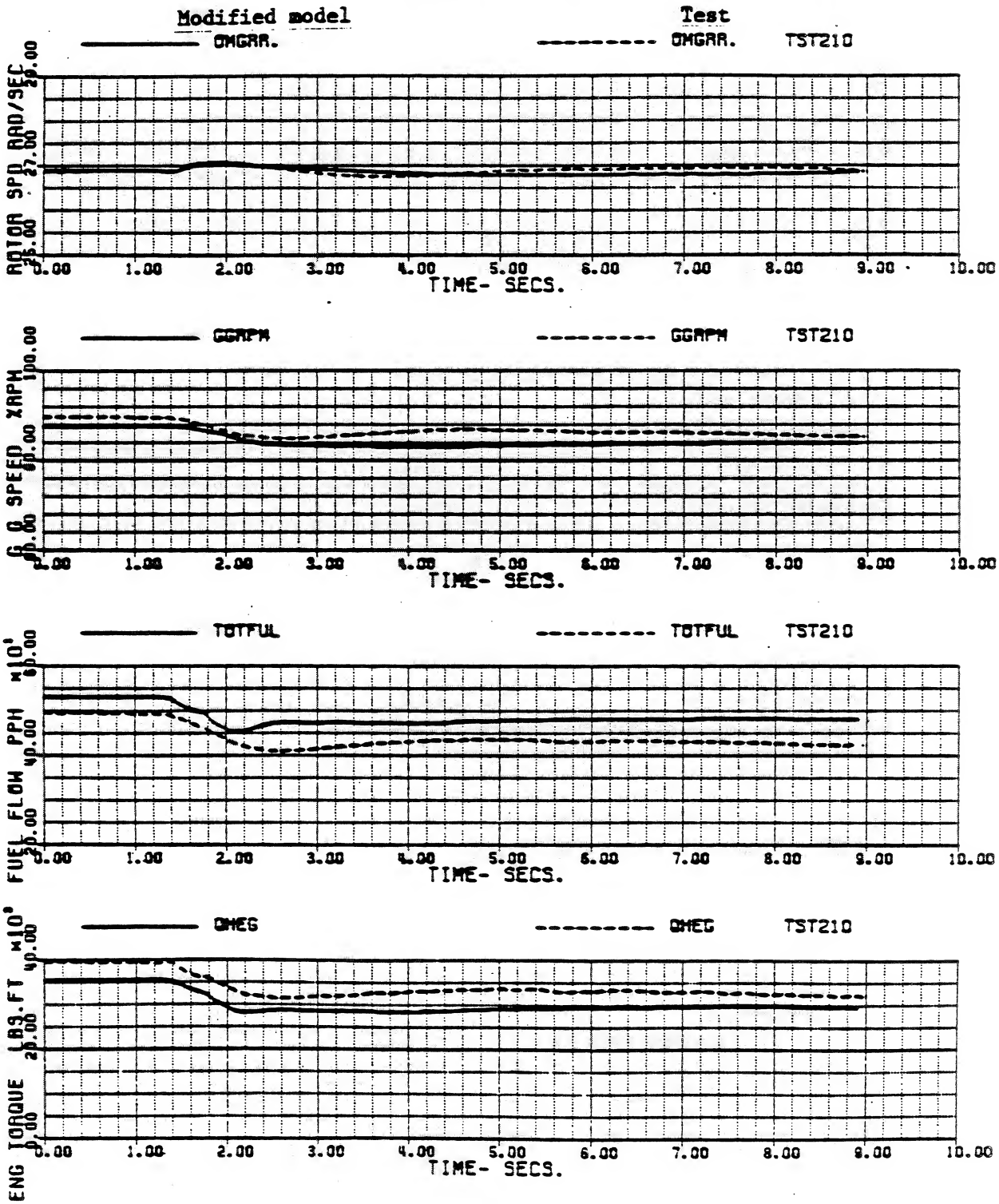

Figure 22b

BLACKHAWK - NASA STUDY 11-APR-84 14:24 (2/2)
AEFA TEST TAPE BHAWK2 7/28/82 FLT 508 RUN 27
HOVER COLL INPUT, LDS LAG 0.75 SEC., UPDATED MODEL

VKT	.9999946E-3	WEIGHT	15940.000	FSCG	359.40000	IH1	39.000000
XB	5.2077971	XB	4.9377300	XC	5.9503980	XP	1.6423207
THETAB	4.5816852	PHIB	-2.4123701	OMGRAT	0.9955555	GGRPM	93.780563

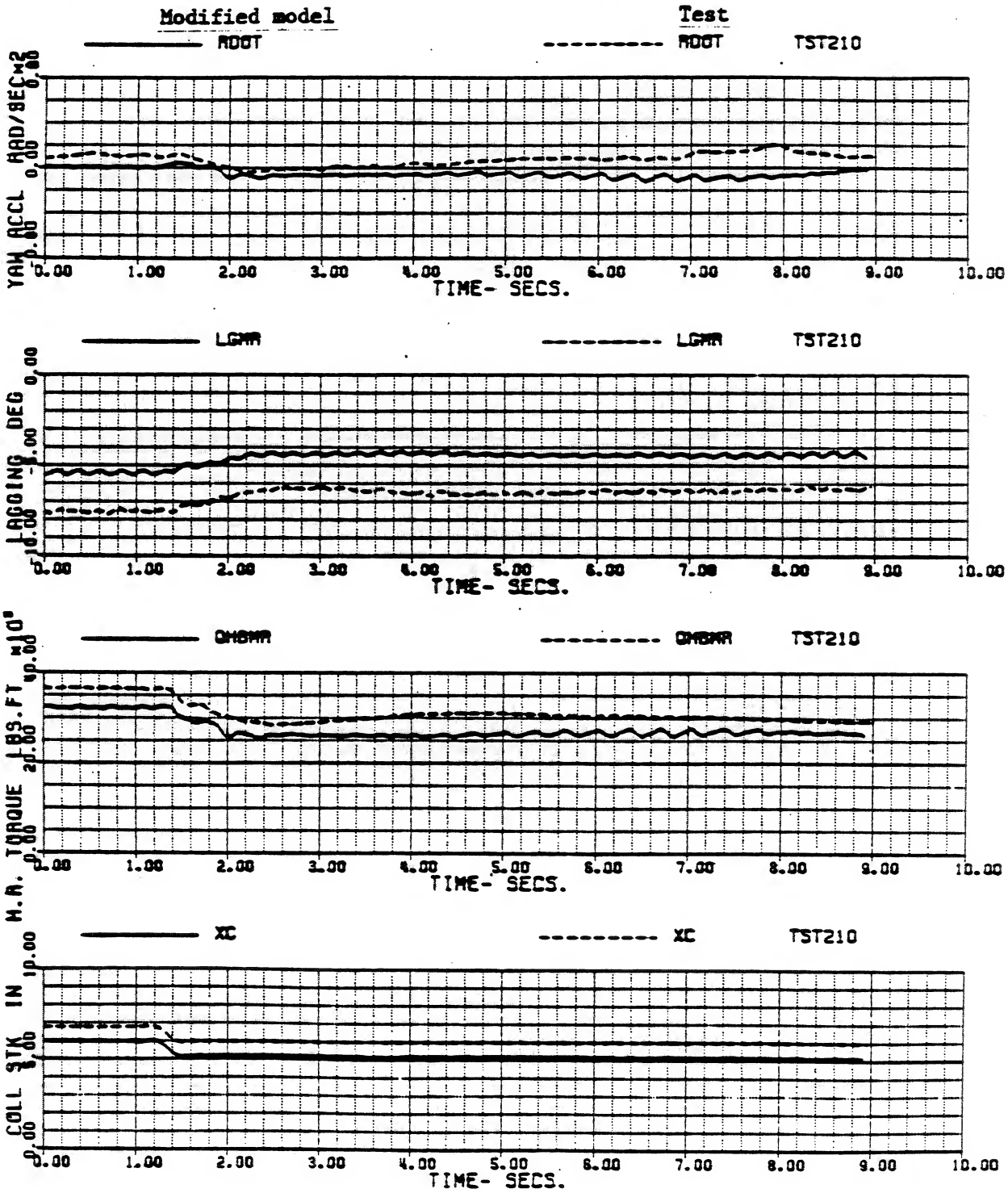

FIGURE 13

BLACK HAWK SIMULATION MODEL VALIDATION

TAIL ROTOR RIGGING

USAAVSCOM PROJECT 79-24 AIRCRAFT S/N 79-23716

YAW SYSTEM STOPS AT 24° AND -9.5° PEDAL

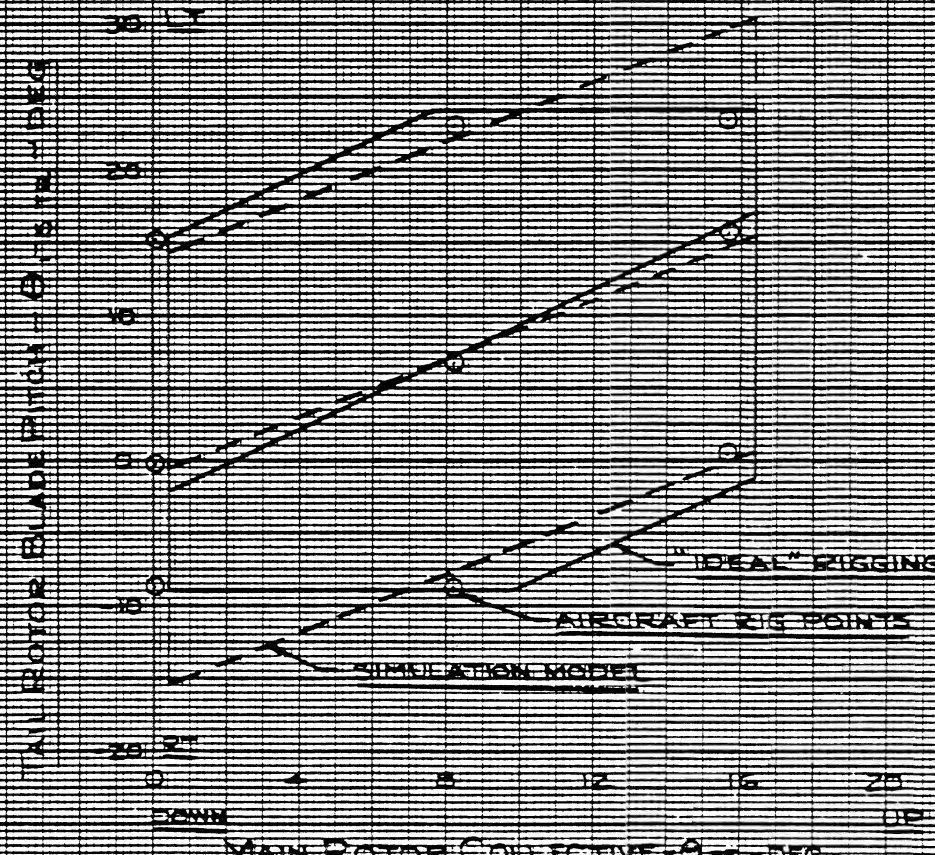

MAIN ROTOR COLLECTIVE -9.5 DEG

Figure 24a

BLACKHAWK - NASA STUDY 17-APR-84 11:13 (1/2)

AEFA TEST TAPE BHAWK3 11/22/82 FLT 66 RUN 27
140 KN PEDAL INPUT, (=4) +DOWNWASH CORRECTION (=5)

VKT	144.00239	WEIGHT	15410.000	FSCG	352.09999	IH1	2.9257000
XA	5.8478359	XB	3.5036866	XC	7.2577255	XP	2.8745256
THETAB	-4.1980354	PHIB	0.	OMGRAT	1.0111110	GGRPM	94.608449

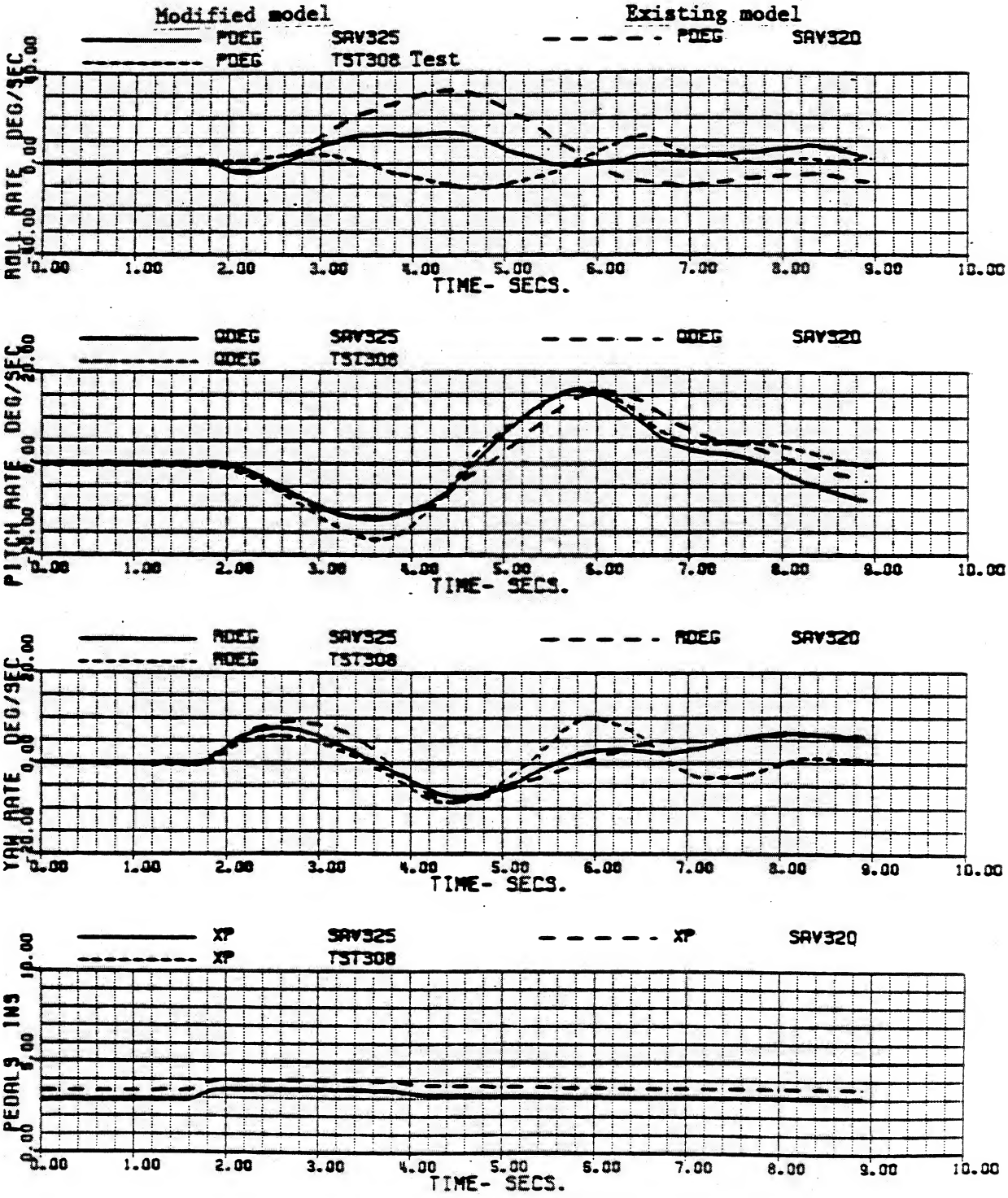

Figure 24b

BLACKHAWK -- NASA STUDY 17-APR-84 11:13 (2/2)

AEFA TEST TAPE BHAWK3 11/22/82 FLT 66 RUN 27
140 KN PEDAL INPUT. (=4) +DOWNWASH CORRECTION (=5)

VKT	144.00239	WEIGHT	15410.000	FSCG	352.09999	IHT	2.9257000
XA	5.8478359	XB	3.5036866	XC	7.2577255	XP	2.8745256
THETA8	-4.1980354	PHIB	0.	OMGRAT	1.0111110	GGRPM	94.608449

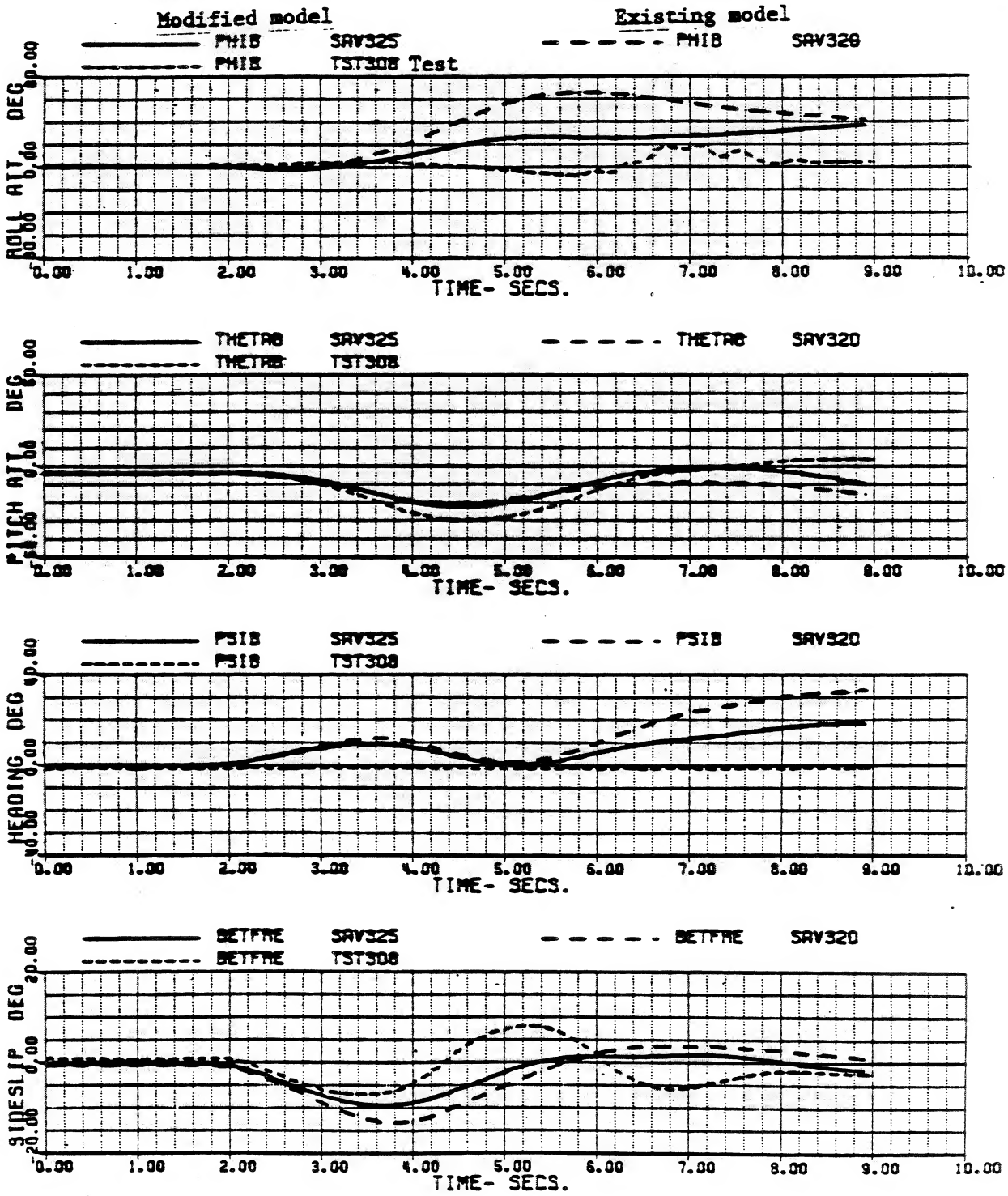

Figure 25a

BLACKHAWK - NASA STUDY 18-APR-84 11:13 (1/2)
AEFA TEST TAPE BHAWK3 11/22/82 FLT 66 RUN 27
140 KN PEDAL INPUT, (=5) +DWSHTR LAG 0.05 SEC (=6)

VKT	144.00261	WEIGHT	15410.000	FSCG	352.09999	IH1	2.9257000
XB	5.8472294	XB	3.5027564	XC	7.2570822	XP	2.8740942
THETAB	-4.1926890	PHIB	0.	OMGRAT	1.0111110	GGAPM	94.626825

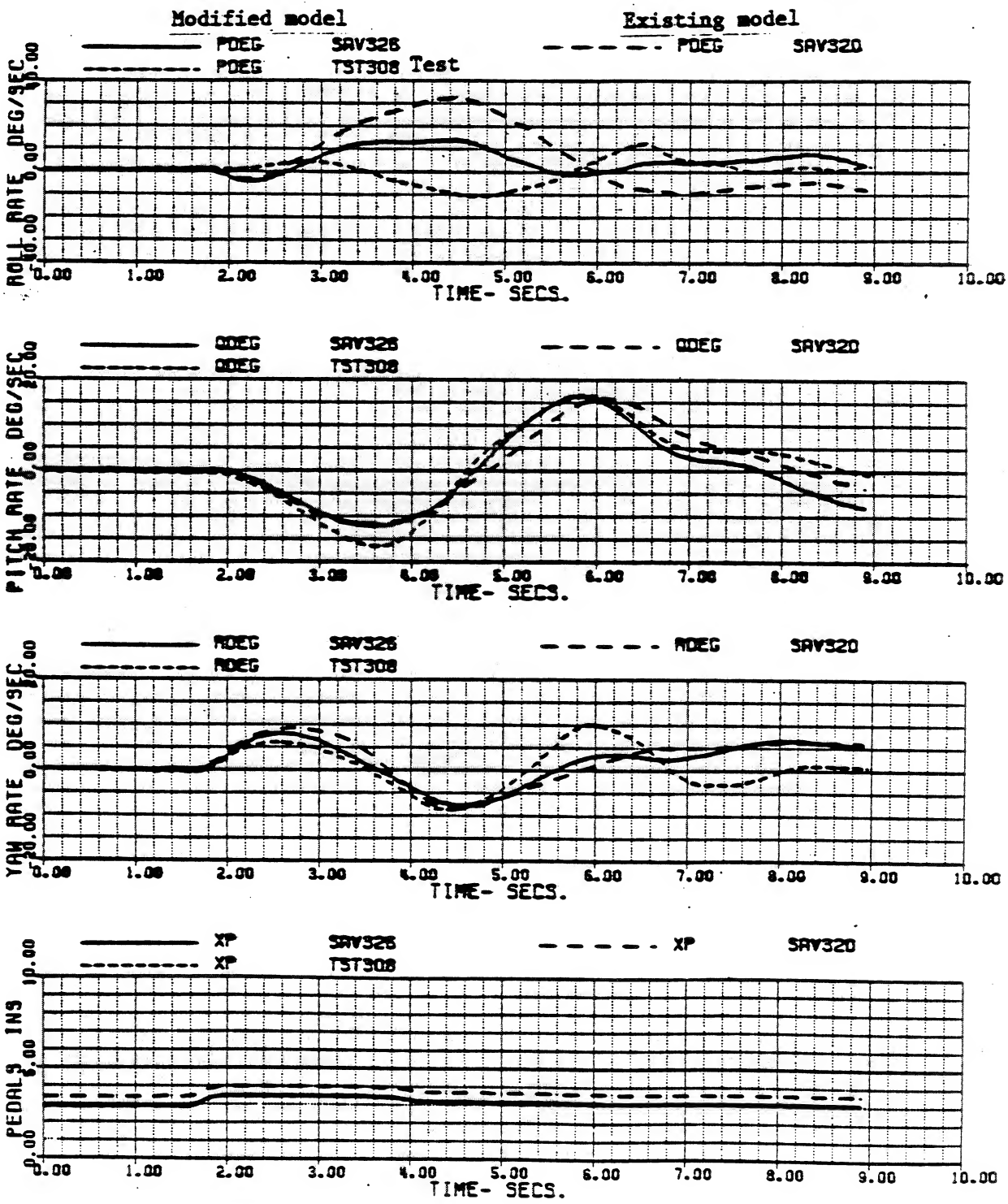

C-25-3

Figure 25b

BLACKHAWK - NASA STUDY 18-APR-84 11:13 (2/2)

AEFA TEST TAPE BHAWK3 11/22/82 FLT 66 RUN 27
140 KN PEDAL INPUT. (#5) +OWSHTR LAG 0.05 SEC (#6)

VKT	144.00261	WEIGHT	15410.000	FSCG	352.09999	IHI	2.9257000
XA	5.8472294	XB	3.5027564	XC	7.2570822	XP	2.8740942
THETA8	-4.1926890	PHIB	0.	OMGRAT	1.0111110	GGRPM	94.626825

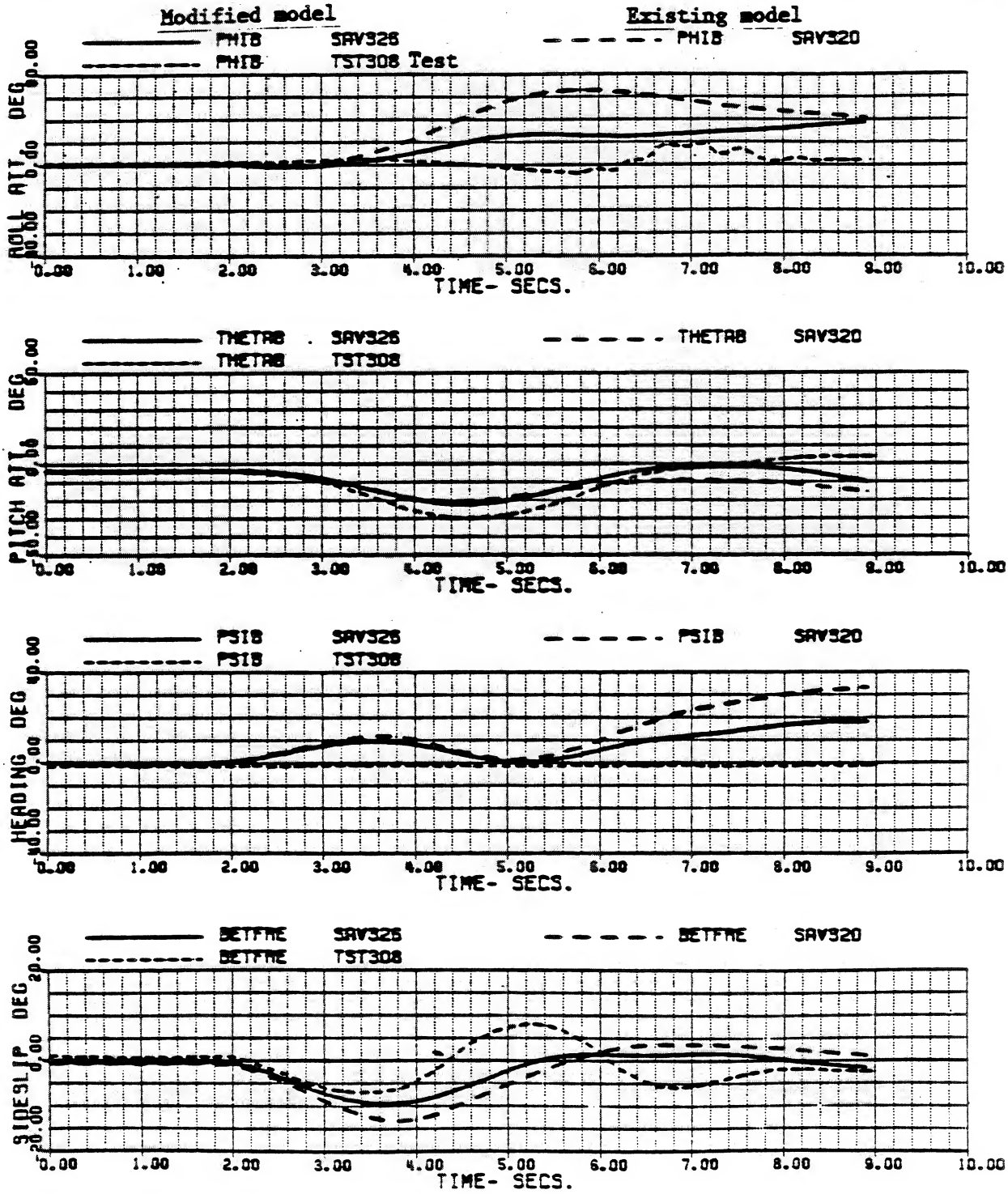

Figure 26

BLACKHAWK - NASA STUDY 19-APR-84 16:53 (1/2)

AEFA TEST TAPE BHAWK3 11/22/82 FLT 66 RUN 27
140 KN PEDAL INPUT, (=6) +OWSHTR ON V.T. (K=1.2) (=8)

VKT	143.98855	WEIGHT	15410.000	FSCG	352.09999	IHI	2.9257000
XA	5.5714135	XB	3.5263118	XC	7.2007847	XP	2.3521451
THETAB	-4.9339745	PHIB	0.	OMGRAT	1.0111110	GGRPM	94.510575

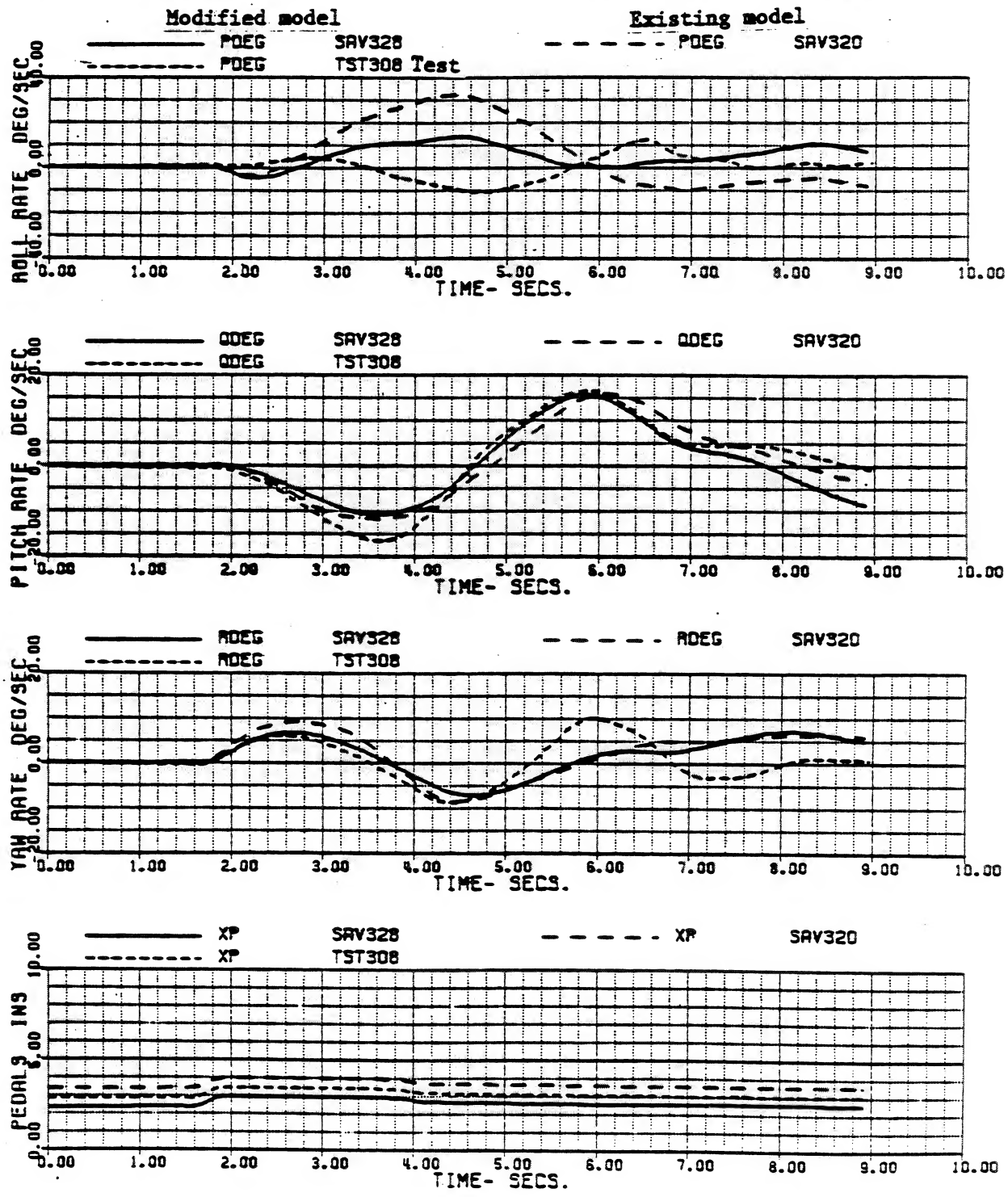

Figure 27

BLACKHAWK - NASA STUDY 19-APR-84 14:05 (1/2)

AEFA TEST TAPE BHAWK3 11/22/82 FLT 66 RUN 27
140 KN PEDAL INPUT, (#6) +H.T. ROLL DAMPING (#7)

VKT	144.00261	WEIGHT	15410.000	FSCG	352.09999	IH1	2.9257000
XA	5.8472294	XB	3.5027564	XC	7.2570822	XP	2.8740942
THETA8	-4.1926890	PHIB	0.	OMGRAT	1.0111110	GGRPM	94.626825

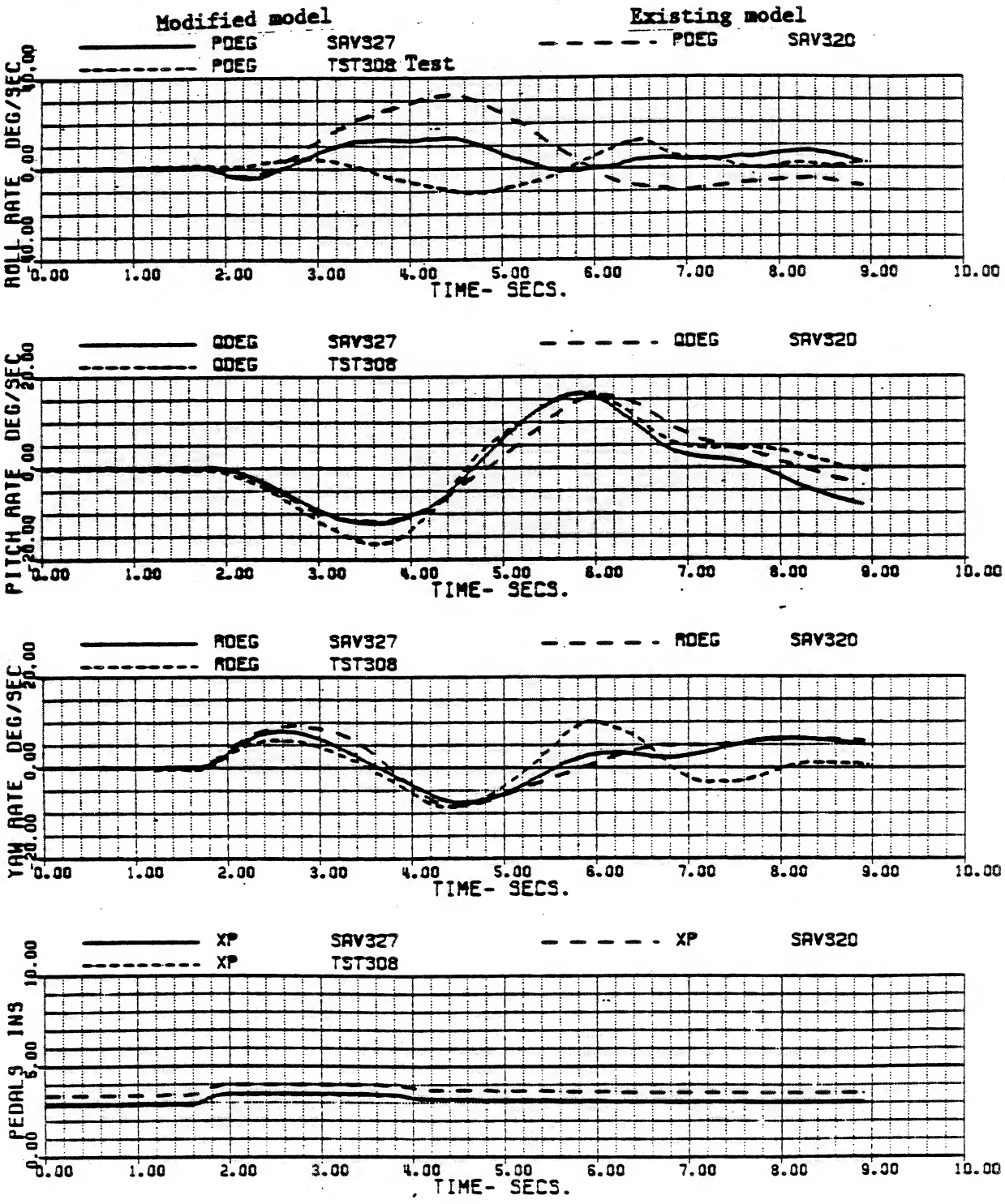

Figure 28

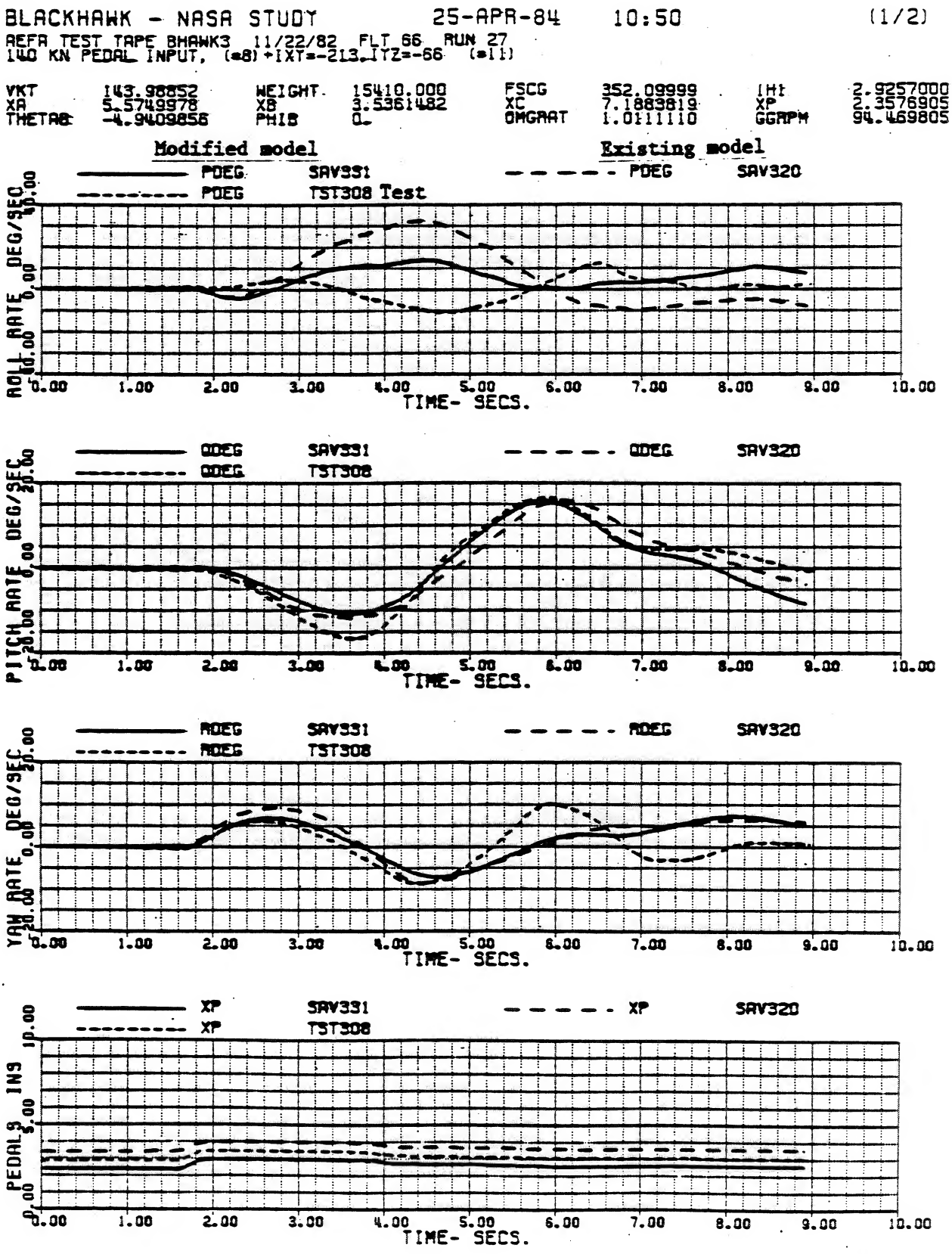
BLACKHAWK - NASA STUDY 25-APR-84 10:50 (1/2)
AEFA TEST TAPE BHAWK3 11/22/82 FLT 66 RUN 27
160 KN PEDAL INPUT, (=8)+IXT=-213.ITZ=-66 (=11)
VKT 143.98852 WEIGHT 15410.000 FSCG 352.09999 IHt 2.9257000
XA 5.5749978 XB 3.5361482 XC 7.1883819 XP 2.3576905
THETAB -4.9409856 PHIB 0. OMGRAT 1.0111110 GGRPM 94.469805
Modified model
Existing model
PDEG SAV331
PDEG TST308 Test
PDEG SAV320
ROLL RATE DEG/SEC
TIME- SECS.
QDEG SAV331
QDEG TST308
QDEG SAV320
PITCH RATE DEG/SEC
TIME- SECS.
RDEG SAV331
RDEG TST308
RDEG SAV320
YAW RATE DEG/SEC
TIME- SECS.
XP SAV331
XP TST308
XP SAV320
PEDALS INS
TIME- SECS.

Figure 29

BLACKHAWK - NASA STUDY 25-APR-84 10:59 (1/2)

AEFA TEST TAPE BHAWK3 11/22/82 FLT 66 RUN 27
140 KN PEDAL INPUT, (=11)+1.50*IXZ(2823.0) (=13)

VKT	143.98851	WEIGHT	15410.000	FSCG	352.09998	IHI	2.9257000
XA	5.5758578	XB	3.5382742	XC	7.1897209	XP	2.3595835
THETA8	-4.9503092	PHIB	0.	OMGRAT	1.0111110	GGRPM	94.456673

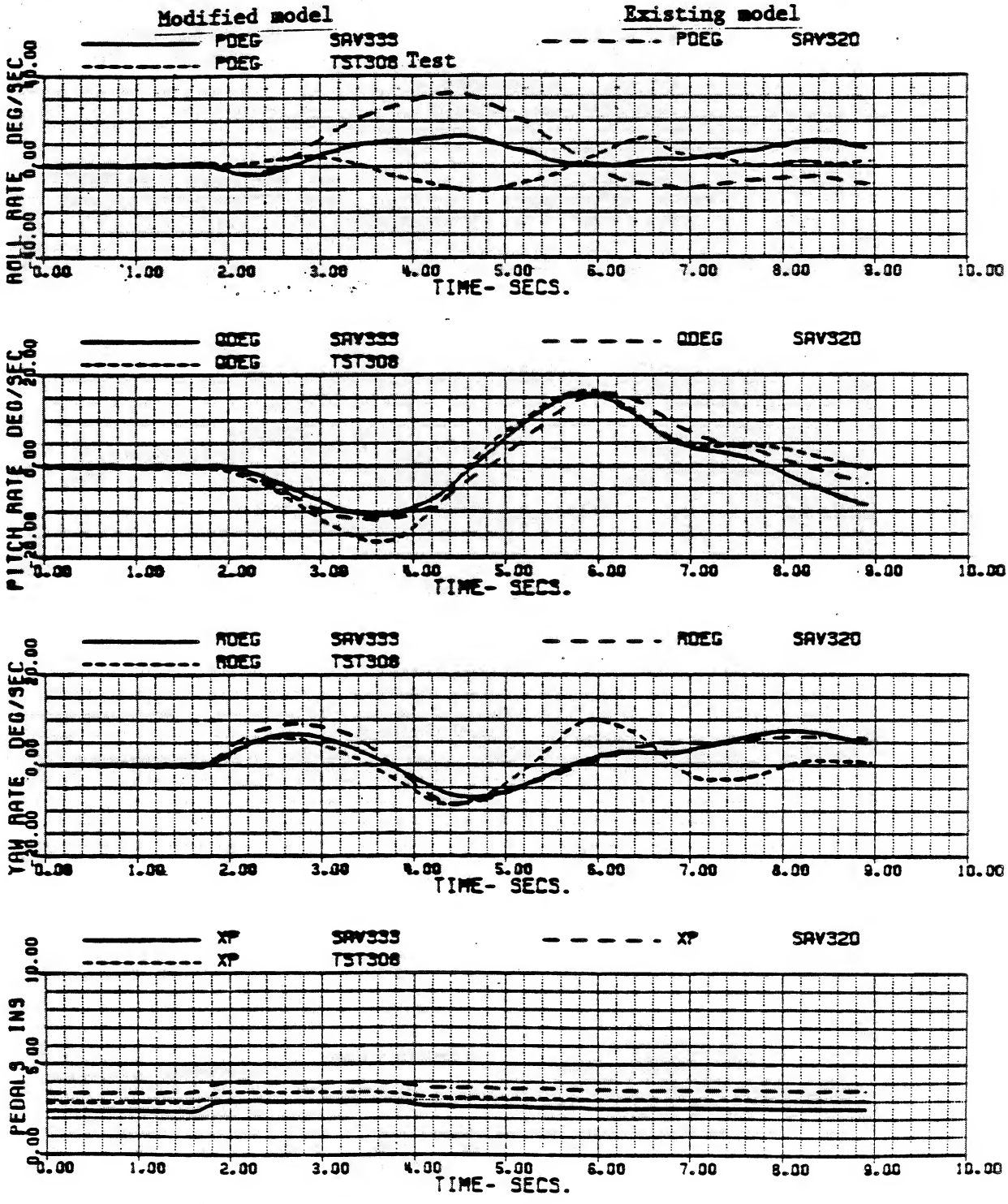

Figure 30a

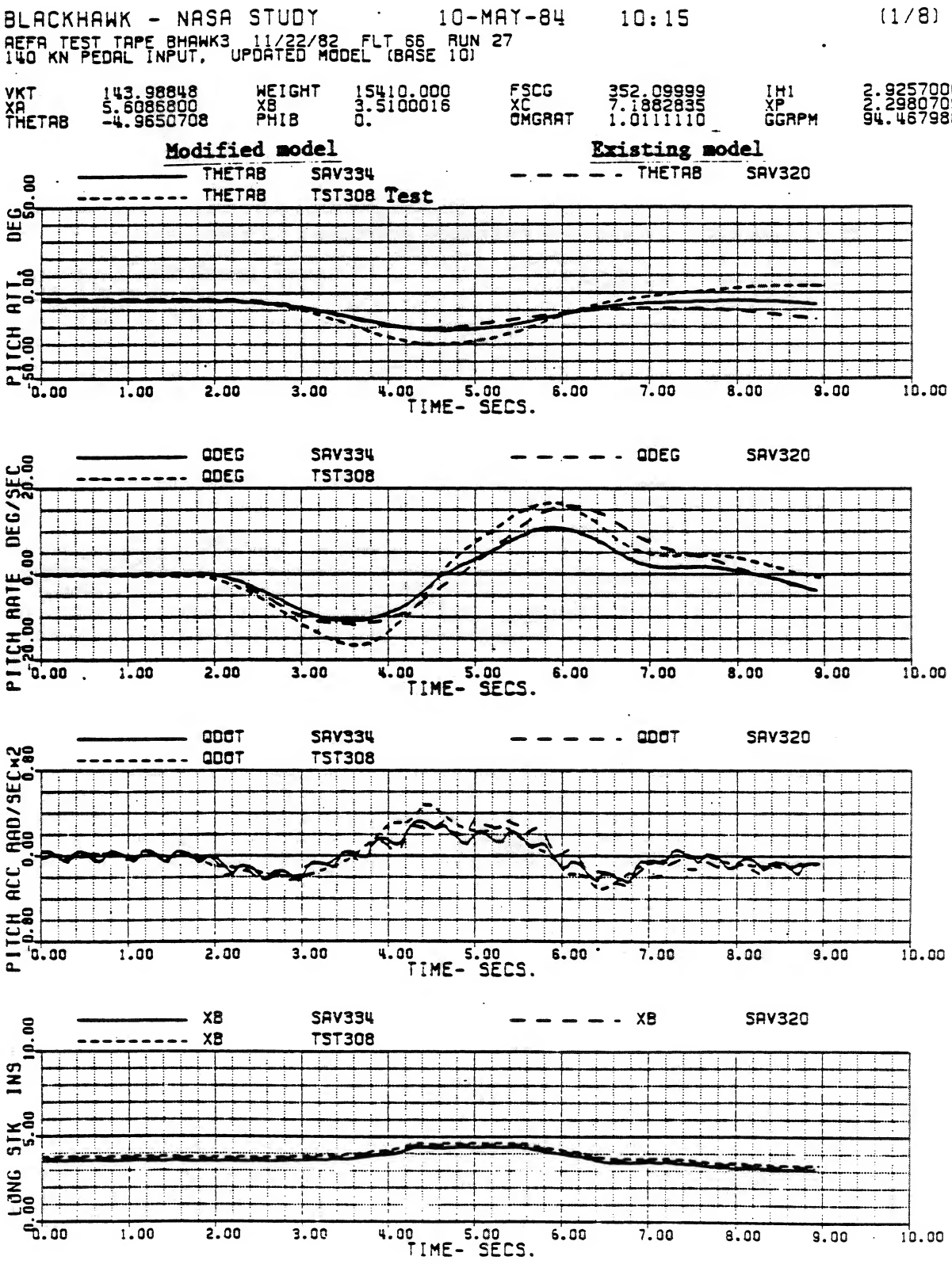
BLACKHAWK - NASA STUDY 10-MAY-84 10:15 (1/8)
AEFA TEST TAPE BHAWK3 11/22/82 FLT 66 RUN 27
140 KN PEDAL INPUT, UPDATED MODEL (BASE 10)
VKT 143.98848 WEIGHT 15410.000 FSCG 352.09999 IM1 2.9257000
XA 5.6086800 XB 3.5100016 XC 7.1882835 XP 2.2980709
THETAB -4.9650708 PHIB 0. OMGRAT 1.0111110 GGRPM 94.467986
Modified model
Existing model
THETAB SAV334
THETAB TST308 Test
THETAB SAV320
PITCH ATT, DEG
50.00
0.00
-50.00
QDEG SAV334
QDEG TST308
QDEG SAV320
PITCH RATE DEG/SEC
20.00
0.00
-20.00
QDOT SAV334
QDOT TST308
QDOT SAV320
PITCH ACC RAD/SEC**2
0.80
0.00
-0.80
XB SAV334
XB TST308
XB SAV320
LONG STK INS
10.00
5.00
0.00
0.00 1.00 2.00 3.00 4.00 5.00 6.00 7.00 8.00 9.00 10.00
TIME- SECS.

Figure 30b

BLACKHAWK - NASA STUDY 10-MAY-84 10:15 (2/8)

AEFA TEST TAPE BHAWK3 11/22/82 FLT 66 RUN 27
140 KN PEDAL INPUT, UPDATED MODEL (BASE 10)

VKT	143.98848	WEIGHT	15410.000	FSCG	352.09999	IH1	2.9257000
XA	5.6086800	XB	3.5100016	XC	7.1882835	XP	2.2980709
THETAB	-4.9650708	PHIB	0.	OMGRAT	1.0111110	GGRPM	94.467986

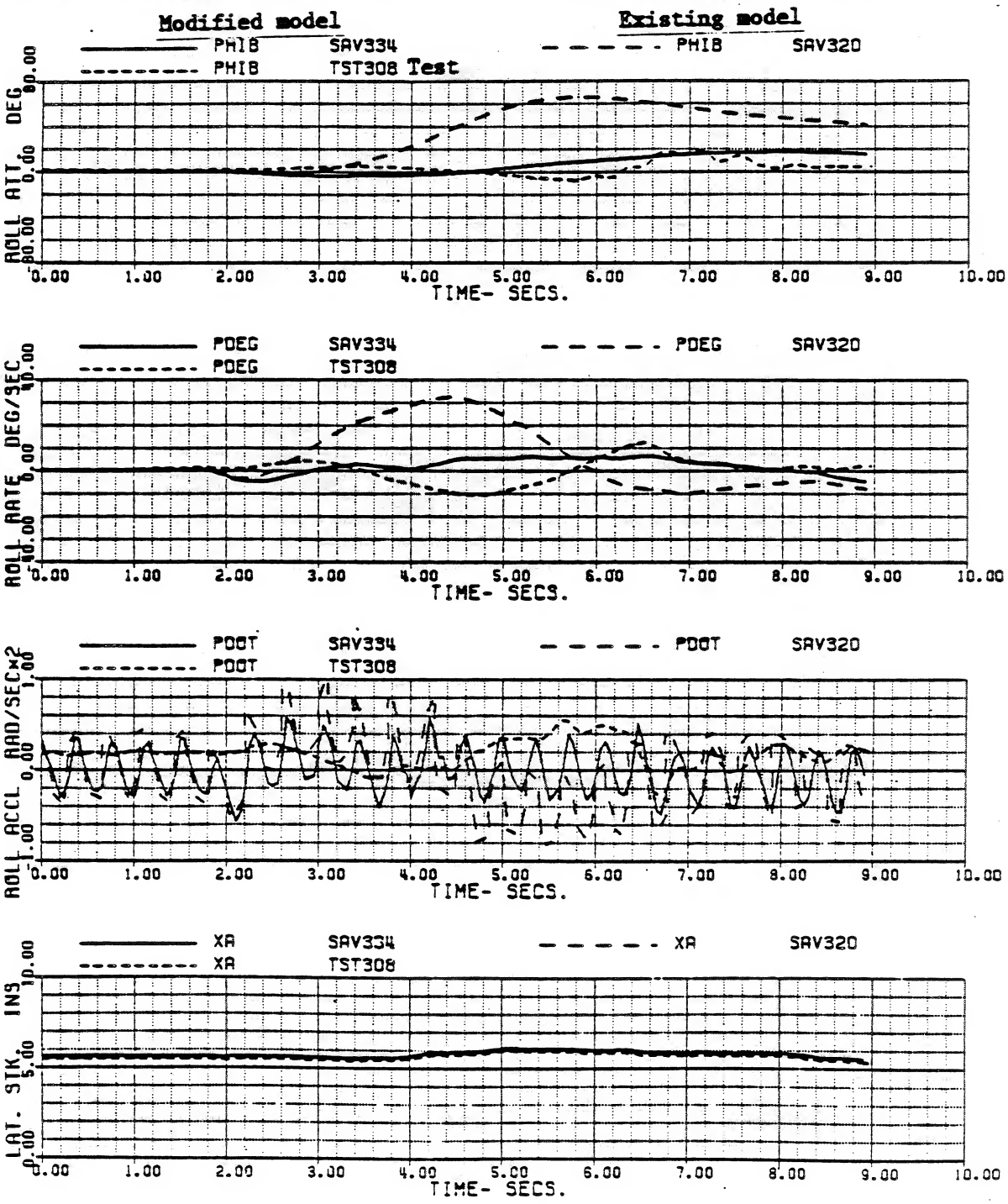

Figure 30c

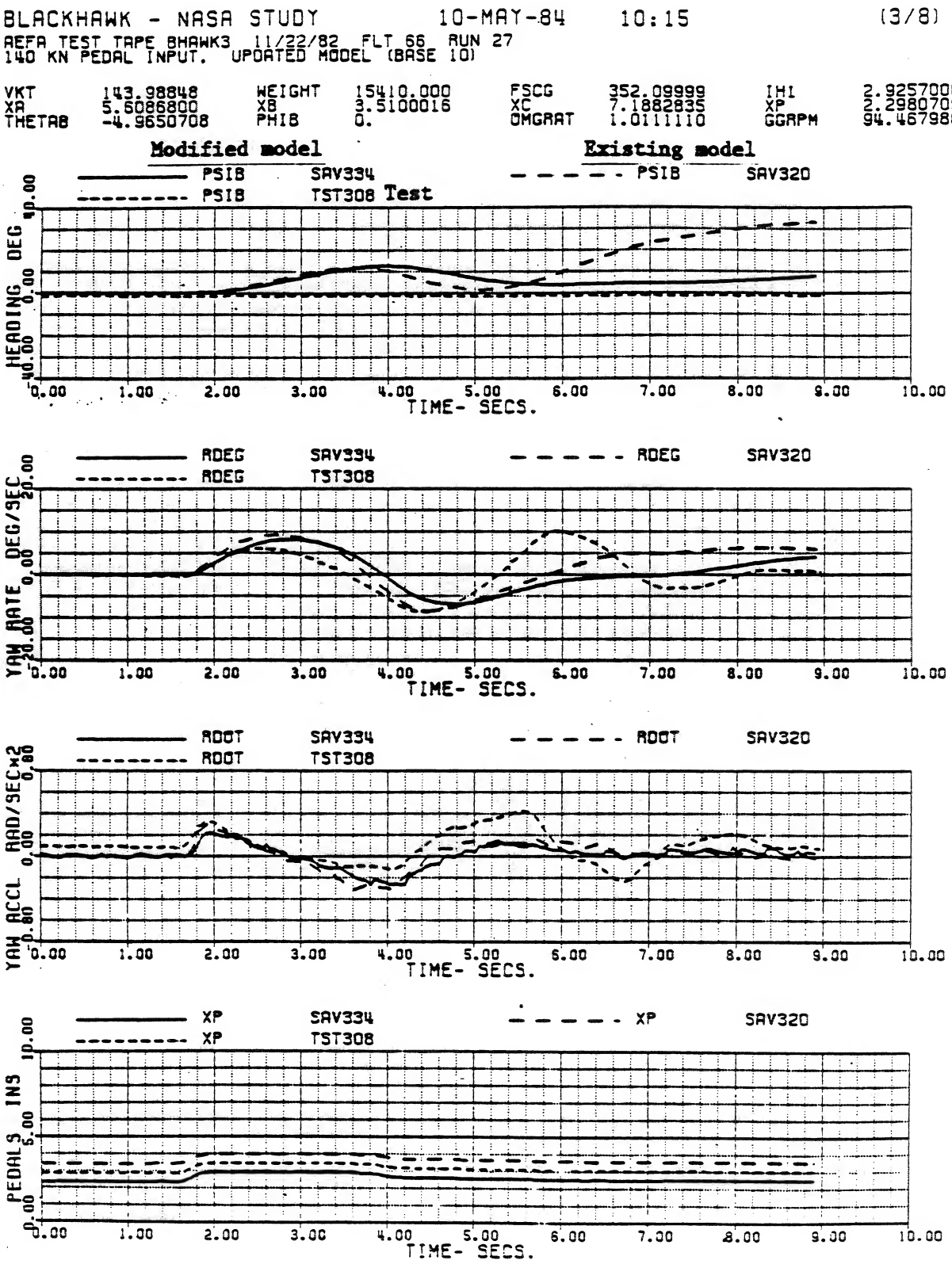
BLACKHAWK - NASA STUDY 10-MAY-84 10:15 (3/8)
AEFA TEST TAPE BHAWK3 11/22/82 FLT 66 RUN 27
140 KN PEDAL INPUT. UPDATED MODEL (BASE 10)
VKT 143.98848 WEIGHT 15410.000 FSCG 352.09999 IHI 2.9257000
XA 5.6086800 XB 3.5100016 XC 7.1882835 XP 2.2980709
THETAB -4.9650708 PHIB 0. OMGRAT 1.0111110 GGRPM 94.467986
Modified model
Existing model
PSIB SAV334
PSIB TST308 Test
PSIB SAV320
HEADING DEG
10.00
0.00
-10.00
0.00 1.00 2.00 3.00 4.00 5.00 6.00 7.00 8.00 9.00 10.00
TIME- SECS.
RDEG SAV334
RDEG TST308
RDEG SAV320
YAW RATE DEG/SEC
20.00
0.00
-20.00
0.00 1.00 2.00 3.00 4.00 5.00 6.00 7.00 8.00 9.00 10.00
TIME- SECS.
RDDT SAV334
RDDT TST308
RDDT SAV320
YAW ACCL RAD/SEC*2
0.80
0.00
-0.80
0.00 1.00 2.00 3.00 4.00 5.00 6.00 7.00 8.00 9.00 10.00
TIME- SECS.
XP SAV334
XP TST308
XP SAV320
PEDALS INS
10.00
5.00
0.00
0.00 1.00 2.00 3.00 4.00 5.00 6.00 7.00 8.00 9.00 10.00
TIME- SECS.

Figure 30d

BLACKHAWK - NASA STUDY 10-MAY-84 10:15 (4/8)
AEFA TEST TAPE BHAWK3 11/22/82 FLT 66 RUN 27
140 KN PEDAL INPUT, UPDATED MODEL (BASE 10)

VKT	143.98848	WEIGHT	15410.000	FSCG	352.09999	IH1	2.9257000
XA	5.6086800	X8	3.5100016	XC	7.1882835	XP	2.2980709
THETAB	-4.9650708	PHI8	0.	OMGRAT	1.0111110	GGRPM	94.467986

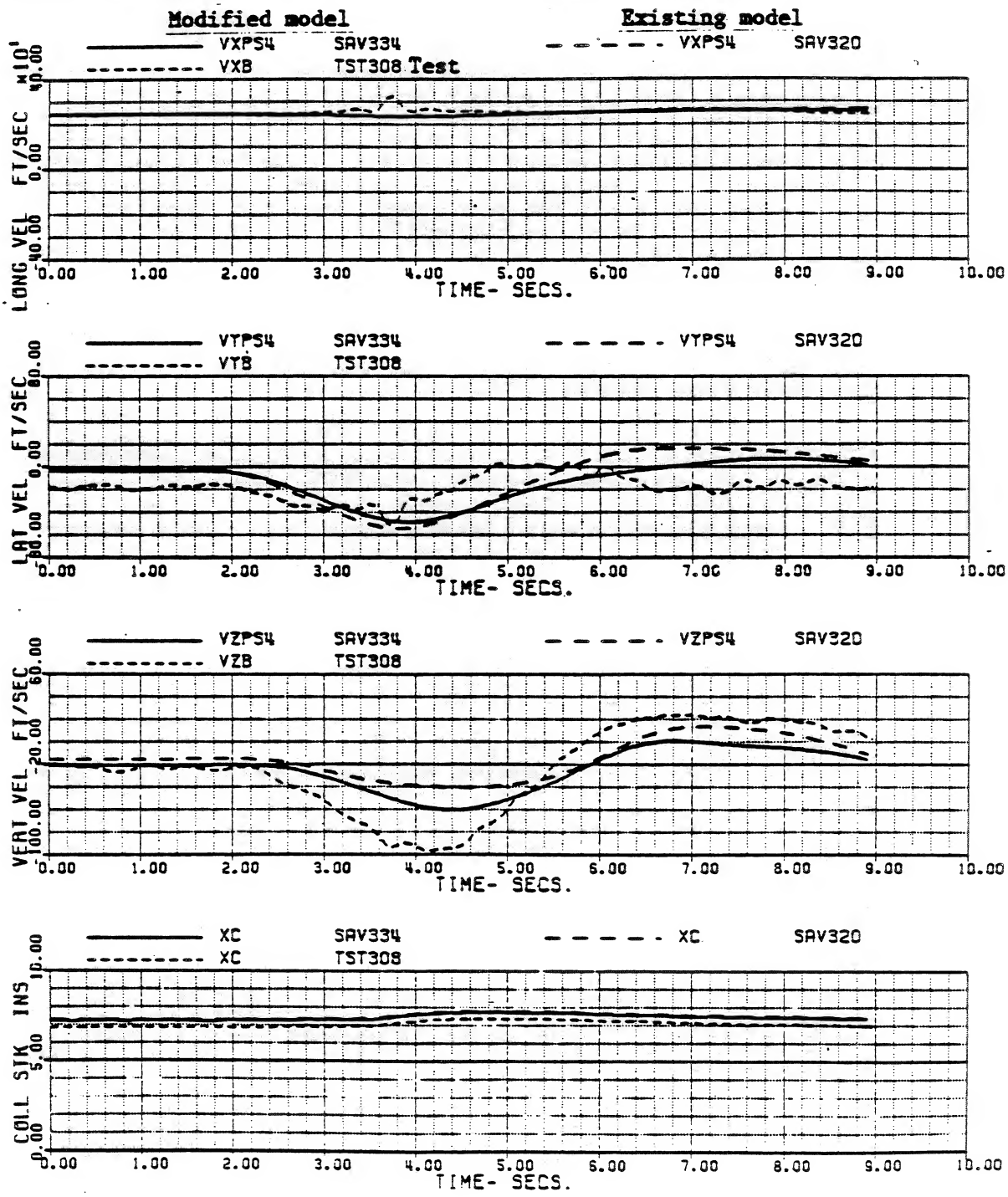

Figure 30e

BLACKHAWK - NASA STUDY 10-MAY-84 10:15 (5/8)

AEFA TEST TAPE BHAWK3 11/22/82 FLT 66 RUN 27
140 KN PEDAL INPUT. UPDATED MODEL (BASE 10)

VKT	143.98848	WEIGHT	15410.000	FSCG	352.09999	IHI	2.9257000
XA	5.6086800	XB	3.5100016	XC	7.1882835	XP	2.2980709
THETAB	-4.9650708	PHIB	0.	OMGRAT	1.0111110	GGRPM	94.467986

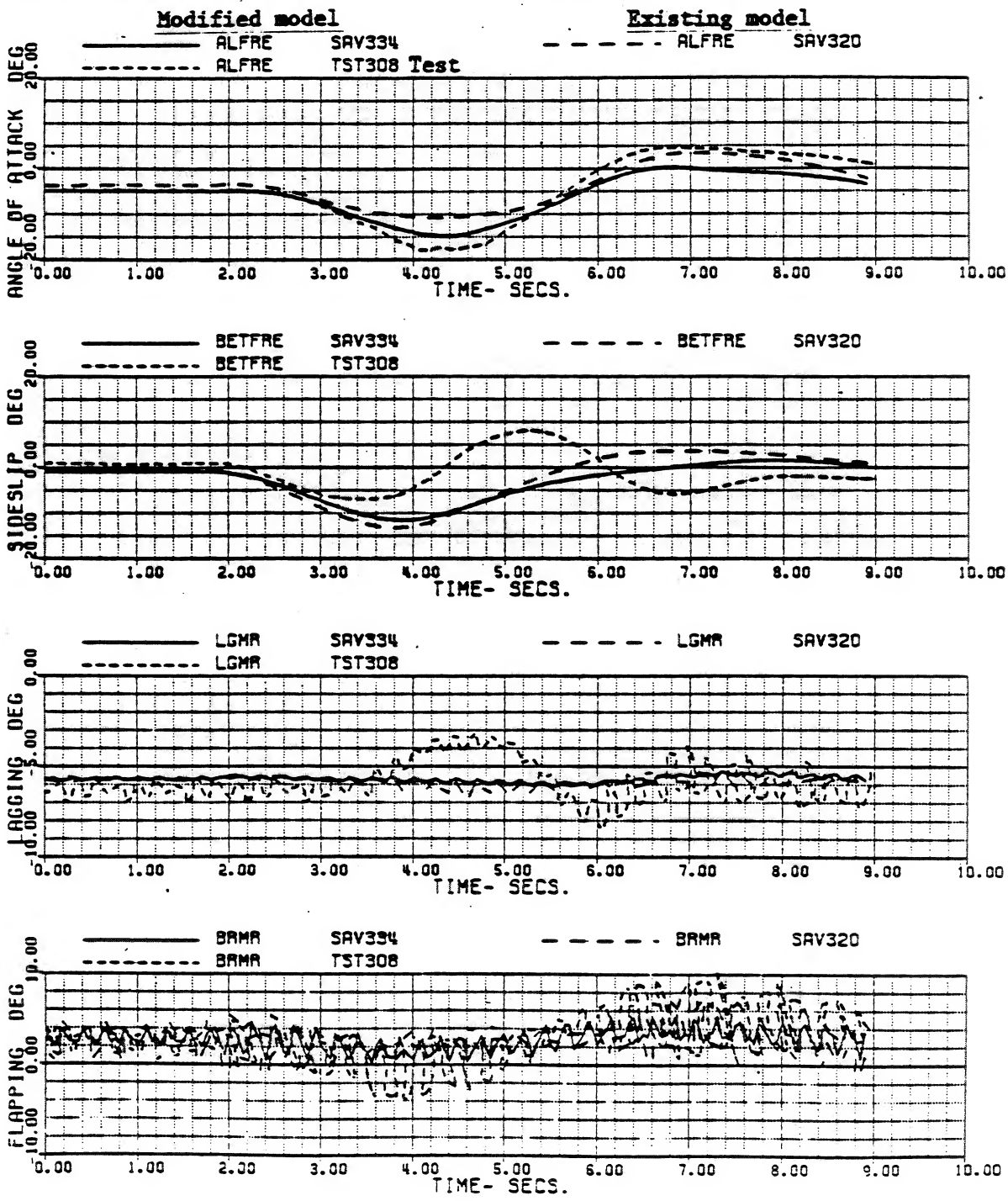

Figure 30f

BLACKHAWK - NASA STUDY 10-MAY-84 10:15 (6/8)

AEFA TEST TAPE BHAWK3 11/22/82 FLT 66 RUN 27
140 KN PEDAL INPUT. UPDATED MODEL (BASE 10)

VKT	143.98848	WEIGHT	15410.000	FSCG	352.09999	IH1	2.9257000
XA	5.6086800	XB	3.5100016	XC	7.1882835	XP	2.2980709
THETAB	-4.9650708	PHIB	0.	OMGRAT	1.0111110	GGRPM	94.467986

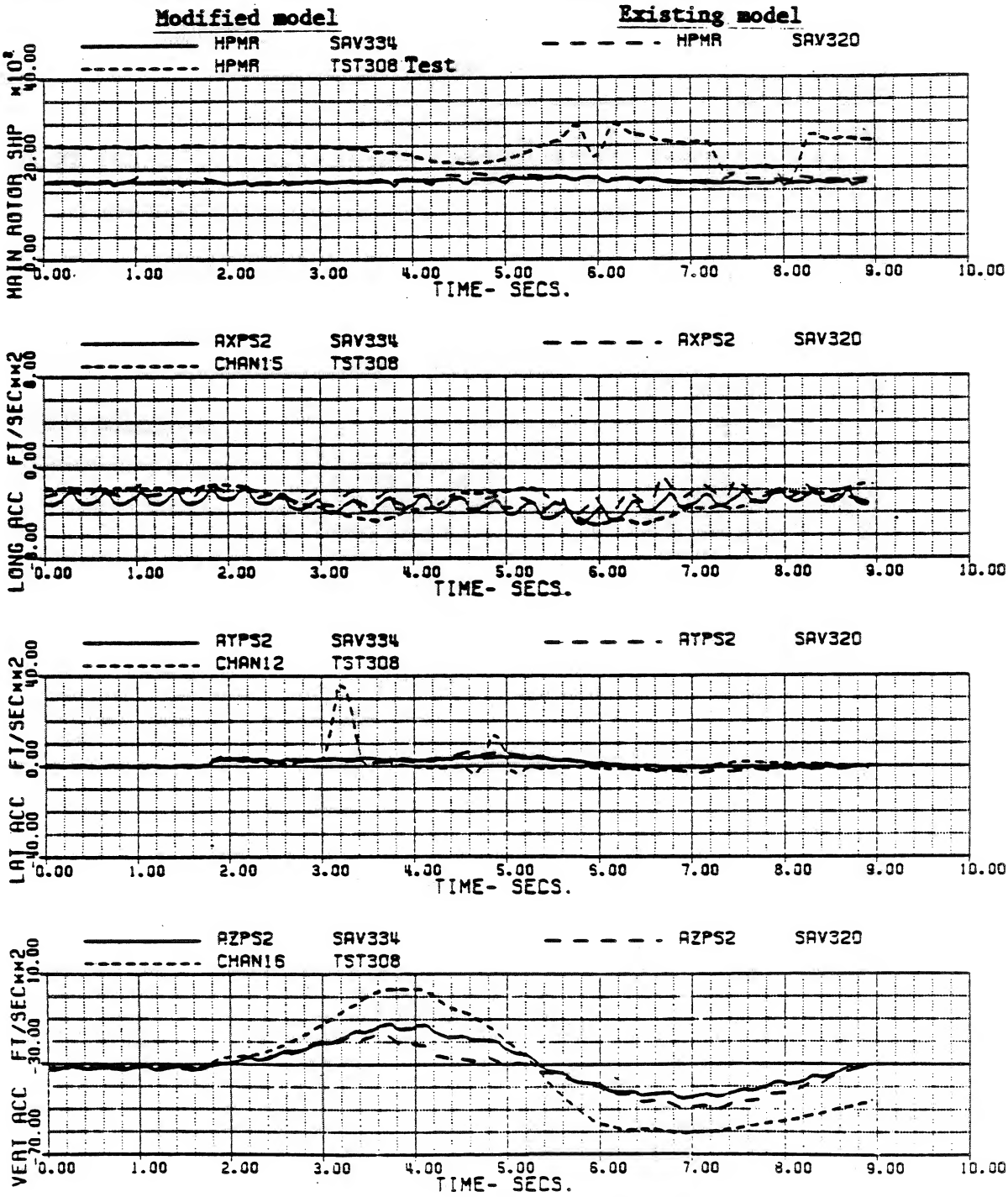

BLACKHAWK - NASA STUDY 10-MAY-84 10:15 (7/8)

AEFA TEST TAPE BHAWK3 11/22/82 FLT 66 RUN 27
140 KN PEDAL INPUT. UPDATED MODEL (BASE 10)

VKT	143.98848	WEIGHT	15410.000	FSCG	352.09999	IH1	2.9257000
XA	5.6086800	XB	3.5100016	XC	7.1882835	XP	2.2980709
THETAB	-4.9650708	PHIB	0.	OMGRAT	1.0111110	GGRPM	94.467986

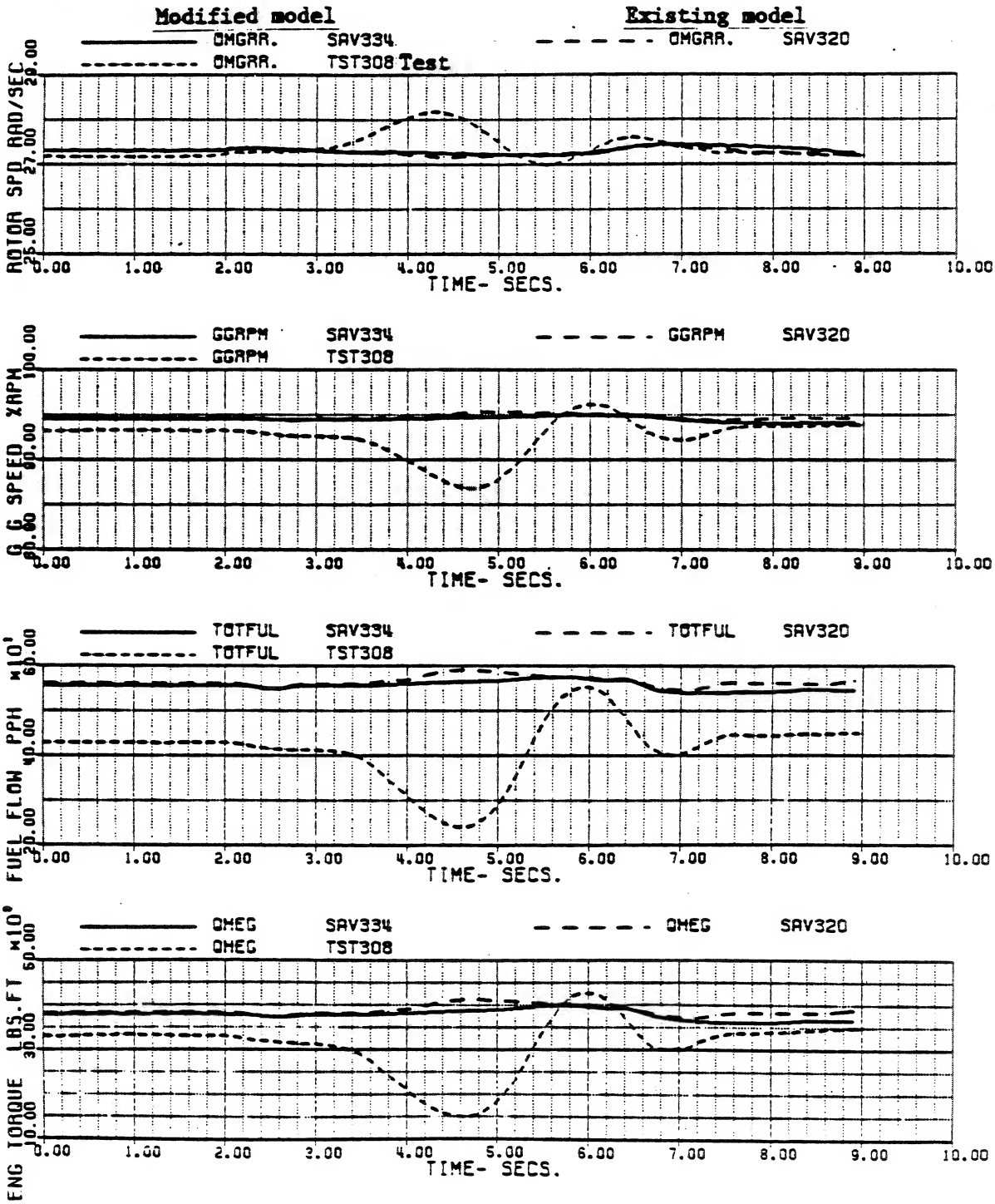

Figure 30h

BLACKHAWK - NASA STUDY 10-MAY-84 10:15 (8/8)

AEFA TEST TAPE BHAWK3 11/22/82 FLT 66 RUN 27
140 KN PEDAL INPUT, UPDATED MODEL (BASE 10)

VKT	143.98848	WEIGHT	15410.000	FSCG	352.09999	IH1	2.9257000
XA	5.6086800	XB	3.5100016	XC	7.1862835	XP	2.2980709
THETAB	-4.9650708	PHIB	0.	OMGRAT	1.0111110	GGRPM	94.467986

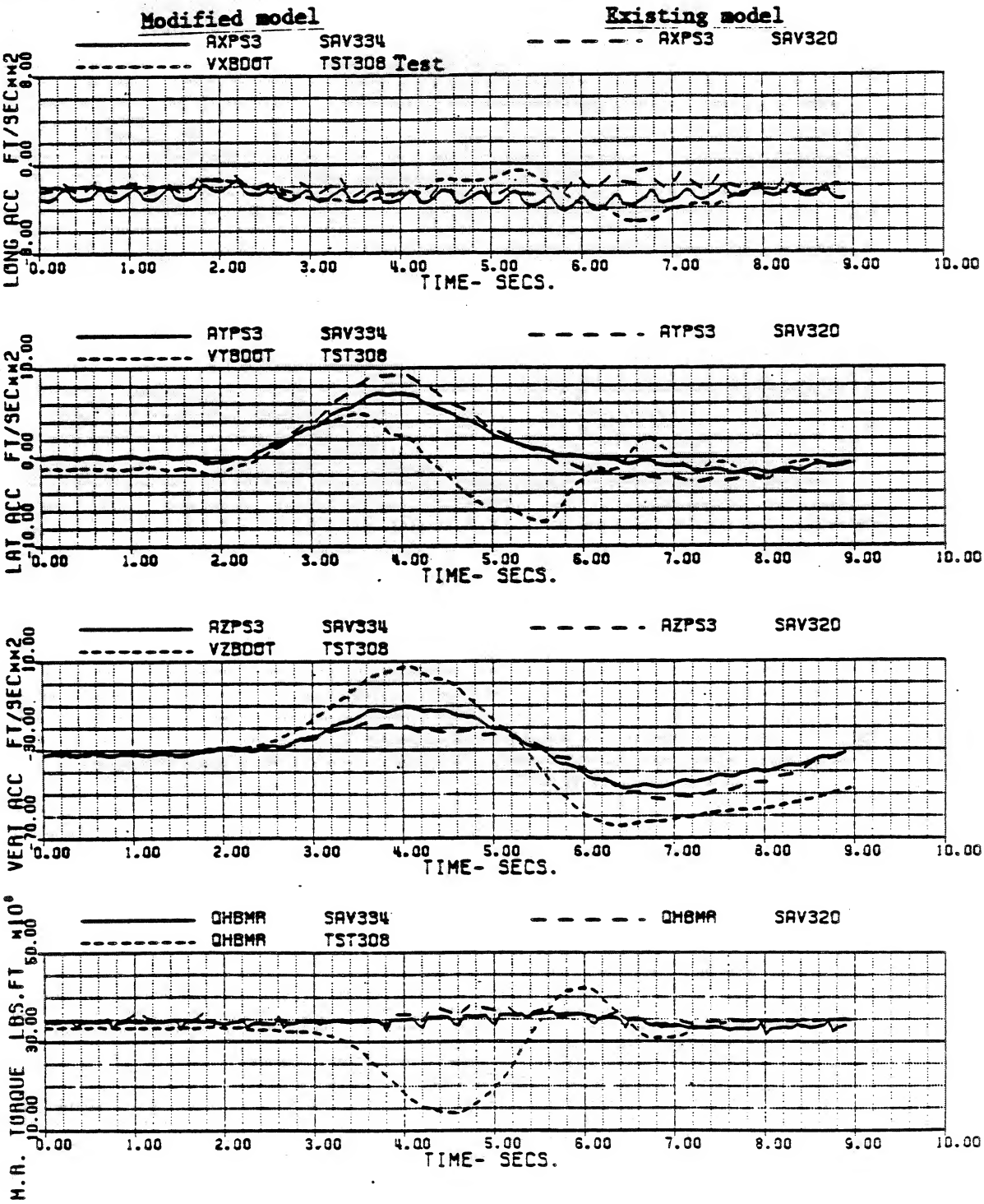

Figure 31a

BLACKHAWK - NASA STUDY 11-MAY-84 14:03 (1/8)
AEFA TEST TAPE BHAWK7 2/1/83
FLT 188 RUN 21 100 KN PEDAL PULSE UPDATED MODEL

VKT	102.99197	WEIGHT	15900.000	FSCG	348.70000	IHI	7.8999999
XA	5.2311698	XB	4.8087467	XC	5.0304511	XP	2.4586541
THETA8	-3.1043404	PHI8	0.	OMGRAT	1.0000000	GGRPM	89.544999

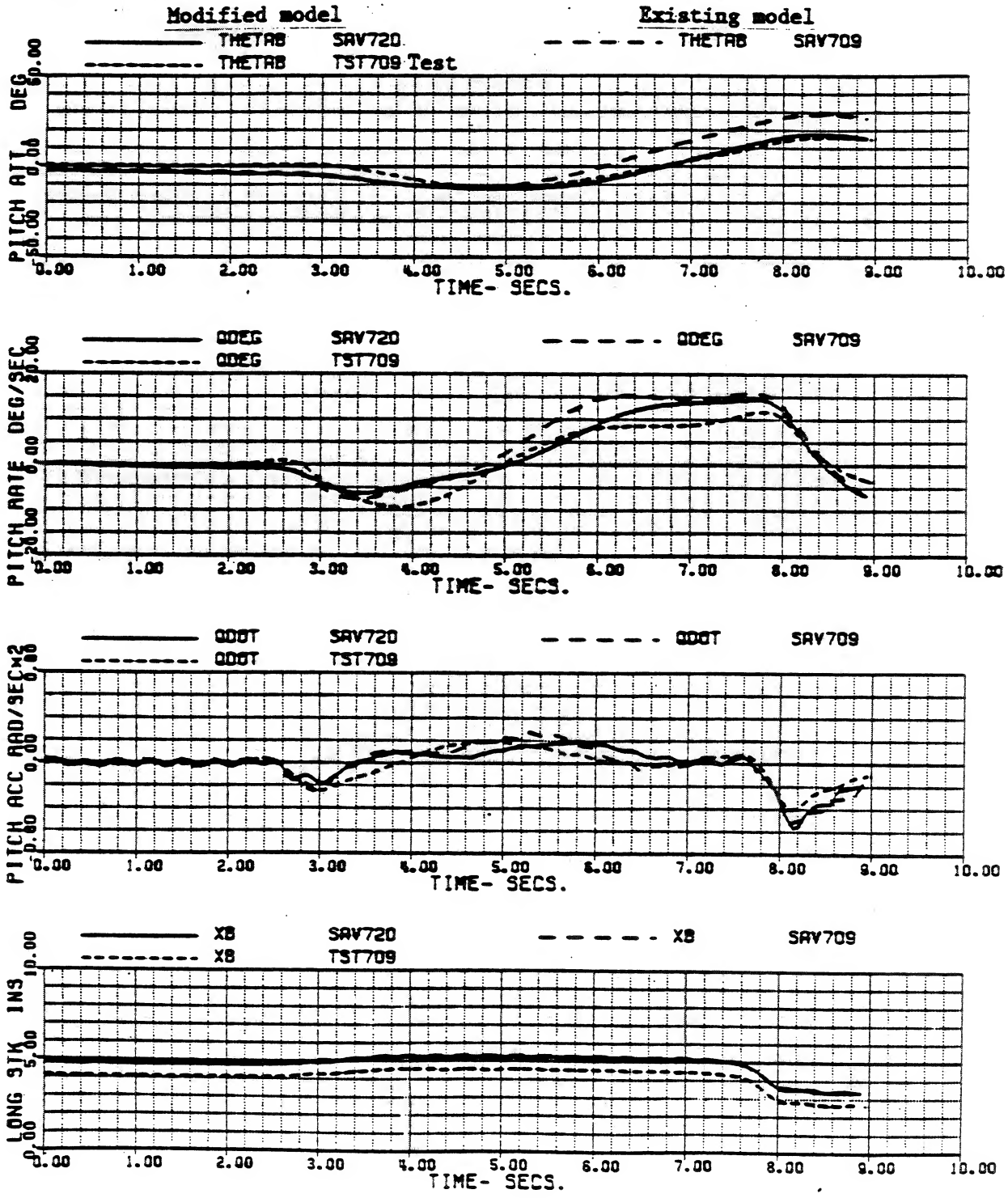

Figure 31b

BLACKHAWK - NASA STUDY 11-MAY-84 14:03 (2/8)
REFA TEST TAPE BHAWK7 2/1/83
FLT 188 RUN 21 100 KN PEDAL PULSE UPDATED MODEL

VKT	102.99197	WEIGHT	15900.000	FSCG	348.70000	IHI	7.8999999
XA	5.2311698	XB	4.8087467	XC	5.0304511	XP	2.4586541
THETAB	-3.1043404	PHIB	0.	OMGRAT	1.0000000	GGRPM	89.544999

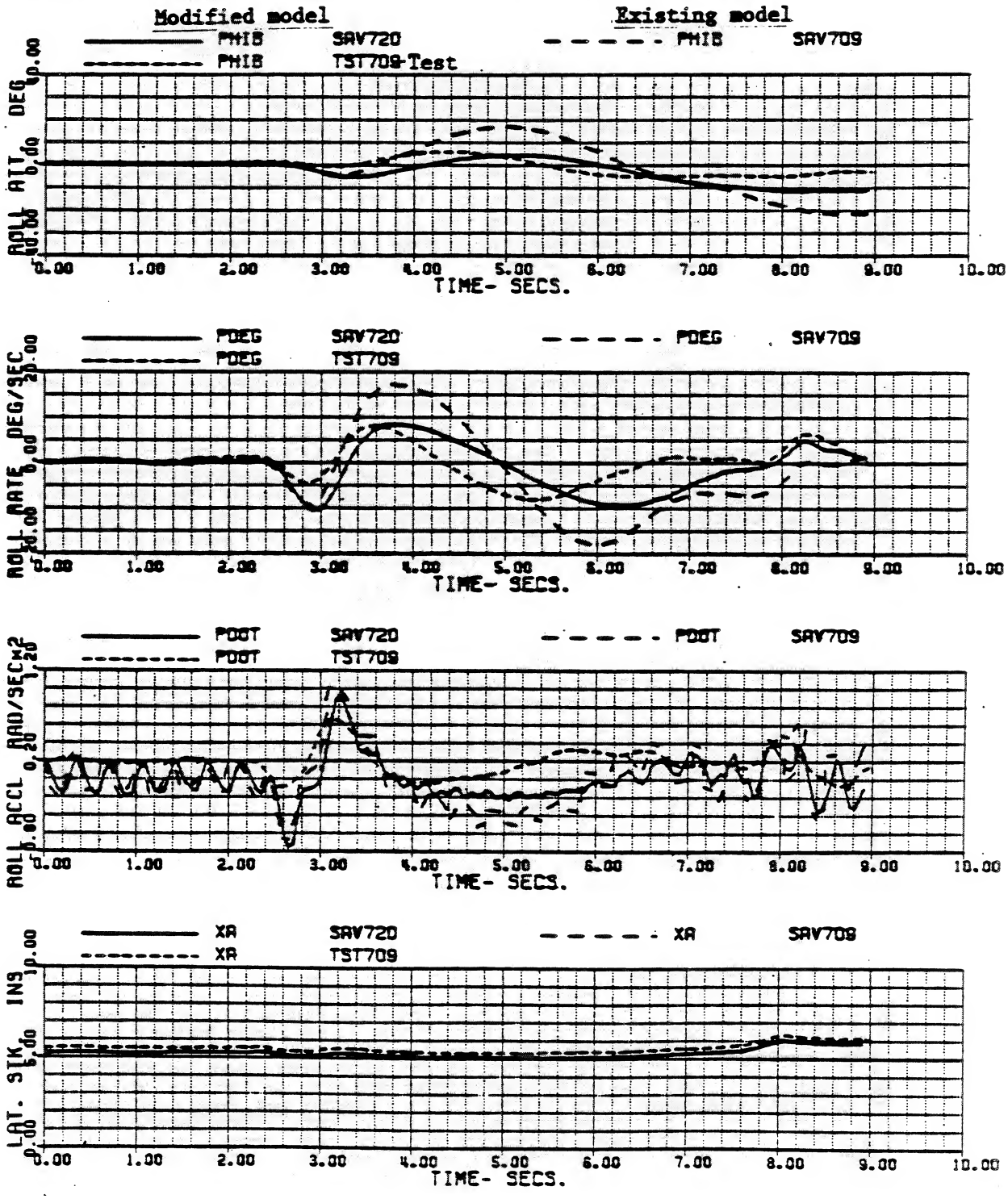

Figure 31c

BLACKHAWK - NASA STUDY 11-MAY-84 14:03 (3/8)
AEFA TEST TAPE BHAWK7 2/1/83
FLT 188 RUN 21 100 KN PEDAL PULSE UPDATED MODEL

VKT	102.99197	WEIGHT	15900.000	FSCG	348.70000	IH1	7.8999999
XA	5.2311698	XB	4.8087467	XC	5.0304511	XP	2.4586541
THETAB	-3.1043404	PHIB	0.	OMGRAT	1.0000000	GGAPM	89.544999

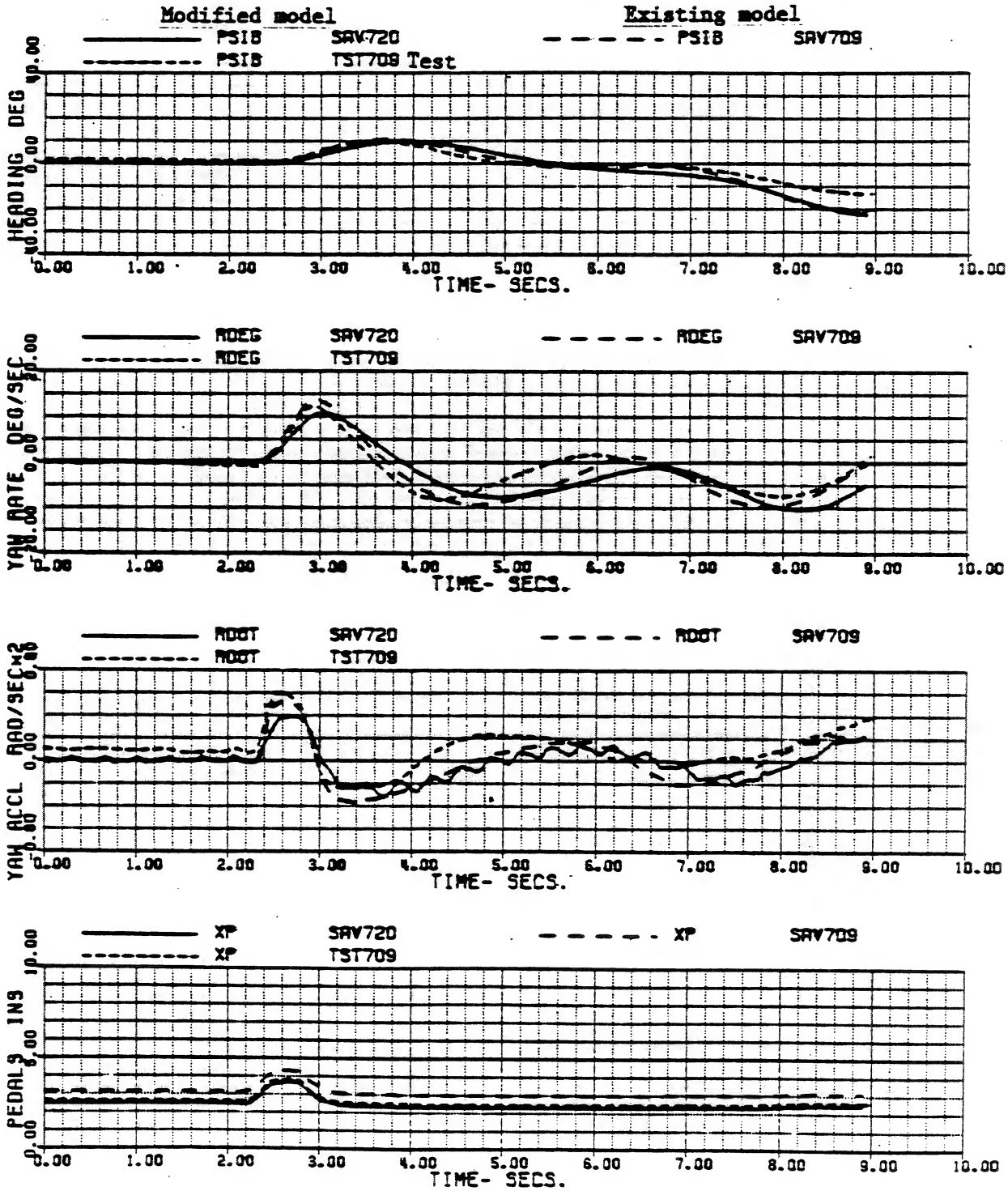

Figure 31d

BLACKHAWK - NASA STUDY 11-MAY-84 14:03 (4/8)
AEFA TEST TAPE BHAWK7 2/1/83
FLT 188 RUN 21 100 KN PEDAL PULSE UPDATED MODEL

VKT	102.99197	WEIGHT	15900.000	FSCG	348.70000	IH1	7.8999999
XA	5.2311698	XB	4.8087467	XC	5.0304511	XP	2.4586541
THETAB	-3.1043404	PHIB	0.	OMGRAT	1.0000000	GGAPM	89.544999

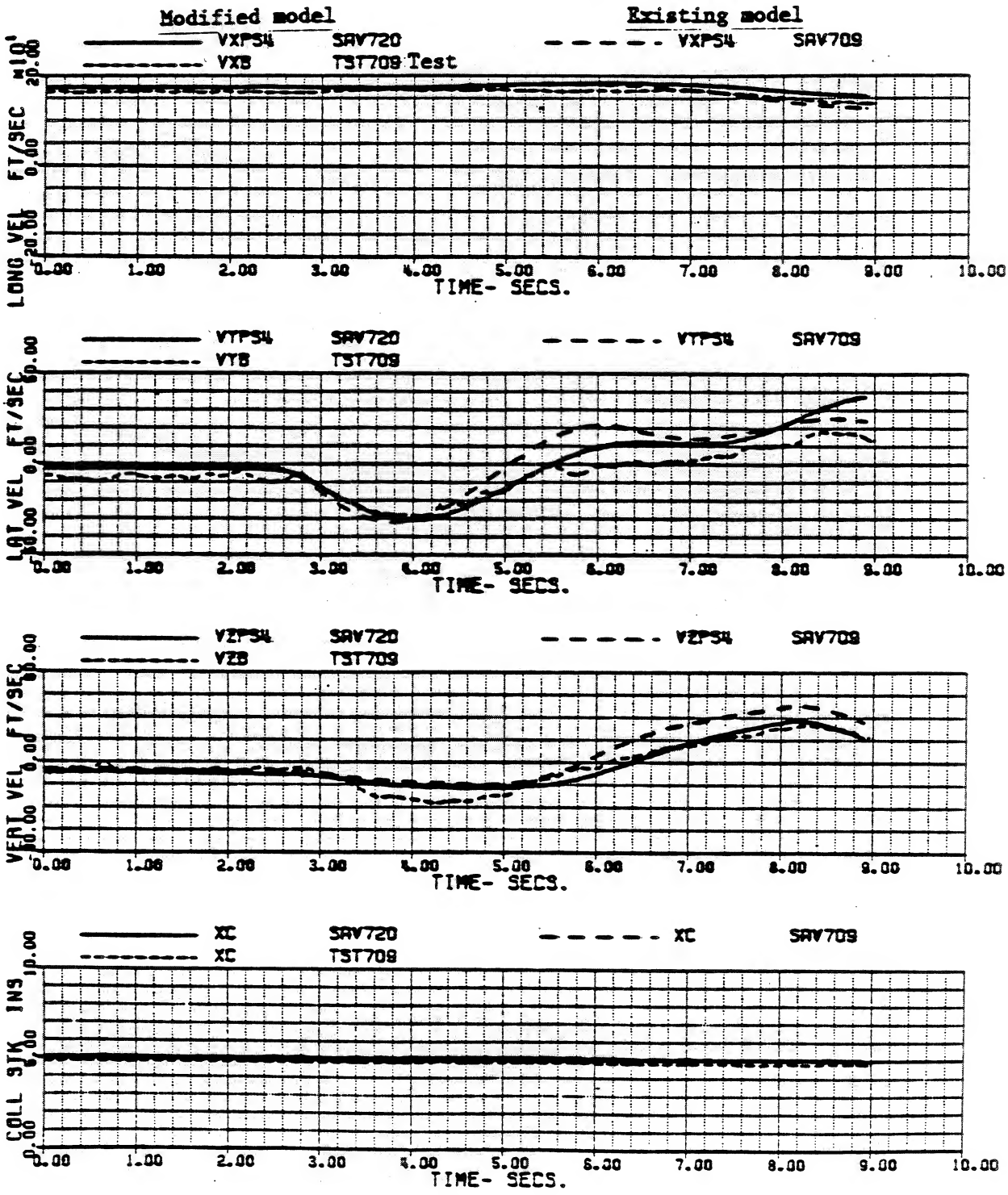

Figure 31e

BLACKHAWK - NASA STUDY 11-MAY-84 14:03 (5/8)
AEFA TEST TAPE BHAWK7 2/1/83
FLT 188 RUN 21 100 KN PEDAL PULSE UPDATED MODEL

VKT	102.99197	WEIGHT	15900.000	FSCG	348.70000	IHT	7.8999999
XA	5.2911698	XB	4.8087467	XC	5.0304511	XP	2.4586541
THETAB	-3.1043404	PHIB	0.	OMGRAT	1.0000000	GGAMA	89.544999

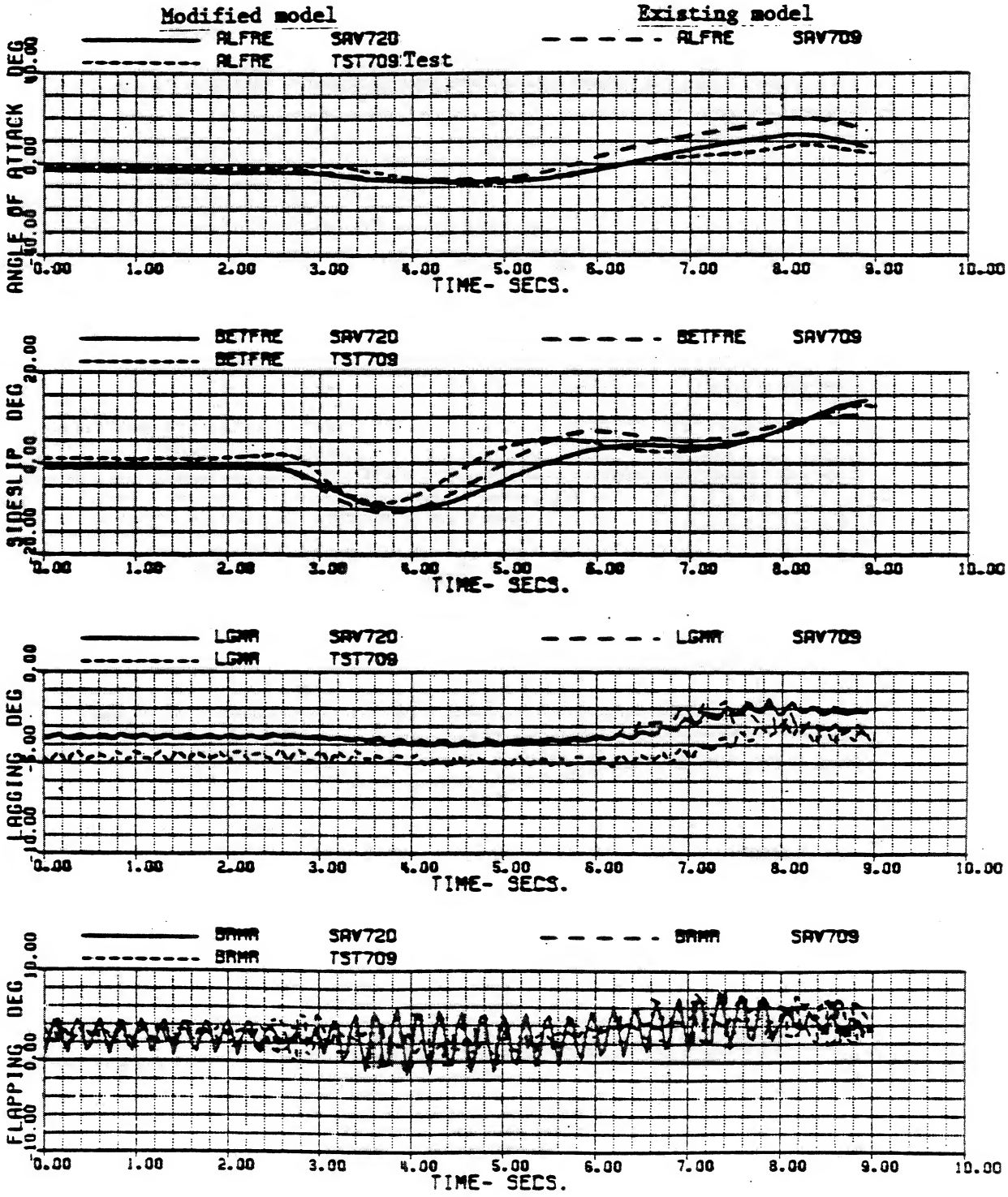

SA 1114

15-MAY
FLT720
.PCO
SAV720
.DAT

Figure 31f

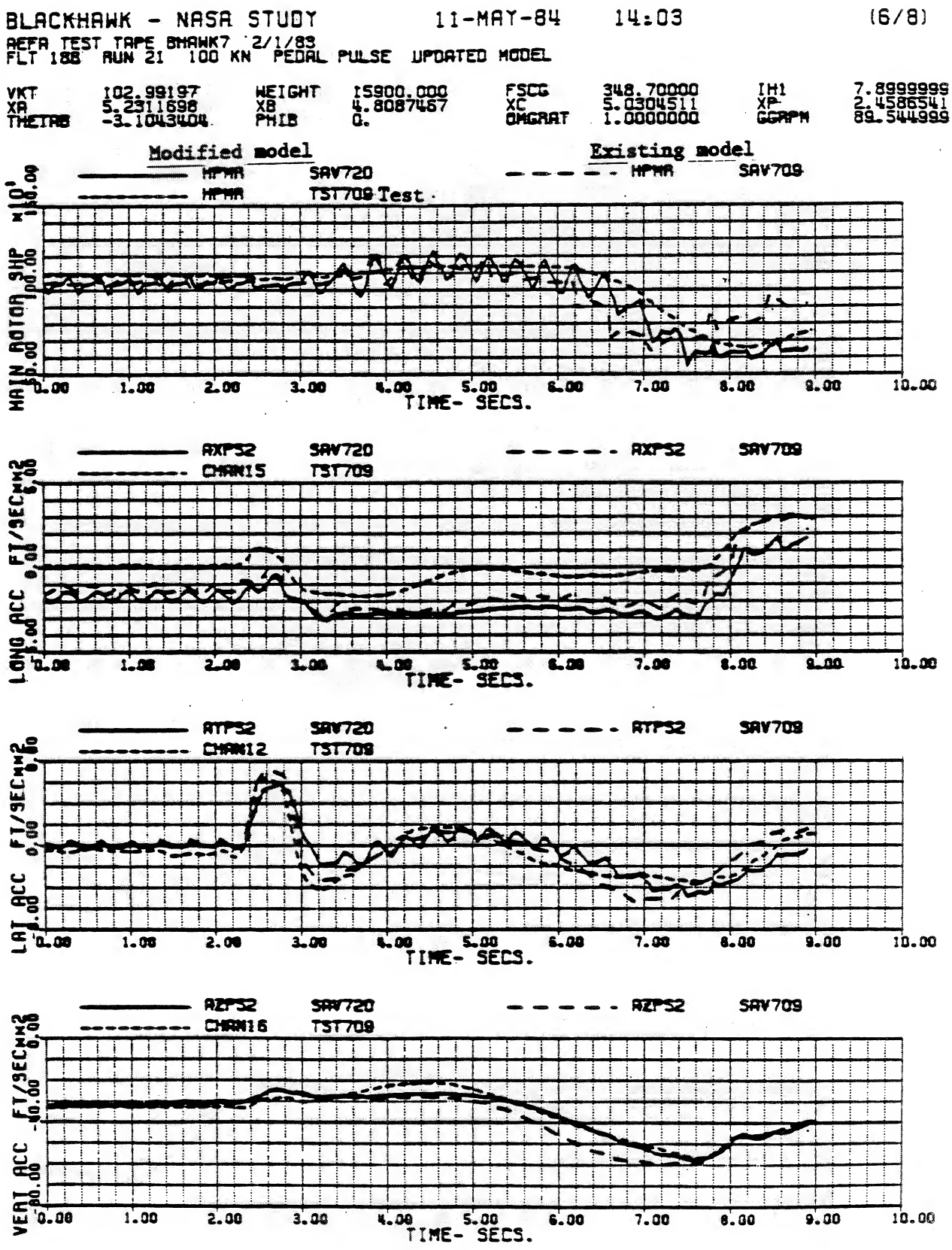

00:05
15-MAY
FLT720
.PCD
SAV720
.DAT

Figure 31g

BLACKHAWK - NASA STUDY 11-MAY-84 14:03 (7/8)
AEFA TEST TAPE BHAWK7 2/1/83
FLT 188 RUN 21 100 KN PEDAL PULSE UPDATED MODEL

VKT	102.99197	WEIGHT	15900.000	FSCG	348.70000	IH1	7.8999999
XA	5.2311698	XB	4.8087467	XC	5.0304511	XP	2.4586541
THETA8	-3.1043404	PHIB	0.	OMGRAT	1.0000000	GGRPM	89.544999

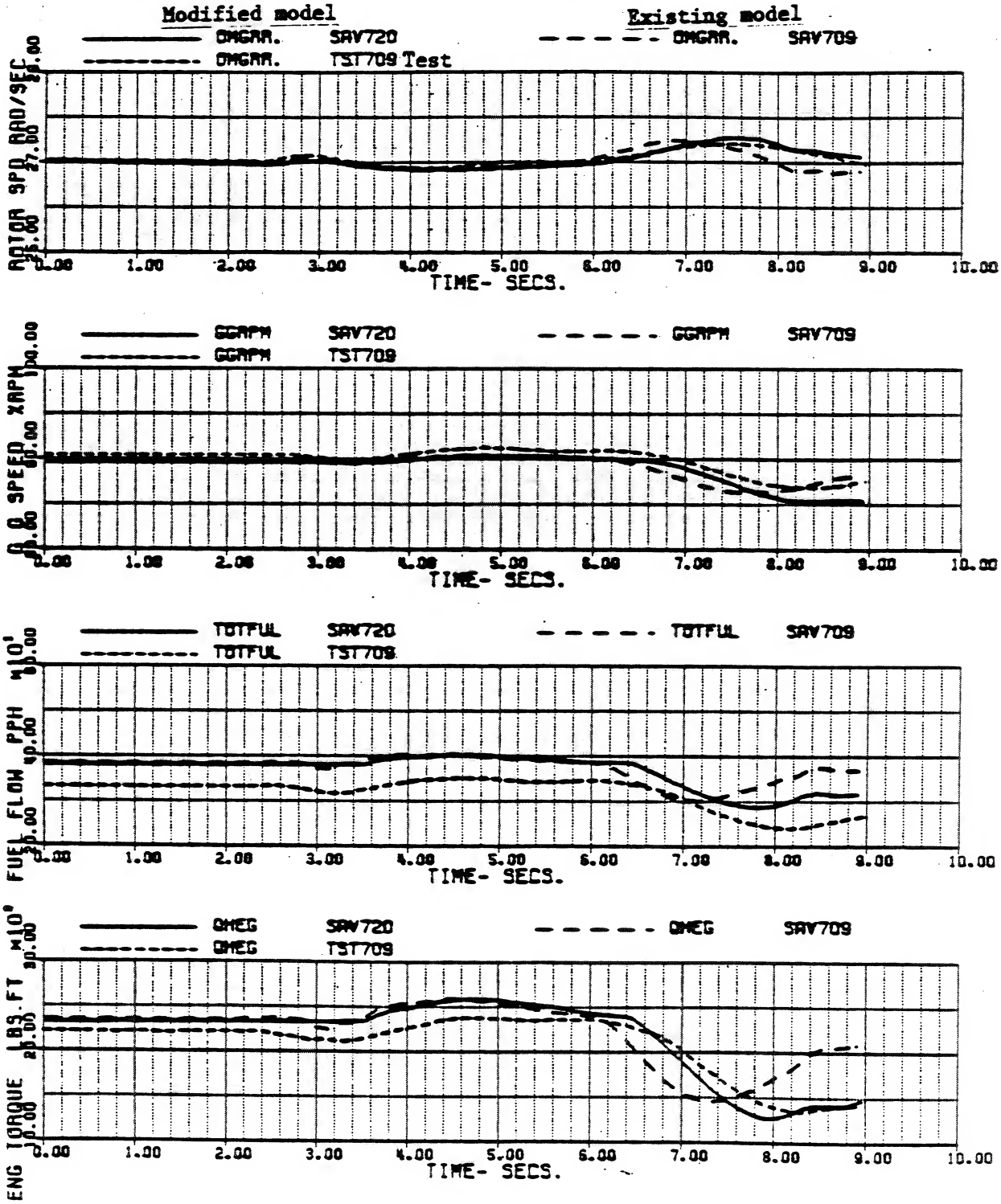

Figure 31h

BLACKHAWK - NASA STUDY 11-MAY-84 14:03 (8/8)
AEFA TEST TAPE BHAWK7 2/1/83
FLT 188 RUN 21 100 KN PEDAL PULSE UPDATED MODEL

VKT	102.99197	WEIGHT	15900.000	FSCG	348.70000	IMI	7.8999999
XA	5.2311698	XB	4.8087467	XC	5.0304511	XP	2.4586541
THETAB	-3.1043404	PHIB	0.	OMGRAT	1.0000000	GGRPM	89.544999

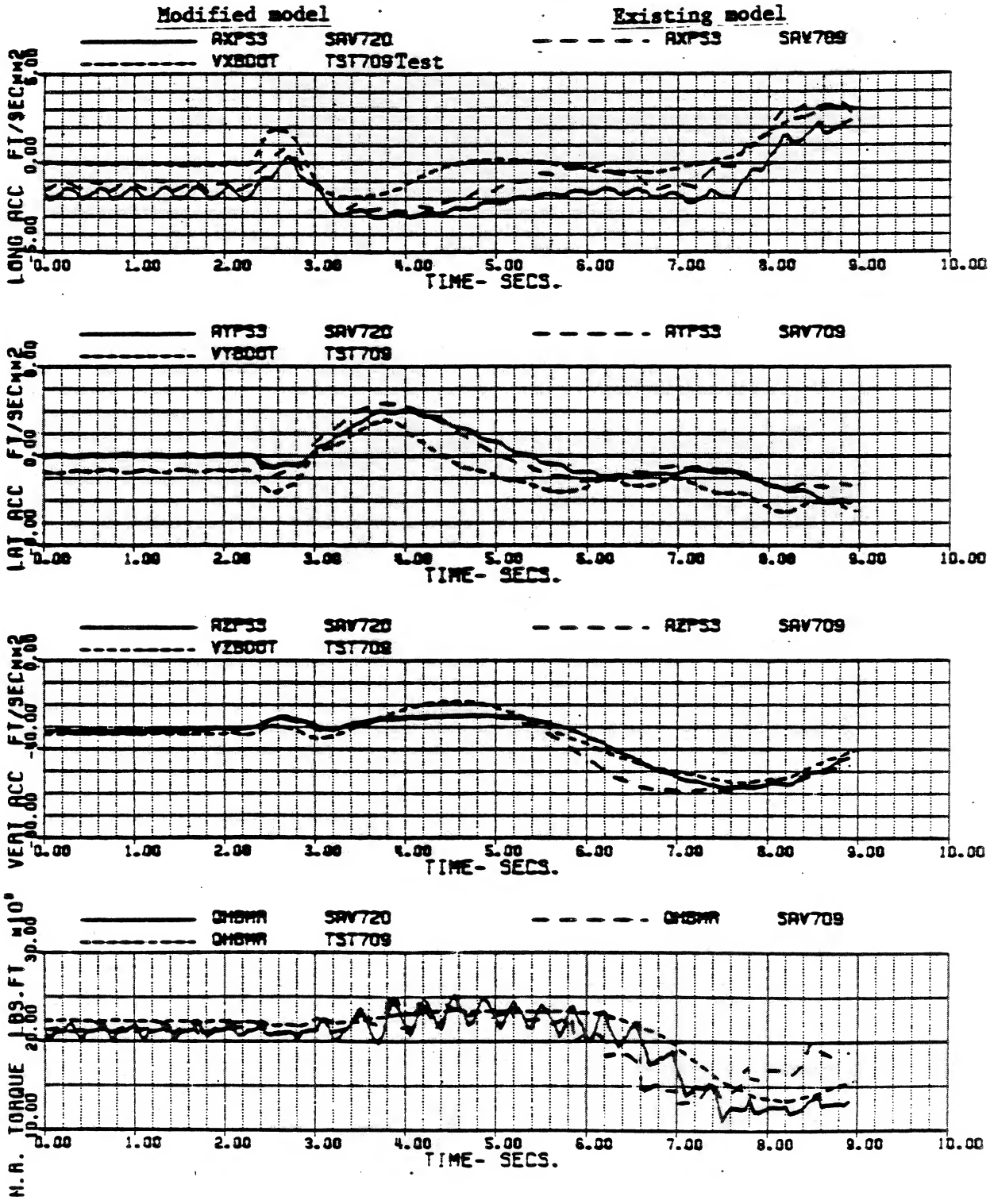

Figure 32a

BLACKHAWK - NASA STUDY 10-MAY-84 09:18 (1/2)
AEFA TEST TAPE BHAWK3 11/22/82 FLT 66 RUN 27
140 KN PEDAL INPUT. UPDATED MODEL (BASE 10)

VKT	143.98846	WEIGHT	15410.000	FSCG	352.09999	IH1	2.9257000
XA	5.6131821	XB	3.5195664	XC	7.1786173	XP	2.3012870
THETAB	-4.9918462	PHIB	0.	OMGRAT	1.0111110	GGRPM	94.427228

Modified model

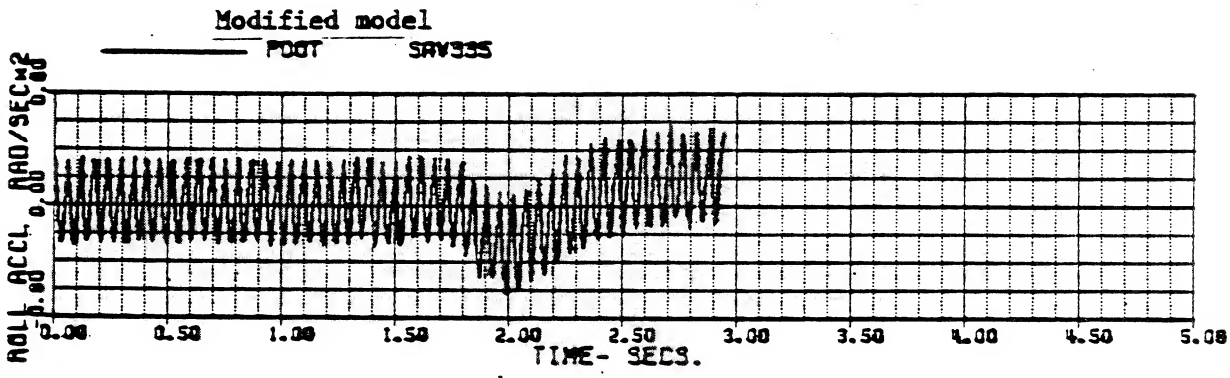

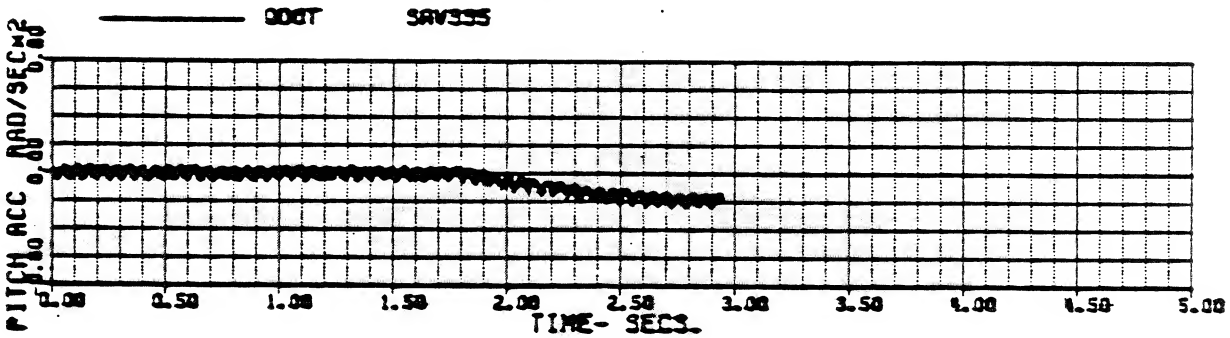

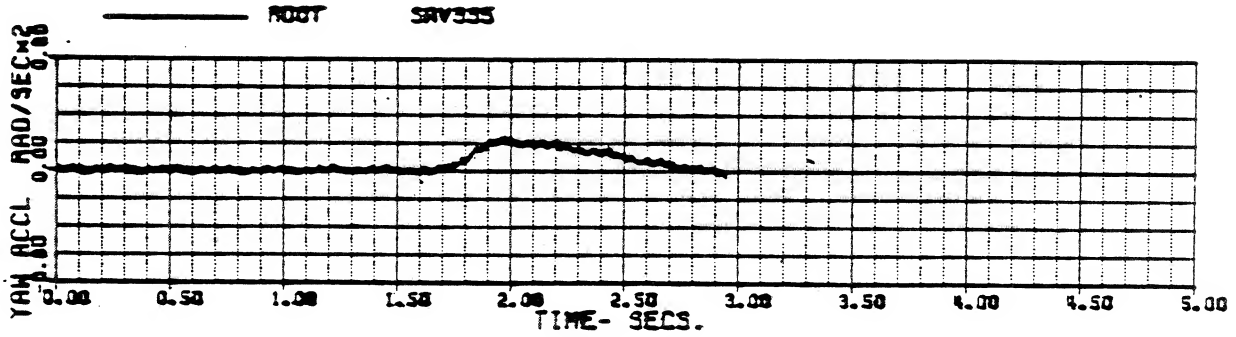

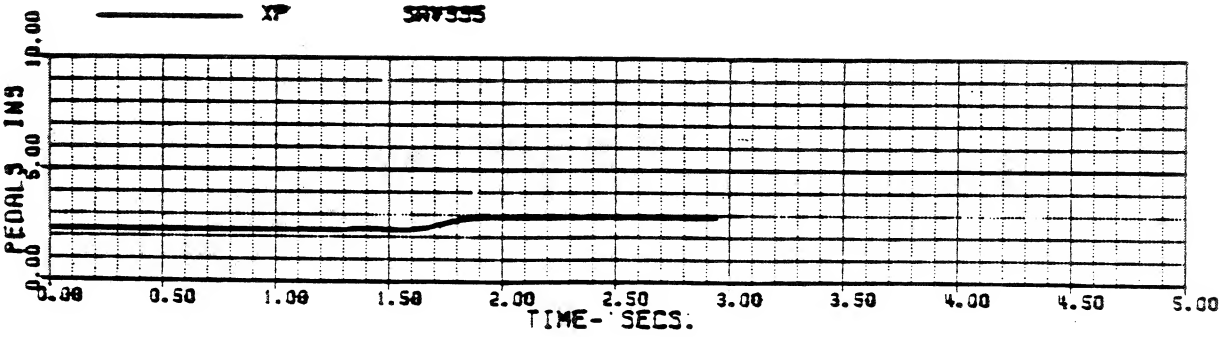

Figure 32b

BLACKHAWK - NASA STUDY 10-MAY-84 09:18 (2/2)

AEFA TEST TAPE BHAWK3 11/22/82 FLT 66 RUN 27
140 KN PEDAL INPUT. UPDATED MODEL (BASE 10)

VKT	143.98846	WEIGHT	15410.000	FSCG	352.09999	IMI	2.9257000
XA	5.6131821	XB	3.5195664	XC	7.1786173	XP	2.3012870
THETAB	-4.9918442	PHIB	0.	OMGRAT	1.0111110	GGRPM	94.427228

Modified model

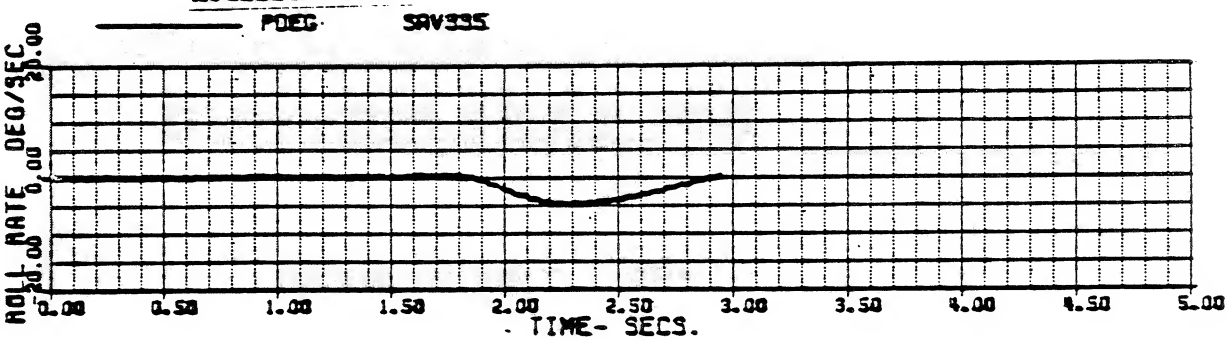

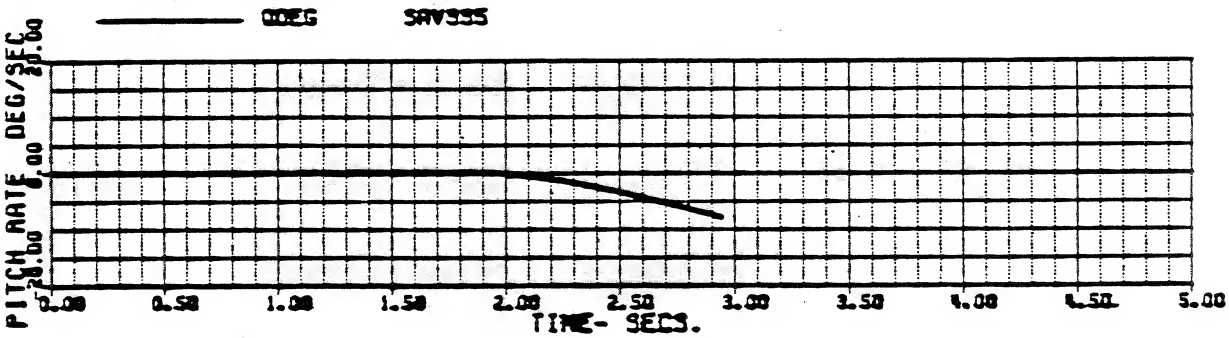

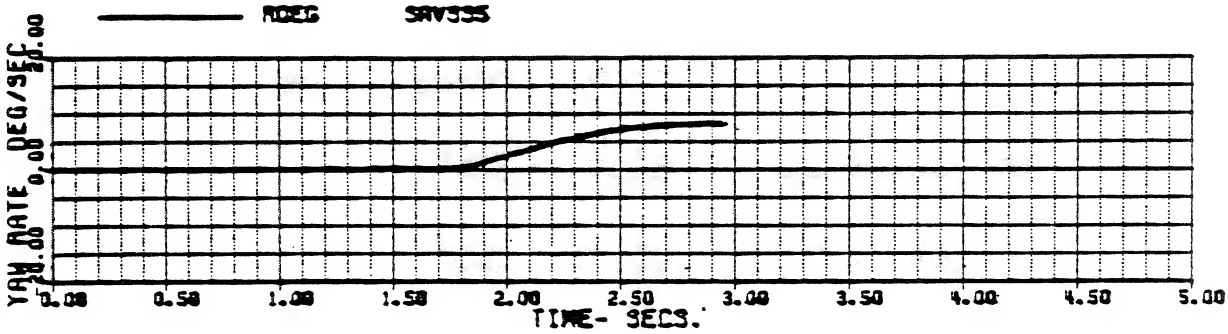

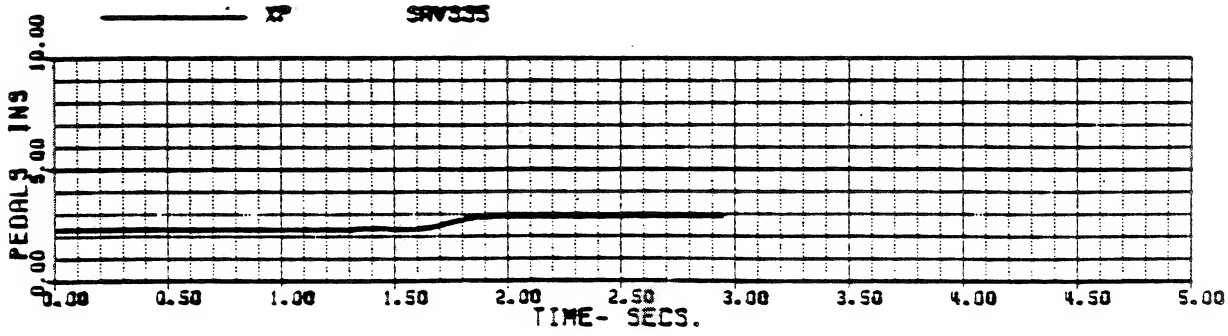

APPENDIX I

MODIFIED DOWNWASH CORRECTION TERMS

[REF. P 5.10-9 REFERENCE (3)]

$$Y_{ADD} = -26.5 * Q_{FRE}$$

$$L_{ADD} = -(160 - 7.5\,\beta^{\circ}_{WF}) * Q_{FRE}$$

$$N_{ADD} = 26.2 * Q_{FRE}$$

IF $\beta^{\circ}_{WF} < 0^{\circ}$ $\quad M_{AD} = 38.9 * \beta^{\circ}_{WF}$ $\quad$ LIMIT MAD > -259

$$M_{ADD} = M_{AD} * Q_{FRE}$$

IF $\beta^{\circ}_{WF} > 0^{\circ}$ $\quad M_{AD} = 58.4 * \beta^{\circ}_{WF}$ $\quad$ LIMIT MAD < 336

$$M_{ADD} = M_{AD} * Q_{FRE}$$

IF $\beta^{\circ}_{WF} \leq -30^{\circ}$ $\quad \beta^{\circ}_{WF} = -30^{\circ}$

IF $\beta^{\circ}_{WF} \geq 30^{\circ}$ $\quad \beta^{\circ}_{WF} = 30^{\circ}$

APPENDIX II

REVISED EQUATIONS OF MOTION

BODY AXES ACCELERATIONS

[REF. P 5.10-6 REFERENCE(3)]

$$VXBDOT = (g/WBD)(SUMXB - WBD\,SIN\theta B) + r \cdot VY'B - q \cdot VZ'B$$

$$VYBDOT = (g/WBD)(SUMYB + WBD\,COS\theta B\,SIN\phi B) + p \cdot VZ'B - r \cdot VX'B$$

$$VZBDOT = (g/WBD)(SUMZB + WBD\,COS\theta B\,COS\phi B) + q \cdot VX'B - p \cdot VY'B$$

$$PDOT = (A \cdot D + B \cdot G + C \cdot H)/J$$

$$QDOT = (A \cdot G + B \cdot E + C \cdot I)/J$$

$$RDOT = (A \cdot H + B \cdot I + C \cdot F)/J$$

WHERE:

$$A = SUMLB - q \cdot hz + r \cdot hy$$

$$B = SUMMB - r \cdot hx + p \cdot hz$$

$$C = SUMNB - p \cdot hy + q \cdot hx$$

$$hx = p \cdot Ix - q \cdot Ixy - r \cdot Ixz$$

$$hy = q \cdot Iy - r \cdot Iyz - p \cdot Ixy$$

$$hz = r \cdot Iz - p \cdot Ixz - q \cdot Iyz$$